

**Establishing the Nature of
Reversible Cardiac Remodeling
in a
Rat Model of Hypobaric Hypoxia-
induced Right Ventricular
Hypertrophy**

Aretha van der Merwe



Thesis presented in partial fulfillment of the requirements
for the degree of Masters of Physiological Sciences at
Stellenbosch University

Supervisor: Prof M. Faadiel Essop

March 2009

DECLARATION

By submitting this dissertation electronically, I declare that the entirety of the work contained therein is my own, original work, that I am the owner of the copyright thereof (unless to the extent explicitly otherwise stated) and that I have not previously in its entirety or in part submitted it for obtaining any qualification.

Date: 24 February 2009

Copyright© 2008 Stellenbosch University

All rights reserved

ABSTRACT

Physiological cardiac hypertrophy is characterized by the heart's ability to increase mass in a reversible fashion without leading to heart failure. In contrast, pathological cardiac hypertrophy leads to the onset of heart failure. For this study, we investigated a model of physiological hypobaric hypoxia-mediated right ventricular (RV) hypertrophy (RVH). Here our hypothesis was that the hypertrophic response and associated changes triggered in the RV in response to chronic hypobaric hypoxia (CHH) (increased RV mass, function and respiratory capacity) are reversible. To test our hypothesis we exposed male Wistar rats to 3 weeks of CHH and thereafter removed the hypoxic stimulus for 3 and 6 weeks, respectively.

Adaptation to 3 weeks of CHH increased the RV to left ventricle (LV) plus interventricular septum ratio by increased (223.5 ± 7.03 vs. 397.4 ± 29.8 , $p < 0.001$ versus normoxic controls), indicative of RVH. Hematocrit levels, RV systolic pressure and RV developed pressure (RVDP) were increased in parallel. Mitochondrial respiratory capacity was not significantly altered when using both carbohydrate and fatty acid oxidative substrates. After the 3-week normoxia recovery period, the RV to LV ratio was increased but to a lesser extent compared to the 3-week hypoxic time-point, i.e. 244.7 ± 11.2 vs. 349.64 ± 3.8 , $p < 0.001$ versus normoxic controls. Moreover, hematocrit levels were completely normalized. However, the RV systolic pressure and the functional adaptations, i.e. increased RVDP induced by CHH exposure still persisted in the 3-week recovery (3HRe) group. Also, pyruvate utilization was increased versus matched controls ($p < 0.04$ vs. matched controls).

Interestingly, we found that at the 6-week recovery time point functional parameters were largely normalized. However, the RV to LV ratio was still increased by 269.3 ± 14.03 vs. 333.9 ± 11.7 , $p < 0.0001$ vs. matched controls. Furthermore, palmitoylcarnitine utilization was increased ($p < 0.03$ vs. matched controls).

In conclusion, we found that exposure to CHH resulted in various adaptive physiological changes, i.e. enhanced hematocrit levels, increased RV mass linked to greater RV contractility and respiratory function. It is important to note that all these changes only occurred in the RV and not in the LV. Furthermore, when a normoxic recovery period (3 and 6 weeks, respectively) were initiated, these physiological parameters largely normalized. Together, the findings of this thesis clearly show the establishment of a reversible model of RV physiological hypertrophy. Our future work will focus on disrupting signaling pathways underlying this process and to thereafter ascertain whether reversibility is abolished. Elucidation of such targets should provide a unique opportunity to develop novel therapeutic agents to treat patients and thereby reduce the burden of heart disease.

OPSOMMING

Fisiologiese kardiak hipertrofie word gekenmerk deur die vermoë van die hart om in spiermassa te vergroot sonder dat dit lei tot die ontwikkeling van hartversakking. Hierdie tipe hipertrofie, is dus omkeerbaar, teenoor patofisiologiese kardiak hipertrofie wat onomkeerbaar is en wat kan lei tot hartversakking. In hierdie studie, was 'n eksperimentele model van fisiologiese hipobariese hipoksie-bemiddelde regter ventrikulêre (RV) hipertrofie (RVH) ondersoek. Ons het dus gehipotetiseer dat die resulterende hipertrofiese respons en bykomende veranderinge teenwoordig in die RV, soos toename in RV massa, funksie and respiratoriese kapasiteit omkeerbaar is. Ons het ons hipotese ondersoek deur manlike Wistar rotte aan 3 weke van kroniese hipobariese hipoksie (KHH) bloot te stel en daarna vir 3- en 6-weke, onderskeidelik onder normoksiese kondisies te huisves.

Op respons tot 3 weke van KHH blootstelling was daar 'n 223.5 ± 7.03 vs. 397.4 ± 29.8 , $p < 0.001$ (vs. normoksie kontrole) toename in die RV tot linker ventrikel (LV) plus interventrikulêre septum verhouding, aanwysend van RVH. Hematokrit vlakke, RV sistoliese druk en RV ontwikkelende druk (RVOD) was ook verhoog. Geen beduidende verandering was in mitochondriale respiratoriese kapasiteit bevind met die toedienning van beide koolhidrate en vetsure as oksidatiewe substrate. Na die 3-weke normoksië herstel periode, was die RV tot LV verhouding nog steeds met 244.7 ± 11.2 vs. 349.64 ± 3.8 , $p < 0.001$ vs. normoksie kontrole verhoog. Terwyl hematokrit vlakke volledig genormaliseer het. Nietemin, die RV sistoliese druk and die aangepaste funksionele veranderinge, b.v. RVOD wat veroorsaak was deur KHH, was nog

steeds teenwoordig in die 3-weke herstel (3HR_e) groep. Eweneens, pirovaat verbruik was verhoog teenoor die normoksie kontrole groep ($p < 0.04$ vs. normoksie kontrole). Interessant, by die 6-weke herstel punt was die funksionele parameters grootliks genormaliseer. Die RV tot LV verhouding was nog steeds verhoog met 269.3 ± 14.03 vs. 333.9 ± 11.7 , $p < 0.0001$ vs. normoksie kontrole). Eweneens, palmitoïelkarnitien was verhoog by die 6-weke herstel tydstop ($p < 0.03$ vs. normoksie kontrole).

Ten slote, ons het bevind dat KHH blootstelling kan verskeie voordelige fisiologiese veranderinge teweegbring, o.a. verhoogde hematokrit vlakke, toename in RV massa wat geassosieer kan word met sterker RV kontraktiliteit and verhoogte respiratoriese funksie. Let wel, hierdie veranderinge was slegs in die RV waargeneem en nie in die LV nie. Die bevindinge in hierdie tesis bewys duidelik die instelling van 'n omkeerbare eksperimentele model van RV fisiologiese hipertrofie. Ons toekomstige navorsing sal grootliks fokus op die ontwinging van sein transduksie paaie wat fisiologiese hipertrofie bevorder en om te bepaal of blokkering van hierdie paaie die omkeerbaarheids vermoë van die hart sal vernietig. Identifisering van sulke teiken sein transduksie paaie sal ons unieke geleenthede bied om nuwe terapeutiese middels te ontwerp wat van toepassing sal wees in die behandeling van pasiënte en dus sodoende die gesondheids las van hartsiektes te verminder.

I dedicate this thesis to my loving parents, my two sisters and my fiancé who supported me throughout this journey.

ACKNOWLEDGEMENTS

Firstly, I need to thank God for the strength to persevere helping me to remain positive when everything seemed to go the wrong way.

Secondly, Prof Essop...Thank you for your guidance and leadership through this year. Thank you for having the patience, to allow me to grow with this project and most importantly, helping me to accomplish this goal in ONE year!

Dr Rob Smith, I'm forever grateful for your guidance and help during the last stretch of my experiments. Thank you for your patience and always being willing to help me with the smallest of problems!

Ben Loos, thank you for always being available when I needed support.

Mandi Albas and her team, thank you for helping me with my histology slides and making life much easier for me.

Dr James Meiring, thank you for your technical support through the year.

Meagan Stevens, thank you for sacrificing your time to help me figure out my stats. “Ek het die bullet vasgebyt”...Thank you for never allowing me to doubt myself.

Bali, Monet and Utra, thank you for your friendship and kind words of wisdom.

Gustav, thank you for never judging me, the insightful conversations and always being willing to help me with the simplest thing even when it meant sacrificing your breakfast or coffee break.

MJ and Ashwin, thank you for making this academic year fun and *different!*

Lastly.....

- My fiancé, Rémi, your support is my energy-booster. Thank you for allowing me the space to accomplish this goal (though it was extremely tough we stuck through it). Thank you for believing and motivating me when I was at my lowest.
- My family, my pillar of strength, thank you for the love and extensive support you have given me through this year. Words are not enough to describe how much it means to me.

Also, I need to thank the National Research Foundation (NRF) for funding my academic year.

The financial assistance of the NRF towards this research is hereby acknowledged. Opinions expressed and conclusions arrived at, are those of the author and are not necessarily to be attributed to the NRF

Table of Contents

	Page
Abbreviations	i
List of Tables	iv
List of Figures	iv
CHAPTER 1: INTRODUCTION	
1.1 EPIDEMIOLOGY	1
1.2 CARDIAC ENERGY METABOLISM UNDER PHYSIOLOGICAL CONDITIONS. 2	
1.2.1. CARBOHYDRATE METABOLISM	3
1.2.2 FATTY ACID METABOLISM	8
1.3 CARDIAC HYPERTROPHY	17
1.3.1 PATHOLOGICAL CARDIAC HYPERTROPHY	18
1.3.2 PHYSIOLOGICAL CARDIAC HYPERTROPHY	23
1.4 HYPOTHESIS	29
1.5 AIMS	30
CHAPTER 2: MATERIALS AND METHODS	
2.1 EXPERIMENTAL DESIGN.....	1
2.2 HEART TISSUE COLLECTION.....	33
2.3 BLOOD COLLECTION AND HEMATOCRIT DETERMINATION	34
2.4 DETERMINATION OF PLASMA METABOLITE LEVELS	35
2.5 HISTOLOGICAL ANALYSIS.....	36
2.6 EVALUATION OF ISOLATED CARDIAC MITOCHONDRIAL FUNCTION	38
2.8 PERFUSION OF ISOLATED RAT HEART	42
2.9 STATISTICAL ANALYSIS.....	44
CHAPTER 3: RESULTS	
3.1 EFFECTS OF CHRONIC EXPOSURE TO HYPOBARIC HYPOXIA	32
3.2 HISTO-ANALYSIS TO INVESTIGATE CARDIAC FIBROSIS.....	52
3.3 PLASMA METABOLITE LEVELS	56
3.4 MITOCHONDRIAL RESPIRATION	58
3.5 DETERMINATION OF CARDIAC FUNCTION VIA THE LANGENDORFF PERFUSION MODE .	62
CHAPTER 4: DISCUSSION	65
CHAPTER 5: REFERENCES	73
CHAPTER 6: APPENDICES	94

ABBREVIATIONS

Introduction:

Acetyl-CoA - acetyl-Coenzyme A

ACC β - acetyl-CoA carboxylase β

Akt - protein kinase B

AMPK - 5' adenosine monophosphate (AMP)-activated protein kinase

ANP/F - atrial natriuretic peptide/factor

ATP - adenosine triphosphate

Ca²⁺ - calcium

CAC - citric acid cycle

CAT - carnitine acyl translocase

CPT-I - carnitine palmitoyltransferase-I

CPT-II - carnitine palmitoyltransferase-II

CVD - cardiovascular disease

CVDs - cardiovascular diseases

c-AMP - cyclic-AMP dependent protein kinase

ERR - estrogen-related receptor family

FABP_{pm} - fatty acid binding protein family

FAT/CD36 - fatty acid translocase

FATP - fatty acid transport protein

F-6-P - fructose-6-phosphate

F-1,6-bisP - fructose 1,6 bisphosphate

G-6-P	-	glucose-6-phosphate
GLUT1	-	glucose transporter 1
GLUT4	-	glucose transporter 4
GH	-	growth hormone
HK	-	hexokinase
IGF-1	-	insulin-like growth factor
IRS-1	-	insulin stimulated receptor 1
LDH	-	lactate dehydrogenase
MCD	-	malonyl-CoA decarboxylase
MCT-1	-	monocarboxylic acid transporter-1
MCH- α	-	α -myosin heavy-chain
MHC- β	-	β -myosin heavy-chain
NAD ⁺	-	nicotinamide adenine dinucleotide
NADH	-	nicotinamide adenine dinucleotide, reduced form
NFAT	-	nuclear factor of activated T-cells
NRF-1	-	nuclear-encoded transcription factor
PDC	-	pyruvate dehydrogenase complex
PDH	-	pyruvate dehydrogenase
PDHP	-	PDH phosphatase
PDK	-	pyruvate dehydrogenase kinase
PDK 1	-	3-phosphoinositide-dependent kinase
PFK-1	-	phosphofructokinase-1

- PDK - pyruvate dehydrogenase kinase
- PGC-1 α - PPAR- γ co-activator 1 α
- PI3-K - phosphatidylinositol-3-kinase
- PPARs - peroxisome proliferator-activated receptors
- PPRE - peroxisome proliferator response element
- RTK - receptor tyrosine kinase
- RXR - retinoid X receptors

Methods:

- CHH - chronic hypobaric hypoxia
- LV - left ventricle
- RV - right ventricle
- RVH - right ventricular hypertrophy
- 3HRe - 3-weeks recovery in normoxia
- 6HRe - 6-weeks recovery in normoxia
- ZT - Zeitgeber time

List of Tables

Page

Results:

Table 1. Functional measurements investigated at each experimental time point. 63

List of Figures

Page

Introduction:

Figure 1. Schematic illustration of the key events in glucose metabolism.5

Figure 2. Illustration of key events that takes place in fatty acid transport into the cardiomyocyte and uptake into the mitochondrion.10

Figure 3. Induction of genes participating in fatty acid oxidation via fatty acids.....13

Figure 4. The PPAR isoforms.....16

Figure 5. Schematic representation of events that may contribute to ventricular dilation, which is a risk factor for heart failure development.20

Figure 6. Physiological cardiac hypertrophy induced by IGF-1 secretion.....24

Figure 7. Description of hypothesis.29

Materials and Methods:

Figure 1. Experimental study design.....32

Figure 2. Diagrammatic illustration of plasma collection.....35

Figure 3. Schematic illustration of histo-analysis.....	36
Figure 4. Mitochondrial isolation.....	40
Figure 5. Evaluation of mitochondrial function.....	42
Figure 6. A simplified schematic illustration of the Langendorff heart perfusion system.	44

Results:

Figure 1. Effects of CHH and normoxia recovery on body weight.	49
Figure 2. Regression of right ventricular hypertrophic response after normoxic exposure.	50
Figure 3. Regression of right ventricular hypertrophic response after normoxic exposure.	51
Figure 4. Unaltered LV to BW ratio in response to experimental conditions.....	52
Figure 5. Complete regression of hematocrit levels after 3- and 6-weeks of normoxia.	53
Figure 6. H&E stained histological sections at different experimental time points.	54
Figure 7. Evaluating regression of right ventricular cardiomyocyte size after normoxic exposure.	55
Figure 8. Sirius red staining demonstrates lack of fibrosis.	56
Figure 9. Fibrosis remained unchanged for both experimental and control groups.	57
Figure 10. Plasma glucose levels normalize following normoxic exposure.	58
Figure 11. Increased TG levels after 6-weeks normoxic exposure.....	59

Figure 12. Effects of CHH on mitochondrial respiratory capacity-pyruvate60

Figure 13. Effects of CHH on mitochondrial respiratory capacity- palmitoylcarnitine..
.....61

Figure 14. Mitochondrial respiratory capacity (pyruvate) remained
unchanged in control and experimental groups.....62

Figure 15. Mitochondrial respiratory capacity (palmitoylcarnitine)
remained unchanged in control and experimental groups.....62

Figure 16. Normalization of right ventricular developed pressure (RVDP)
in response to normoxic exposure.....64

Figure 17. Left ventricular developed pressure (LVDP) remained
unaltered during experimental period.65

Chapter 1

Introduction

1.1 Epidemiology

Over the past two decades, CVDs have emerged as the number one cause of mortality in developed nations (Fuster et al., 2004). Recently, CVD mortality data show that it is responsible for ~ 2,400 deaths daily in the US, and that for every one in three American adults a cardiovascular pathology can be recognized (Heart disease and stroke statistics, 2008). However, the burden of CVD is not only restricted to developed nations (Yusuf et al., 2001) since recent studies also reported an increase in CVD incidences in developing countries (Damasceno et al., 2007; Reddy, 2004; Yusuf et al., 2004; Yusuf et al., 2001). In Africa, cardiovascular pathologies arise primarily from non-ischemic causes (Damasceno et al., 2007). For example, rheumatic heart disease and hypertensive heart disease accounts for ~75% of CVD incidences, whereas *cor pulmonale* and pericarditis are responsible for ~20% (Damasceno et al., 2007; Tibazarwa et al., 2008). However, this pattern is gradually changing as a consequence of epidemiological transition or urbanization (Pearson, 1999). This process is generally characterized by the so-called “westernized” way of living defined by over-consumption of high-energy dense foods, reduced levels of physical activity and high rates of cigarette smoking (Pearson, 1999; Reddy, 2004; Wilson et al., 2007). This will eventually increase the prevalence of obesity, diabetes mellitus, coronary heart disease and hypertension in our developing countries (Damasceno et al., 2007), all major driving forces for the development of CVDs (Reddy, 2004; Van Gaal et al., 2006; Yusuf et al., 2004). Therefore, CVD has become a global epidemic with projections indicating ~24,2 million annual deaths by 2030 (WHO, 2008).

Although CVD can result from poor lifestyle habits, cardiac hypertrophy may be an important risk factor (Leong et al., 2003). For example, 15-20% of individuals present with cardiac hypertrophy, more than 90% of these individuals are hospitalized with CVD (Leong et al., 2003). Generally, cardiac hypertrophy is an adaptive response of the heart to prolonged pressure- or volume overload (Dorn II, 2007; Frey et al., 2004; Hunter and Chien, 1999; McMullen and Jennings, 2007). Hallmarks of this response include an increase in cardiomyocyte size, enhanced protein synthesis, and the addition of sarcomeres (Frey and Olson, 2003, Frey et al., 2004; Hunter and Chien, 1999). At the molecular level cardiac hypertrophy is typified by the re-expression of the so-called fetal gene program in cardiomyocytes, approximating gene expression profiles observed in the fetal heart (Frey et al., 2004; Razeghi et al., 2001; Rajabi et al., 2007). Moreover, cardiac hypertrophy is also associated with a change in the heart's energy metabolism, i.e. increased glycolytic ATP production (Sambandam et al., 2002). To further explore the latter, I will provide an overview of energy metabolism in the healthy and hypertrophied heart.

1.2 Cardiac energy metabolism under physiological conditions

The healthy mammalian adult heart is an “omnivorous” organ, deriving its energy from numerous fuel sources depending on availability and the surrounding metabolic environment (Taegtmeyer et al., 2005). The non-hypertrophied heart is a relatively small organ that daily consumes about ~6 kg of ATP (Neubauer, 2007). This high energy demand of the heart is met by catabolizing various metabolic fuels, including fatty acids, glucose and lactate (Calvani *et al.*, 2000; Kodde *et al.*, 2007; Neubauer, 2007; Stanley *et al.*, 2005; Stanley and Sabbah, 2005). Breakdown of fatty acids accounts for ~60-90% of ATP production, whereas glucose and lactate oxidation provides ~10-40% of ATP generated (Kodde *et al.*, 2007; Neubauer, 2007; Stanley

et al., 2005). Before participating in energy metabolism, metabolic fuels are taken up into cardiomyocytes through specific transport proteins located at the sarcolemmal surface (Coort *et al.*, 2007; Dolinsky and Dyck, 2006; Neubauer, 2007; Stanley *et al.*, 2005). Upon entering the cardiomyocyte, fuel substrates are metabolized by numerous metabolic pathways that are stringently regulated by various enzymes in the cytosol and mitochondria (Kodde *et al.*, 2007; Stanley *et al.*, 2005). In addition, substrate utilization is also regulated at the transcriptional level by various transcriptional modulators, e.g. the PPARs, PGC-1 α and the ERR family (An and Rodrigues, 2006; Finck, 2007; Huss and Kelly, 2005). Fuel substrate selection by the heart can also be influenced by nutritional status (e.g. starvation or over-nourishment), diabetes mellitus (considering that the diabetic predominantly utilizes fatty acid as a fuel source), stress and exercise (Brownsey *et al.*, 1997; Duncan and Finck, 2007; Lehman *et al.*, 2000; Vander *et al.*, 1998). Together, these regulatory mechanisms ensure proper myocardial substrate uptake and intracellular utilization thereby linking cardiac energy metabolism to the overall function of the normal mammalian heart (Taegtmeyer *et al.*, 2005). In light of this, I will now review carbohydrate and fatty acid metabolism in the healthy myocardium.

1.2.1. Carbohydrate metabolism

Glucose and lactate are the main carbohydrates that participate in the heart's energy metabolism. This process usually occurs through cellular glucose and lactate uptake and its catabolism by several metabolic pathways, e.g. glycolysis and pyruvate oxidation (Stanley *et al.*, 2005). A brief overview of glucose metabolism, i.e. glucose uptake and breakdown for energy production will be presented.

Glucose enters the cardiomyocyte via specific glucose transporters, i.e. GLUT1 and GLUT4 (Stanley *et al.*, 2005). In the cardiomyocyte, GLUTs can be either located at the plasma membrane or found within intracellular compartments (An and Rodrigues, 2006). The insulin-insensitive glucose transporter, GLUT1, is present in the plasma membrane and regulates basal glucose uptake, whereas GLUT4 transporters are stored in intracellular vesicles that translocates to the sarcolemma under the influence of insulin stimulation (An and Rodrigues, 2006; Bertrand *et al.*, 2008; Brownsey *et al.*, 1997).

Following a meal, plasma glucose concentrations are normally elevated and pancreatic β -cells are stimulated to secrete insulin (Vander *et al.*, 1998). Insulin binds to its tetrameric receptor, composed of two extracellular α -subunits (binds growth factors e.g. insulin, insulin-like growth factor [IGF-1], growth hormone [GH]) and two transmembrane β -subunits (possessing tyrosine kinase activity) (Bertrand *et al.*, 2008; Brownsey *et al.*, 1997). Binding of insulin to its receptor enhances tyrosine kinase activity of its β -subunits, causing autophosphorylation of tyrosyl residues of the intracellular domain (Bertrand *et al.*, 2008; Engelman *et al.*, 2006; Saad *et al.*, 1994). Once activated and phosphorylated, receptor tyrosine kinase (RTK) phosphorylates the cytosolic adaptor protein, insulin stimulated receptor 1 (IRS-1), which in turn binds to and activates the lipid enzyme, phosphatidylinositol 3-kinase (PI3-K) (Figure 1) (Engelman *et al.*, 2006; Saad *et al.*, 1994). PI3-K is a heterodimeric protein composed of two subunits, a p110 α catalytic subunit and a p85 regulatory subunit (Engelman *et al.*, 2006; Luo *et al.*, 2005).

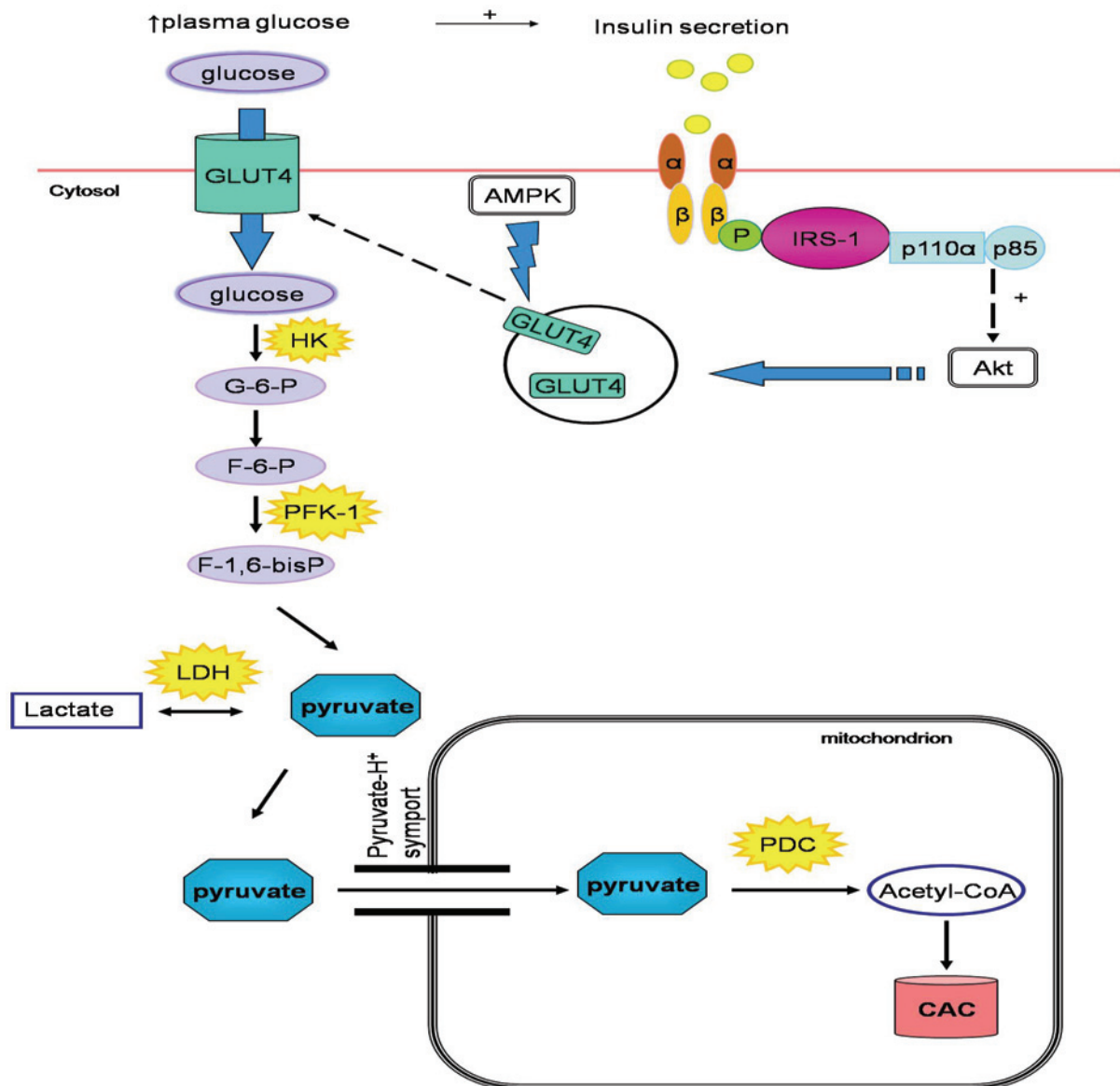


Figure 1. Schematic illustration of the key events in glucose metabolism. *The pancreatic beta cells secrete insulin in response to high plasma glucose concentrations. Insulin binds to its membrane receptor (a tetrameric receptor composed of two α and β subunits) and initiates an intracellular signalling cascade via the PI3-K/Akt pathway. The PI3-K/Akt pathway stimulates GLUT4 translocation to the sarcolemma, hence, facilitating glucose entry into the cardiomyocyte. AMPK (5' adenosine monophosphate (AMP)-activated protein kinase) also stimulates GLUT4 translocation in an insulin/PI3-K/Akt independent manner. Glucose is rapidly converted to G-6-P (glucose-6-phosphate) by HK (hexokinase). G-6-P is then further broken down to F-6-P (fructose-6-phosphate) and pyruvate. F-6-P is phosphorylated to F-1,6-bisP (fructose 1,6 bisphosphate) by PFK-1 (phosphofruktokinase-1), the rate limiting enzyme of glycolysis. Lactate enters the cell to be converted to pyruvate in a reversible reaction catalyzed by LDH (lactate dehydrogenase). Pyruvate enters the mitochondria via a specific pyruvate-H⁺ symport. Inside the mitochondrion, pyruvate is decarboxylated to acetyl-CoA via PDC (pyruvate dehydrogenase complex), the rate-limiting step of glucose oxidation. Acetyl-CoA enters the citric acid cycle (CAC) for energy production.*

Once activated, PI3-K(p110 α) phosphorylates the 3' hydroxyl group on the inositol ring of phosphatidylinositol-4,5-bisphosphate to produce phosphatidylinositol-3,4,5-

triphosphate (PIP₃) (Luo et al., 2005). PIP₃ is a lipid second messenger, that activates numerous downstream targets by binding to their pleckstrin homology domains (Dorn and Force, 2005; Engelman et al., 2006; Luo et al., 2005). The protein serine/threonine kinase, Akt (also referred to as protein kinase B) and PDK1 are recruited to the sarcolemma, whereupon PDK1 phosphorylates and activates Akt (Bertrand et al., 2008; Dorn and Force, 2005; Engelman et al., 2006; Luo et al., 2005). The insulin-mediated PI3-K/Akt signalling cascade initiates GLUT4 translocation to the sarcolemmal surface to allow for glucose entry into the cardiomyocyte (Bertrand et al., 2008; Brownsey et al., 1997).

A second method of GLUT4 translocation to the sarcolemma is through the activation of AMPK that increases glucose uptake in an insulin/PI3-K/Akt independent manner (Dolinsky and Dyck, 2006) (Figure 1). AMPK is a heterotrimeric enzyme, comprised of two regulatory subunits, β and γ and a catalytic subunit, α (Hardie, 2003). This protein is often referred to as the “fuel sensor” of the cell since it is able to activate catabolic pathways to generate ATP and inhibit anabolic pathways that consume unnecessary energy (Arad et al., 2007; Hardie, 2003; Towler and Hardie, 2007).

Once glucose is imported into the cardiomyocyte, it is rapidly phosphorylated to glucose-6-phosphate via hexokinase (Kodde *et al.*, 2007; Petersen and Shulman, 2006). The newly synthesized glucose-6-phosphate have several main destinations: a) it can be stored as glycogen via a reaction catalysed by glycogen synthase, b) metabolized to pyruvate via glycolysis and glucose oxidation, c) converted to fructose-6-phosphate which may enter the hexosamine biosynthetic pathway and d)

converted to ribose-5-phosphate via the pentose phosphate pathway (Kodde *et al.*, 2007; Rossetti, 2000).

Within the cardiomyocyte, glucose metabolism occurs in the cytosol and the mitochondrion. This process can be divided into two separate components: a) glycolysis, the breakdown of glucose to pyruvate in the cytosol, and b) glucose oxidation, the decarboxylation of pyruvate (glycolysis end-product) to acetyl-CoA within the mitochondrion (Ussher and Lopaschuk, 2006). Pyruvate generated in the glycolytic pathway is transported into the mitochondria via a specific pyruvate- H^+ symport, where it is decarboxylated by a multi-enzyme complex, PDC, to produce acetyl-CoA (Voet and Voet, 2004) (Figure 1). PDC is an important rate-limiting enzyme that couples glycolysis to the citric acid cycle (Lydell *et al.*, 2002; Sidhu *et al.*, 2008). PDC comprises of three enzymatic subunits: a) pyruvate dehydrogenase (PDH) or E_1 , b) dihydrolipoyl transacetylase (E_2) and c) dihydrolipoyl dehydrogenase (E_3) (Sidhu *et al.*, 2008; Voet and Voet, 2004). PDH is responsible for the decarboxylation of pyruvate to acetyl-CoA, an irreversible rate-limiting step in glucose oxidation (Stanley *et al.*, 2005; Voet and Voet, 2004). PDC activity can be regulated by a) increased mitochondrial $[NADH]/[NAD^+]$ and $[acetyl-CoA]/[free\ CoA]$ ratios, and b) phosphorylation/dephosphorylation of PDH via PDK and PDHP (Sidhu *et al.*, 2008; Voet and Voet, 2004).

PDK inhibits the activity of PDC by phosphorylating PDH at a specific serine residue (Voet and Voet, 2004). Four PDK-isoforms are known to date, whereof three are found in the heart, i.e. PDK-1, PDK-2, and PDK-4 (Sugden, 2008). PDK-4 is a “lipid sensitive” isoform that is found in the heart (Stanley *et al.*, 2005; Sugden, 2008). Therefore, PDK activity is indirectly enhanced by increased rates of fatty acid

oxidation which leads to elevated mitochondrial $[NADH]/[NAD^+]$ and $[acetyl-CoA]/[free\ CoA]$ ratios (Stanley and Sabbah, 2005). This reduction in PDH activity is brought about by increased mitochondrial $[NADH]/[NAD^+]$ and $[acetyl-CoA]/[free\ CoA]$ ratios as well as PDK activity, leading to a decline in pyruvate oxidation (Stanley and Sabbah, 2005). However, PDH activity is enhanced by dephosphorylation by PDH phosphatase (Stanley et al., 2005). PDH phosphatase activity can be increased by intracellular Ca^{2+} concentrations and indirectly by insulin secretion (Voet and Voet, 2004) thereby increasing PDH activity to promote pyruvate oxidation.

A second source of cytosolic pyruvate is lactate (Stanley et al., 2005). Lactate enters the cardiomyocyte via its membrane transporter, the monocarboxylic acid transporter-1 (MCT-1) (Stanley et al., 2005) (Figure 1). Intracellular lactate is converted to pyruvate in a reversible reaction catalyzed by lactate dehydrogenase (LDH) (Kodde *et al.*, 2007). However, during ischemia-reperfusion the reduction in PDC activity results in delinking of glycolysis from glucose oxidation leading to increased lactate and proton (H^+) build up in the myocardium (Stanley *et al.*, 2005; Ussher and Lopaschuk, 2006).

1.2.2 Fatty acid metabolism

The heart is a relatively small organ with limited storage capacity for fuel substrates therefore relying on substrates supplied by the circulation (Kodde *et al.*, 2007). For example, fatty acids are taken up by the cardiomyocytes either via passive diffusion or by a carrier-mediated transport system involving the plasma membrane fatty acid binding protein family ($FABP_{pm}$), fatty acid translocase (FAT/CD36) and fatty acid

transport protein (FATP) (Coort et al., 2007; Kodde et al., 2007). These transporters bind to fatty acid moieties thereby facilitating entry into cardiomyocytes (Stanley *et al.*, 2005). Inside cardiomyocytes, fatty acids are converted to long-chain fatty acyl-CoAs (activated fatty acids) via an ATP-dependent acylation reaction catalysed by acyl-CoA synthetase (Calvani *et al.*, 2000). Cytosolic long-chain fatty acyl-CoAs are unable to cross the inner mitochondrial membrane to undergo β -oxidation and as a result depends on the carnitine shuttle to facilitate its transport across the inner mitochondrial membrane (Figure 2) (Calvani *et al.*, 2000). The carnitine shuttle comprises of three mitochondrial membrane transporters, i.e. carnitine palmitoyltransferase-I (CPT-I), carnitine palmitoyltransferase-II (CPT-II) and carnitine acyl translocase (CAT) (Calvani et al., 2000). Before long-chain fatty acyl-CoAs can be transported across the inner mitochondrial membrane, its acyl group is transferred to cytosolic carnitine to produce long-chain acyl-carnitine in a reaction catalysed by CPT-I (Calvani *et al.*, 2000; Voet and Voet, 2004).

The resulting long-chain acyl-carnitine enters the intermembrane space where it is converted to acyl-carnitine via CAT and transported across the inner mitochondrial membrane (Calvani *et al.*, 2000; Stanley *et al.*, 2005). The third enzyme involved in fatty acid transport into the mitochondrion, CPT-II, catalyses the synthesis of mitochondrial matrix long-chain acyl-CoAs from acyl-carnitine by replacing the carnitine portion with a CoA group (as presented in Figure 2) (Voet and Voet, 2004). The released carnitine is then returned to the cytosol to replenish the cytosolic carnitine pool (Voet and Voet, 2004). Acyl-CoA will eventually enter the β -oxidation pathway to form acetyl-CoA necessary for ATP generation (Calvani *et al.*, 2000).

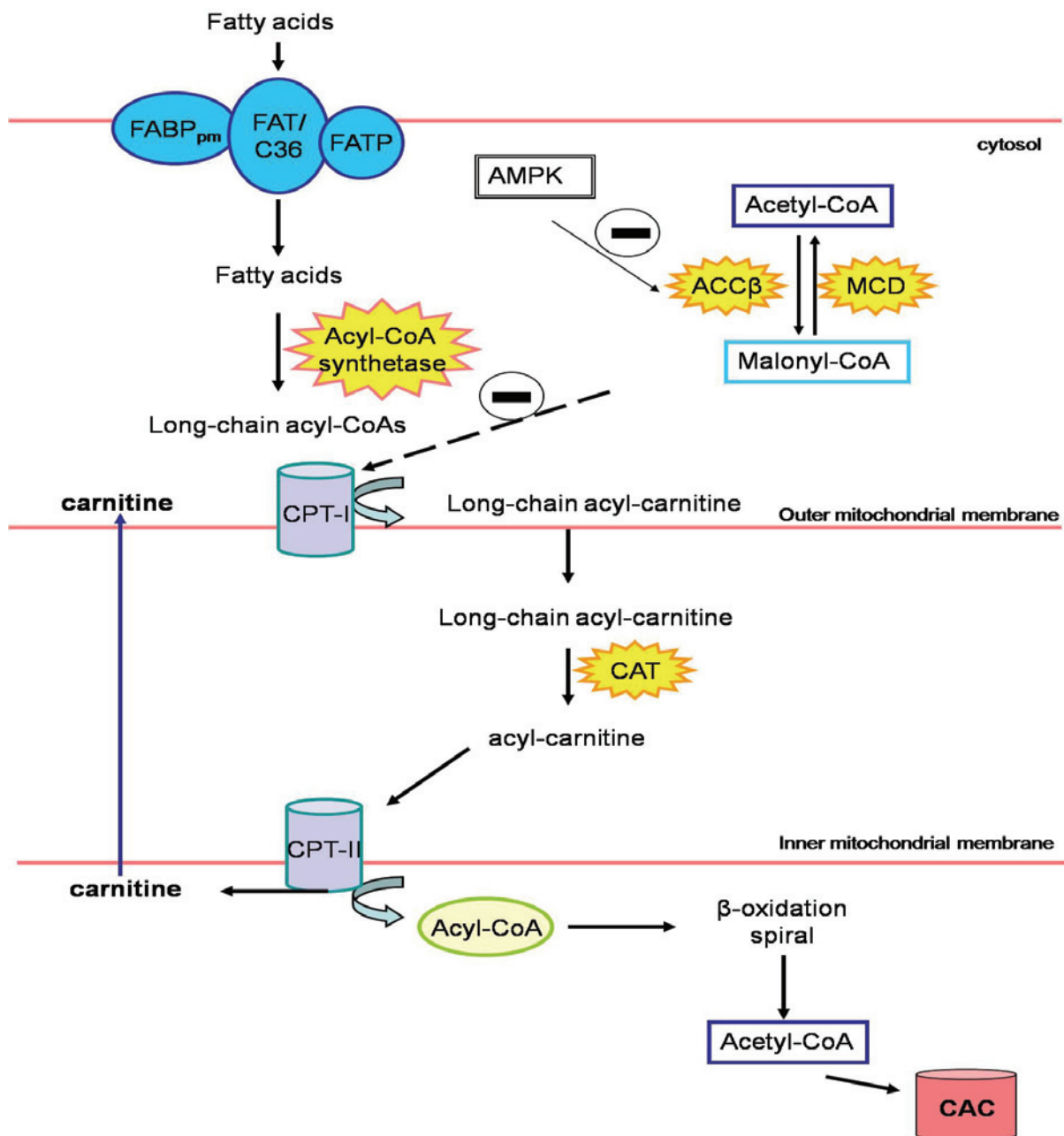


Figure 2. Illustration of key events that takes place in fatty acid transport into the cardiomyocyte and uptake into the mitochondrion. *Transport of fatty acids into cardiomyocytes are facilitated by fatty acid membrane transport proteins such as FAT/CD36, FATP and FABP_{pm}. Within the cytosol, they are acted upon by acyl-CoA synthetase to produce long-chain acyl-CoAs. Long-chain acyl-CoAs are unable to cross the outer mitochondrial membrane. Their transport into the mitochondrion is facilitated by the carnitine shuttle. The carnitine shuttle comprises three enzymes: carnitine palmitoyltransferase-I (CPT-I), carnitine palmitoyltransferase-II (CPT-II) and acyl translocase (CAT). Acyl-carnitine generated by the carnitine shuttle, enters the fatty acid β - oxidation spiral to produce acetyl-CoA that will fuel the citric acid cycle (CAC). This process is influenced by the actions of AMPK on acetyl-CoA carboxylase β (ACCβ). ACCβ promotes malonyl-CoA synthesis from acetyl-CoA while malonyl-CoA decarboxylase (MCD) degrades it. Malonyl-CoA is an endogenous inhibitor of CPT-I, thus decreasing fatty acid oxidation.*

Of the three carnitine specific enzymes involved in the transport of long-chain fatty acyl-CoAs across the inner mitochondrial membrane, CPT-I is the rate-determining enzyme that regulates mitochondrial fatty acid uptake (Calvani *et al.*, 2000; Folmes and Lopaschuk, 2007; Stanley *et al.*, 2005). The activity of CPT-I is inhibited by malonyl-CoA, a key regulator of cardiac fatty acid oxidation (Folmes and Lopaschuk, 2007; Stanley *et al.*, 2005). The enzyme acetyl-CoA carboxylase beta (ACC β) is responsible for the conversion of acetyl-CoA to malonyl-CoA (Folmes and Lopaschuk, 2007; Stanley *et al.*, 2005). An increase in cardiac malonyl-CoA levels inhibits mitochondrial fatty acid oxidation and fatty acid uptake, while a decrease in malonyl-CoA levels results in an increase in mitochondrial fatty acid oxidation (Folmes and Lopaschuk, 2007).

The activity of ACC β is inhibited by a variety of kinases such as AMPK, cyclic-AMP dependent protein kinase (c-AMP) and protein kinase C (Rasmussen and Wolfe, 1999). Inactivation of ACC β by AMPK phosphorylation results in a decrease in malonyl-CoA synthesis. This diminishes the inhibitory effect of malonyl-CoA on CPT-I, resulting in a concomitant rise in mitochondrial fatty acid oxidation (Stanley *et al.*, 2005). The enzyme malonyl-CoA decarboxylase (MCD) is responsible for the degradation of malonyl-CoA to acetyl-CoA (Folmes and Lopaschuk, 2007). Therefore, high rates of MCD activity is associated with reduced myocardial malonyl-CoA content and increased levels of fatty acid oxidation in the heart (Stanley *et al.*, 2005).

Following their transport across the inner mitochondrial membrane, fatty acyl-CoAs enter the mitochondrial matrix to undergo β -oxidation to produce acetyl-CoA that will feed into the citric acid cycle (Stanley *et al.*, 2005). The process of fatty acid β -

oxidation involves four enzymatically catalyzed reactions that are able to catabolize short-, medium- and long-chain fatty acids (Ussher and Lopaschuk, 2006). The enzyme catalyzing the last reaction in this process, 3-ketoacyl CoA thiolase that generates acetyl-CoA, is also the therapeutic target of Trimetazidine, a metabolic drug aimed at partial inhibition of fatty acid oxidation (Ussher and Lopaschuk, 2006).

A number of studies have demonstrated that regulation of myocardial fatty acids metabolism also occurs at the transcriptional level (Finck, 2007; An and Rodrigues, 2006). For example, the PPAR family, belonging to a large family of nuclear receptors, are crucial role players in fatty acid metabolism (Finck, 2007; An and Rodrigues, 2006). PPARs are activated by fatty acids that function as ligands (Neubauer, 2007; Young *et al.*, 2002). Once activated, PPARs form heterodimers with retinoid X receptors (RXR) (Finck, 2007; Grimaldi, 2007). The PPAR/RXR complex then translocates to the nucleus where it induces transcriptional activation of genes encoding enzymes regulating cardiac fatty acid metabolism (Figure 3). The PPAR/RXR heterodimer binds to specific response elements, i.e. the peroxisome proliferator response element (PPRE), in the promoter region of target genes (Grimaldi, 2007; Kodde *et al.*, 2007). This PPRE is a direct repeat of 6 nucleotides, AGGTCA, divided by one spacer nucleotide (Grimaldi, 2007).

In order to initiate the transcriptional activation of the target genes, the PPAR/RXR complex must recruit additional transcriptional co-activators (Finck, 2007). Puigserver and Spiegelman (2003) referred to co-activators as proteins or protein complexes “that increases the rate of transcription by interacting with transcription factors but does not itself bind to DNA in a sequence specific manner”.

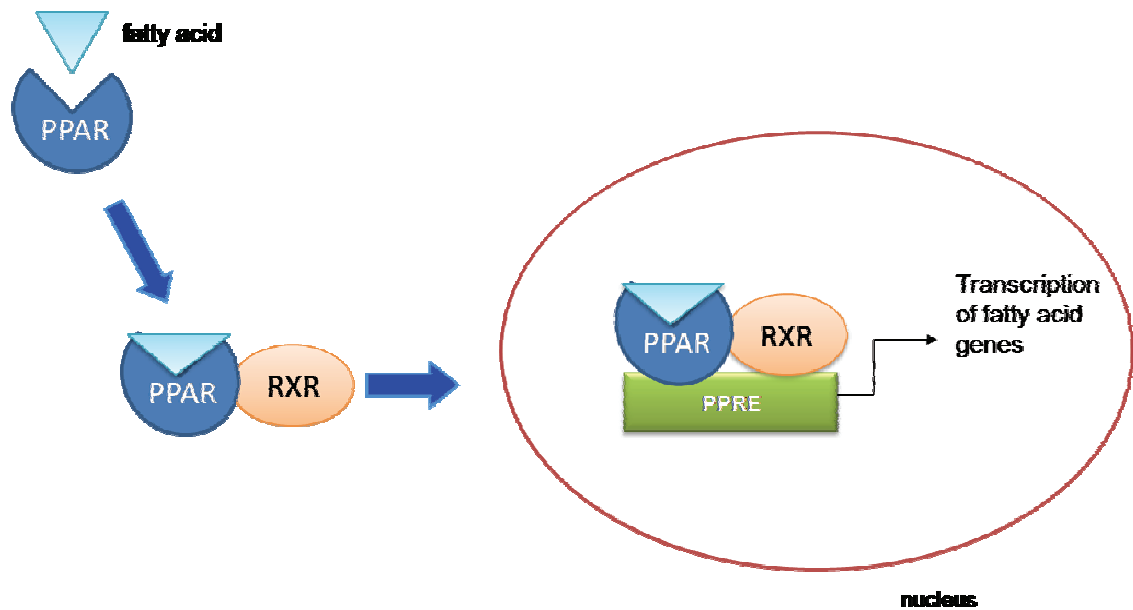


Figure 3. Induction of genes participating in fatty acid oxidation via fatty acids.

Fatty acids act as ligands for the PPAR (peroxisome proliferator-activated receptors) family. Once activated by these ligands, PPAR forms a complex with RXR (retinoid X receptors) and enters the nucleus where it binds to a specific promoter region, PPRE, to induce transcription of genes that are involved in fatty acid metabolism.

Two classes of co-activators are required for optimal functioning of the transcriptional machinery (Duncan and Finck, 2008). Class I co-activators possess histone acetylase (HAT) activity to enhance DNA unwinding, thus providing easy access to the target genes (Duncan and Finck, 2008; Finck, 2007). Conversely, class II co-activators are unable to induce DNA unwinding, but can interact with the RNA polymerase machinery (Duncan and Finck, 2008). This class of co-activators includes the steroid receptor co-activators (SRC), PPAR-interacting protein (PRIP), p300, PPAR-binding protein (PBP) and PPAR- γ co-activator 1 α (PGC-1 α) (Finck, 2007).

PGC-1 α is also a co-activator of the PPAR transcriptional regulators. PGC-1 α levels are highly induced in the postnatal heart when there is a switch in fuel substrate utilization from glucose to fatty acids as the main energy source. This fuel substrate switch is accompanied by a robust increase in mitochondrial number (mitochondrial biogenesis) and oxidative capacity (Finck and Kelly, 2007; Liang and Ward, 2006; Puigserver and Spiegelman, 2003). PGC-1 α is a key regulator of energy metabolism and is activated under conditions of food scarcity, physical activity and disease states such as diabetes (Duncan and Finck, 2008; Finck and Kelly, 2007; Liang and Ward, 2006; Lehman et al., 2000; Puigserver and Spiegelman, 2003).

In the heart, PGC-1 α exerts its effects by interacting with three families of transcription factors including 1) the PPAR family, 2) ERR family and 3) nuclear respiratory factor 1 (NRF-1) (Duncan and Finck, 2008; Finck and Kelly, 2007; Huss and Kelly, 2005; Huss et al., 2007). Cardiac fatty acid metabolism is regulated by both the PPARs and ERR family (Finck and Kelly, 2007; Huss and Kelly, 2005; Huss et al., 2007).

The PPAR family is activated by fatty acids and upon activation induces transcriptional activation of genes encoding enzymes involved in fatty acid metabolism (Finck, 2007). There are three PPAR isoforms known to date, i.e PPAR α , PPAR β (also referred to as PPAR δ) and PPAR γ . The distribution of these isoforms is different in the various tissues where they are expressed (Kodde *et al.*, 2007). However, all three PPAR isoforms function as regulators of cardiac fatty acid metabolism (Neubauer, 2007).

PPAR α and PPAR β are highly expressed in the heart to regulate cardiac fatty acid metabolism, since fatty acids are the chief fuel substrate (Kodde *et al.*, 2007; An and Rodrigues, 2006). As a result, high intracellular fatty acid levels activates PPAR α and PPAR β to induce the expression of genes involved in fatty acid oxidation and cellular fatty acid uptake (An and Rodrigues, 2006). Additionally, PPAR α also reduces glucose utilization in the heart due to the inhibitory effects of high rates of fatty acid oxidation on glucose metabolism (Kodde *et al.*, 2007).

Therapeutically, PPAR β agonists e.g. L-168041 and GW 1516 have been documented to play an important role in the control of the metabolic syndrome (Grimaldi, 2007). For example, GW 1516 increased insulin sensitivity in genetically or diet-induced obese db/db mice (Liebowitz *et al.*, 2000). Furthermore, L-168041 and GW 1516 have also been reported to regulate atherosclerosis by increasing plasma HDL (high-density lipoprotein, generally referred to as the “good” cholesterol) levels in insulin resistant db/db mice and obese rhesus monkeys, respectively (Liebowitz *et al.*, 2000; Wang *et al.*, 2003b).

PPAR γ is highly expressed in adipose tissue and functions as a regulator of gene expression of genes involved in fatty acid storage and adipogenesis (Finck, 2007). Although, PPAR γ is not expressed to a sufficient extent in the heart, it may regulate fatty acid oxidation indirectly by reducing the circulating fatty acid levels and supply to the heart (An and Rodrigues, 2006). PPAR γ is the metabolic target of thiazolidinediones (TZDs), a group of metabolic treatment drugs that are administered to patients with type 2 diabetes mellitus (Petersen and Shulman, 2006). Figure 4 summarizes key functions of PPAR isoforms.

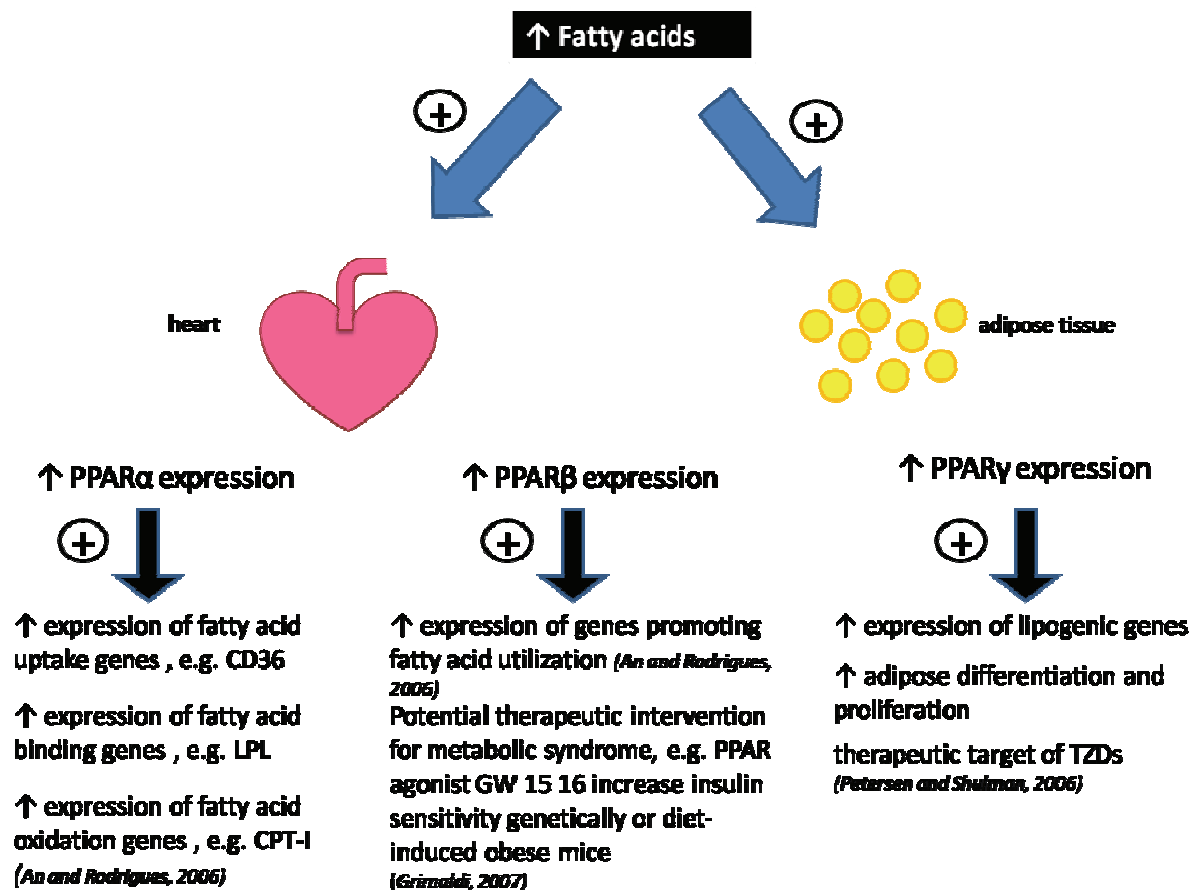


Figure 4. The PPAR isoforms. Fatty acids induce the expression of the PPAR isoforms in the specific tissues, e.g. PPARα and PPARβ expression in the heart and PPARγ expression in adipose tissue.

The ERR family belongs to a subfamily of orphan nuclear receptors, comprised of three members, i.e. ERRα, ERRβ and ERRγ (Huss and Kelly, 2005). Cardiac ERRα expression is dramatically increased following birth when the transition from glucose to fatty acids as primary energy source occurs. Furthermore, ERRα activity may be upregulated by PGC-1α, since its expression is also increased after birth (Finck and Kelly, 2007; Huss and Kelly, 2005; Huss et al., 2007). The nuclear-encoded transcription factor, NRF-1, is also a target of PGC-1α co-activation (Scarpulla, 2002). Co-activation of NRF-1 by PGC-1α initiates the transcription of genes that participates in mitochondrial oxidative phosphorylation, mitochondrial DNA transcription and mitochondrial biogenesis (Scarpulla, 2002).

In summary, optimal fuel substrate supply to the heart is an important component of its energy producing capacity. Fatty acids and carbohydrates are the main energy sources in the heart, but not mentioned is that ketones and amino acids may also act as energy fuels. Under physiological conditions, metabolic and signaling pathways that govern the breakdown and uptake of substrates are tightly regulated to match the heart's high energy demand. Not discussed in this section are alterations that occur in cardiac energy metabolism in response to pathophysiological states. For example, during myocardial ischemia the heart may switch to greater glucose utilization since it is a more O₂-efficient fuel to use when O₂ is limited (Stanley and Sabbah, 2005). Since the focus of my thesis is on the development of cardiac hypertrophy, I will now review this. The discussion will also refer to energy metabolism of the hypertrophied heart.

1.3 Cardiac Hypertrophy

Wang et al. (2003a) defined cardiac hypertrophy as “an adaptive response of the heart to hemodynamic overload, during which terminally differentiated cardiomyocytes increase in size without undergoing cell division”. Therefore, the adult mammalian heart is believed to be a post-mitotic organ, capable of growing only by increasing individual cardiomyocyte size but not cardiomyocyte number, and it does this a) during normal cardiac development, b) pregnancy, c) exercise and d) chronic hemodynamic overload (DeBosch et al., 2006; Chandrasekar et al., 2005; Czubyrt and Olson, 2004; Frey et al., 2004; Hunter and Chien, 1999; McMullen and Jennings, 2007; Sano and Schneider, 2005).

Phenotypically two types of cardiac hypertrophies that occur in response to alterations in pressure and volume loads can be distinguished (Frey et al., 2004; Hunter and Chien, 1999; Opie et al., 2006). Firstly, concentric hypertrophy caused by prolonged pressure overload is characterized by cardiomyocyte growth in width and the addition of sarcomeres in parallel (Dorn II, 2007; Frey et al., 2004; Hunter and Chien, 1999). Secondly, eccentric hypertrophy is stimulated by volume-overload. Here, cardiomyocytes grow in length due to the addition of sarcomeres in series (Dorn II, 2007; Frey et al., 2004; Hunter and Chien, 1999). Cardiac hypertrophy induced by pressure-overload is usually viewed as a “compensatory” response to preserve cardiac pump function but prolonged activation of these responses may increase the risk for heart failure development (Dorn II, 2007; Hill and Olson, 2008). In contrast, volume-overloaded hearts, e.g. the athlete’s heart, exhibit the “desirable” type of cardiac hypertrophy, i.e. reversible and does not lead to heart failure development (Berenji et al., 2005; Dorn II, 2007; McMullen and Jennings, 2007). However, cardiac hypertrophy is present in both athlete’s and hypertensive hearts, but what predicts the nature of the response may be the disturbance in extracellular matrix (ECM) activity (Brower et al., 2006; Miner and Miller, 2006). Historically, the ECM was viewed only as structural support for cardiomyocytes, but only more recently has it been discovered to be a “complex microenvironment” that participates in the remodeling of the myocardium (Spinale, 2007). In light of this, I will briefly review pathological and physiological hypertrophy to distinguish between these two phenomena.

1.3.1 Pathological cardiac hypertrophy

Pathological cardiac hypertrophy may be categorized into two stages, i.e. an early or “compensated” and a “decompensated” stage (Figure 5) (Czubryt and Olson, 2004).

The early stages of pathological hypertrophy is marked by an adaptive response of the heart to increase wall thickness in response to a specific stressor (e.g. hypertension and valvular heart disease) (Czubryt and Olson, 2004). This is usually irreversible and is accompanied by enhanced fibrosis (Czubryt and Olson, 2004; McMullen and Jennings, 2007; Zhu et al., 2007). This hypertrophic response is usually initiated by two major triggers, i.e. biomechanical stress and neuro-hormonal activation (Berenji et al., 2005; Hill and Olson, 2008). The precise mechanisms whereby biomechanical stress induces cardiac hypertrophy are still unclear (Berenji et al., 2005). However, it is thought that stretch-sensitive ion channels and integrins present on the sarcolemmal surface may be involved in conducting the biomechanical stress signaling in the heart (Berenji et al., 2005; Bökel and Brown, 2002; Hilfiker-Kleiner et al., 2006; Hill and Olson, 2008; Srivastava and Yu, 2006). Mechanical stress resulting from hemodynamic overload or altered cardiac functioning, promotes the secretion of neuro-hormonal factors such as angiotensin II (Ang-II) and endothelin-I (ET-I) (Czubryt and Olson, 2004; Frey and Olson, 2003; Heineke and Molkentin, 2006; Hill and Olson, 2008). These factors bind to specific transmembrane hepta-helical receptors to induce an intracellular hypertrophic signaling cascade (Heineke and Molkentin, 2006).

Ca^{2+} , an important regulator of cardiac excitation-contraction coupling in the normal heart, also participates in hypertrophic signaling when dysregulated (Bers, 2002; Chakraborti et al., 2007). Increased intracellular Ca^{2+} concentrations are a potent activator of the Ca^{2+} /calmodulin-dependent serine-threonine protein phosphatase, calcineurin (Wilkins et al., 2004). Calcineurin activity induces dephosphorylation of the transcription factors of the nuclear factor of activated T-cells (NFAT) family, leading to translocation of NFAT proteins to the nucleus where they initiate

transcription of hypertrophic genes (Frey and Olson, 2003). Prolonged activation of these compensated responses may result in the transition to decompensated hypertrophy (Diwan et al., 2008).

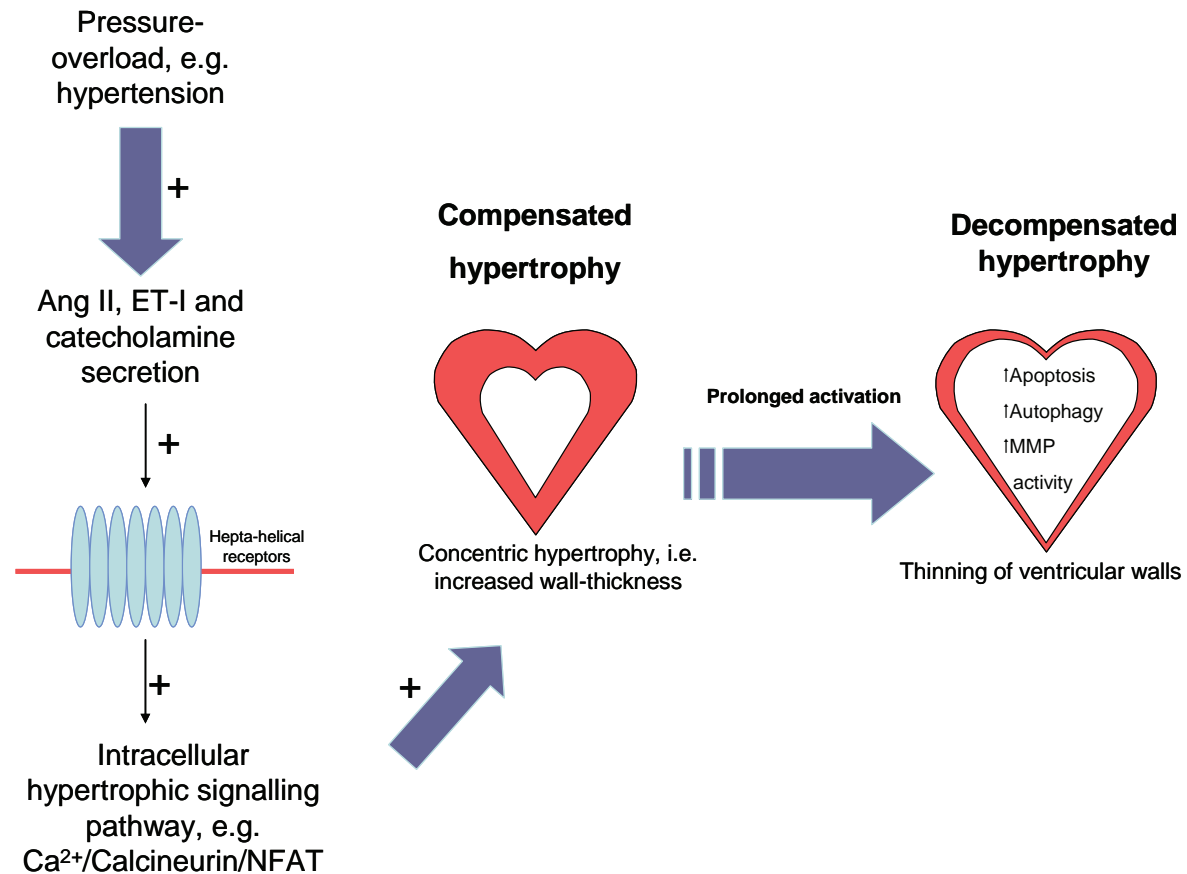


Figure 5. Schematic representation of events that may contribute to ventricular dilation, which is a risk factor for heart failure development. *Pathological cardiac hypertrophy may initially be described as compensatory when first initiated by a pathological stimulus, e.g. hypertension. In response to pressure-overload neuro-hormonal factors, e.g. angiotensin-II (Ang II), endothelin-1 (ET-1) and catecholamines, are secreted and binds to hepta-helical receptors on the sarcolemmal surface to induce an intracellular hypertrophic signaling response that will bring about compensated cardiac hypertrophy. However, prolonged activation of this compensatory pathway may have several detrimental effects on the heart, e.g. cardiomyocyte loss through apoptosis and autophagy, and break down of ventricular collagen by increased matrix metalloproteinase (MMP) activity. As a consequence, the ventricular walls become thin leading to dilated cardiomyopathy and predisposing to heart failure development.*

The heart is believed to undergo decompensated hypertrophy when it is unable to cope with the presenting pathological stimulus (Diwan and Dorn II, 2007; Dorn II,

2007). This is usually associated with reduced cardiac function and increased deposition of interstitial fibrosis (Frey et al., 2004). The transition from compensated to decompensated cardiac hypertrophy is associated with thinning of the ventricular walls resulting from various mechanisms for e.g. apoptosis, autophagy and ECM remodeling (Diwan et al., 2008; Spinale, 2007; Swynghedauw, 1999; Zhu et al., 2007).

Recent studies have shown that apoptosis and autophagy occur in response to hemodynamic stress (Diwan et al., 2008; Zhu et al., 2007). The loss of cardiomyocytes through these processes can be detrimental. Consequently, the synchrony and communication between adjacent cardiomyocytes are lost, causing unsynchronized heart beats (Duffy, 2008). The lost cardiomyocytes are replaced by fibrotic tissue, possibly due to increased Ang-II secretion (Opie et al., 2006). Only recently has it been discovered that angiotensin has receptors on fibroblasts, thereby inducing its fibrogenic effects (Swynghedauw, 1999). Resident cardiac fibroblasts are responsible for the production of two main fibrillar collagens, Type I and II, which maintains cardiac architecture (Miner and Miller, 2006). Therefore, increased collagen synthesis is associated with greater collagen production and enhanced myocardial stiffness (Swynghedauw, 1999). However, ECM remodeling is associated with the induction and activation of a family of endopeptidases, i.e. matrix metalloproteinases (MMPs) (Spinale, 2007). MMPs function to break down collagen leading to ventricular dilation. This causes decompensation of hypertrophy which may lead to dilated cardiomyopathies (Dorn II, 2007; Opie et al., 2006; Miner and Miller, 2006; Spinale, 2007; Swynghedauw, 1999).

Metabolically, the pathological hypertrophied heart is characterized by enhanced glycolytic metabolism as the source of ATP production (Leong et al., 2002; Ritchie and Delbridge, 2005). However, it is well known that the rate of glycolysis exceeds that of glucose oxidation in the pathologically hypertrophied heart (Leong et al., 2003; Lydell et al., 2002; Sambandam et al., 2002). The hypertrophied heart is therefore dependent on anapleurotic reactions since the pyruvate produced in the glycolytic pathway is not converted to acetyl-CoA (Kodde et al., 2007). Pyruvate produced via glycolysis has several destinations, e.g. a) carboxylated via pyruvate carboxylase to oxaloacetate, b) converted to malate by malic enzymes, c) transaminated with glutamine to form alanine and α -ketoglutarate and d) lactic acid under hypoxic conditions (Kodde *et al.*, 2007; Stanley et al., 2005). These citric acid cycle intermediates produced from pyruvate carboxylation and transamination will then replenish the citric acid cycle to replenish and help with energy production (Kodde *et al.*, 2007; Stanley *et al.*, 2005). It is well-recognized that cardiac function and metabolism are “extrinsically” linked (Taegtmeyer et al., 2005). However, recent studies have shown that pathological hypertrophied hearts exposed to periods of ischemia-reperfusion are worse off when compared to non-hypertrophied hearts (Allard, 2005; Sambandam et al., 2002). Moreover, the metabolic drug Trimetazidine, a partial inhibitor of fatty acid oxidation, stimulated glucose oxidation in pathological hypertrophied hearts following ischemia-reperfusion and thereby improved cardiac function (Saeedi et al., 2005).

This switch in fuel substrate from fatty acids to glucose in the pathological hypertrophied heart may partly be due to the reduced myocardial mitochondrial density coupled with the decrease in transcript levels of PGC-1 α , NRF-1 and PPAR α , key regulators of fatty acid oxidation and mitochondrial biogenesis (Goffart

et al., 2004; Scarpulla, 2002). At the gene level, the fetal pattern of gene expression manifests, resulting in upregulation of fetal genes (e.g. atrial natriuretic peptide/factor (ANP/F) and β -myosin heavy-chain (MHC- β) and downregulation of genes normally expressed in the adult heart (e.g. MHC- α and sarco/endoplasmic reticulum Ca^{2+} -ATPase) (Swynghedauw, 1999).

In summary, pathological cardiac hypertrophy is a complex process that occurs in response to hemodynamic overload. This increased pressure-overload will initially be the index event to a sequence of various detrimental steps that will ultimately lead to heart failure. Although, this form of cardiac hypertrophy occurs in two stages, therapeutic intervention can still be administered to prevent or slow heart failure development (Frey et al., 2004).

1.3.2 Physiological cardiac hypertrophy

This form of cardiac hypertrophy normally occurs during growth, pregnancy and exercise training, and is generally associated with volume-overload (Dorn II, 2007; McMullen and Jennings, 2007). At the cellular and molecular level, physiological hypertrophy is characterized by a proportional increase in myocyte length and width. As a result, normal sarcomeric organization, enhanced cardiac function and minimal change in cardiac gene expression patterns usually accompanies this condition (Hunter and Chien, 1999; Luo et al., 2005; McMullen et al., 2007). Most importantly, physiological cardiac hypertrophy is reversible and does not lead to dilation or heart failure development (McMullen and Jennings, 2007). Interestingly, cardiac fibrosis is absent in physiologically hypertrophied hearts (McMullen and Jennings, 2007).

The PI3-K/Akt signaling pathway is an important predictor of physiological cardiac hypertrophy and can be activated by growth factors (e.g. insulin or insulin-like growth factor-1 [IGF-1]) binding to receptor tyrosine kinases (RTKs) (Heineke and Molkentin, 2006). IGF-1 may be released in response to mechanical stress or exercise (Hill and Olson, 2008; Kemi et al., 2008). IGF-1 binds to the RTK receptor whereby it induces PI3-K/Akt signaling, causing an intracellular signaling cascade that promotes physiological cardiac growth (Figure 6) (Heineke and Molkentin, 2006; Luo et al., 2005).

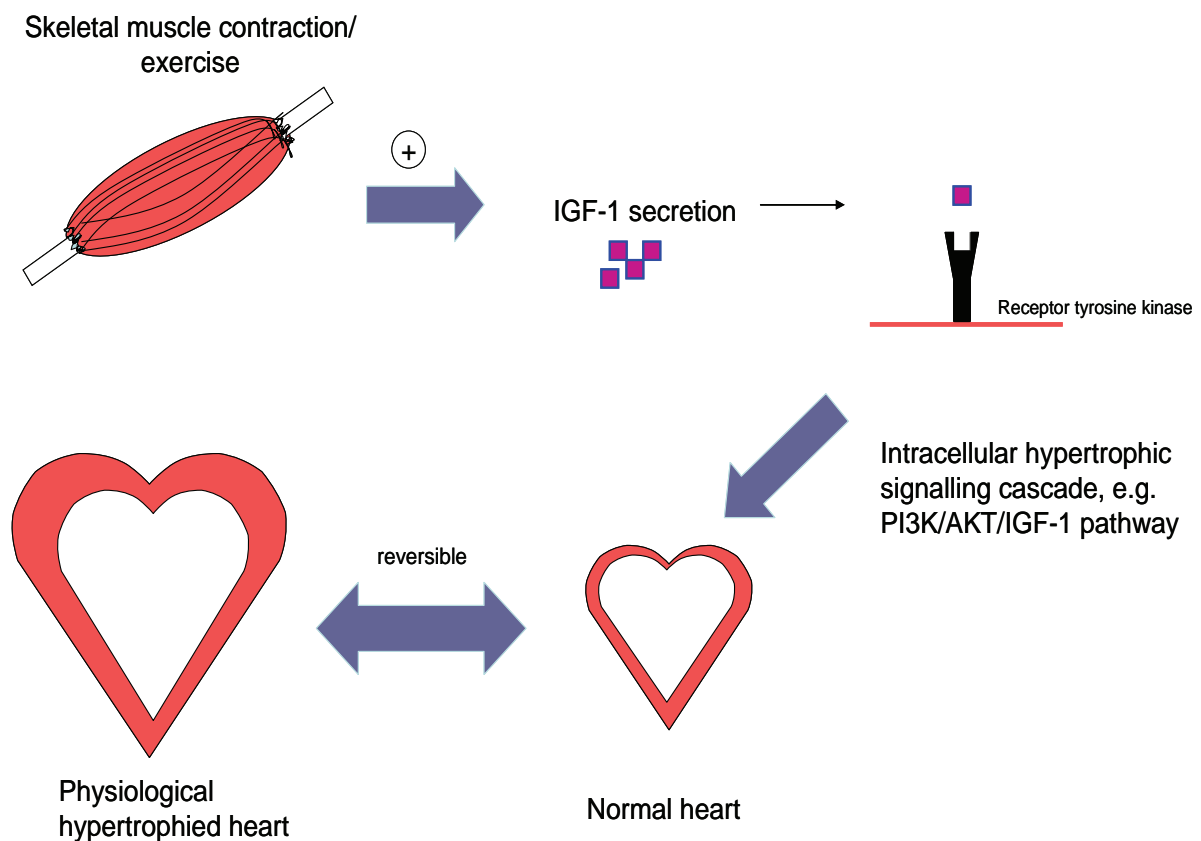


Figure 6. Physiological cardiac hypertrophy induced by IGF-1 secretion. *Exercise and mechanical stress are the main stimulators of insulin-like growth factor-1 (IGF-1) secretion. IGF-1 binds to plasma membrane receptor tyrosine kinases (RTK) to induce the PI3K/AKT pathway to stimulate physiological cardiac hypertrophy. Physiological hypertrophy is reversible and does not lead to the onset of heart failure.*

Metabolically, the physiological hypertrophied heart demonstrates increased rates of fatty acid oxidation, especially long-chain fatty acids including oleic and palmitic acid for energy production (Duncan and Finck, 2008; Finck and Kelly, 2007; Sambandam et al., 2002). This may be largely due to increased mitochondrial density that is associated with upregulation of PGC-1 α , NRF-1 and PPAR α (Goffart et al., 2004). In this setting, PGC-1 α plays an important role as a regulator of energy metabolism and activator of mitochondrial biogenesis to provide the necessary energy to the enlarged cardiomyocytes (hypertrophy) (Goffart et al., 2004). Unlike the pathological hypertrophied heart, glucose oxidation is increased in the physiological hypertrophied heart (Allard, 2005).

Physiological cardiac hypertrophy induced by hypobaric hypoxia

It is well-established that chronic hypobaric hypoxia exposure leads to cardiopulmonary remodeling (Hainsworth and Drinkhill, 2007). This includes for e.g. increased pulmonary hypertension and pulmonary vascular resistance resulting from hypoxic pulmonary vasoconstriction (HPV) and remodeling of the pulmonary arteries (Han et al., 2007; Hislop and Reid, 1978; Howell et al., 2004; Moudgil et al., 2005). Under physiological conditions the right ventricle (RV) is a highly compliant, thin-walled chamber when compared to the left ventricle (LV) (Klinger and Hill, 1991). In response to pressure-overload the RV increases in mass, i.e. hypertrophies to compensate for higher load to provide adequate blood supply to the pulmonary circulation (Pokreisz et al., 2007; Zungu et al., 2007). Moreover, exposure to chronic hypobaric hypoxia leads to increased erythropoietin (EPO) production, mainly in the kidneys (Savourey et al., 2004).

Right ventricular hypertrophy (RVH) may also occur in response to disease and is referred to as *cor pulmonale* (Klinger and Hill, 1991). For the purpose of this thesis, however, I will review RVH resulting only from hypobaric hypoxia conditions and not as a result of various disease states.

It has been recognized that physiological cardiac hypertrophy of the right side of the heart can be induced by hypobaric hypoxia or high altitude hypoxia (HAH) (Adroque et al., 2005; Cormo et al., 2002; Essop, 2007; Ostadal and Kolar, 2007; Rumsey et al., 1999; Sharma et al., 2004; Zungu et al., 2007). HAH has been recognized to have various cardioprotective effects which includes 1) reduced prevalence of myocardial infarctions in native high altitude dwellers ; 2) enhanced oxygen-carrying capacity of the blood; 3) remodeling of the pulmonary system, e.g. right ventricular hypertrophy (RVH) and 4) heightened adrenergic activity, hence, increased cardiac output (Hainsworth and Drinkhill, 2007; Kolar and Ostadal, 2004; Ostadal and Kolar, 2007). This increase in adrenergic activity can be initially viewed as being beneficial, especially during the early or moderate stage of heart failure, which is marked by a hyperadrenergic state that is activated in response to decreased pump function of the heart to preserve cardiac output and thereby allow for adequate oxygen and nutrient supply to all tissues (Essop and Opie, 2004). However, prolonged activity may be detrimental since this may lead to mitochondrial uncoupling.

The effects of chronic hypobaric hypoxia (CHH) on the RV have been studied in some detail before (Adroque et al., 2005; Sharma et al., 2004; Zungu et al., 2007; Zungu et al., 2008). Here the effects of varying lengths of hypobaric hypoxia exposure (e.g. 1-, 2-, 4-, 10- and 12-weeks) were investigated (Adroque et al., 2005; Sharma et al., 2004; Zungu et al., 2007; Zungu et al., 2008). For example, chronic

exposure to hypobaric hypoxia for 1-week resulted in alterations in expression patterns of metabolic genes involved in fatty acid and glucose oxidation as well as genes involved in cardiac functioning (Sharma et al., 2004). These authors found that key regulators of fatty acid metabolism, e.g. PPAR α and medium-chain acyl-CoA dehydrogenase (MCAD) were decreased in the RV but not in LV. Moreover, CHH exposure for 1-week resulted in no significant difference in regulators involved in glucose metabolism. For example, there was no change in GLUT1 and GLUT4 levels in both ventricles, whereas PDK-4 levels remained at baseline levels. Functionally, MHC- α and β remained unchanged in both ventricles following 1-week of CHH exposure, but SERCA 2a expression was decreased only in the RV (Sharma et al., 2004).

However, 2-weeks exposure to CHH resulted in increased PPAR α expression only in the RV, whereas MCAD expression was induced in both ventricles. At this experimental time point, glucose metabolic gene expression in the RV resembled that of the adult metabolic gene program, i.e. increased GLUT4, PDK-4 levels and decreased GLUT1 levels. In the LV, GLUT1 and GLUT4 levels remained unchanged whereas PDK-4 expression increased. Genes involved in cardiac function, e.g. MHC- α and β were increased in both ventricles, whereas SERCA 2a expression was only upregulated in the RV. Here, the researchers identified genes whose expression are influenced by pressure-overload, i.e. PPAR α , GLUT1, GLUT4 and SERCA 2a, versus hypoxia-treatment, i.e. PDK-4, MHC- α and β and MCAD.

In a later study, Zungu et al. (2007) demonstrated that cardiac contractile function and oxidative capacity was improved at 2-weeks of CHH exposure. For instance, mitochondrial state 3 respiration was increased only in the RV. The rate of ADP

phosphorylation and ADP/O ratio remained unchanged for both ventricles. Metabolically, this study demonstrated an increase in the right ventricular transcript levels of PGC-1 α and NRF-1 (Zungu et al., 2007), both important modulators that participate in mitochondrial fatty acid oxidation, glucose oxidation and mitochondrial biogenesis (Duncan and Finck, 2008; Finck and Kelly, 2007; Liang and Ward, 2006; Scarpulla, 2002). Mitochondrial DNA content was increased in the RV in accordance with the decreased levels of proton leakage. In the LV, mitochondrial DNA content and proton leakage remained unchanged. These changes were associated with functional adaptation of the RV, i.e. right ventricular developed pressure (RVDP). Together, the work done by Sharma et al., (2004) and Zungu et al., (2007) demonstrated that the adult metabolic-gene pattern is still expressed following 2-weeks of CHH exposure and that RV contractile and mitochondrial respiratory function was improved, respectively. Since there was also a lack of fibrosis in the RV (Sharma et al., 2004) and an “adult-like” expression of metabolic genes (increased fatty acid oxidation), these data suggest a model of right ventricular physiological hypertrophy.

A more recent study performed by Zungu et al. (2008) investigated the effects of CHH exposure at 4-weeks on the rat heart. Here they showed that the right ventricular hypertrophic response is associated with enhanced contractile and mitochondrial respiratory function at a late time point. These data therefore suggest that physiological hypertrophic response observed at the 2-weeks time point may be sustained at later time points, i.e. 4-weeks exposure.

1.4 Hypothesis

Although these studies suggest a robust model of physiological right ventricular hypertrophy, it is still unclear whether this adaptation is reversible or not. ***In light of this we hypothesized that chronic exposure to hypobaric hypoxia induces RVH but that attenuation of the chronic stimulus results in reversibility of the hypertrophic response (Figure 7). Therefore, we predict that increased RV mass, function and respiratory capacity will normalize following removal of the hypoxic stimulus.***

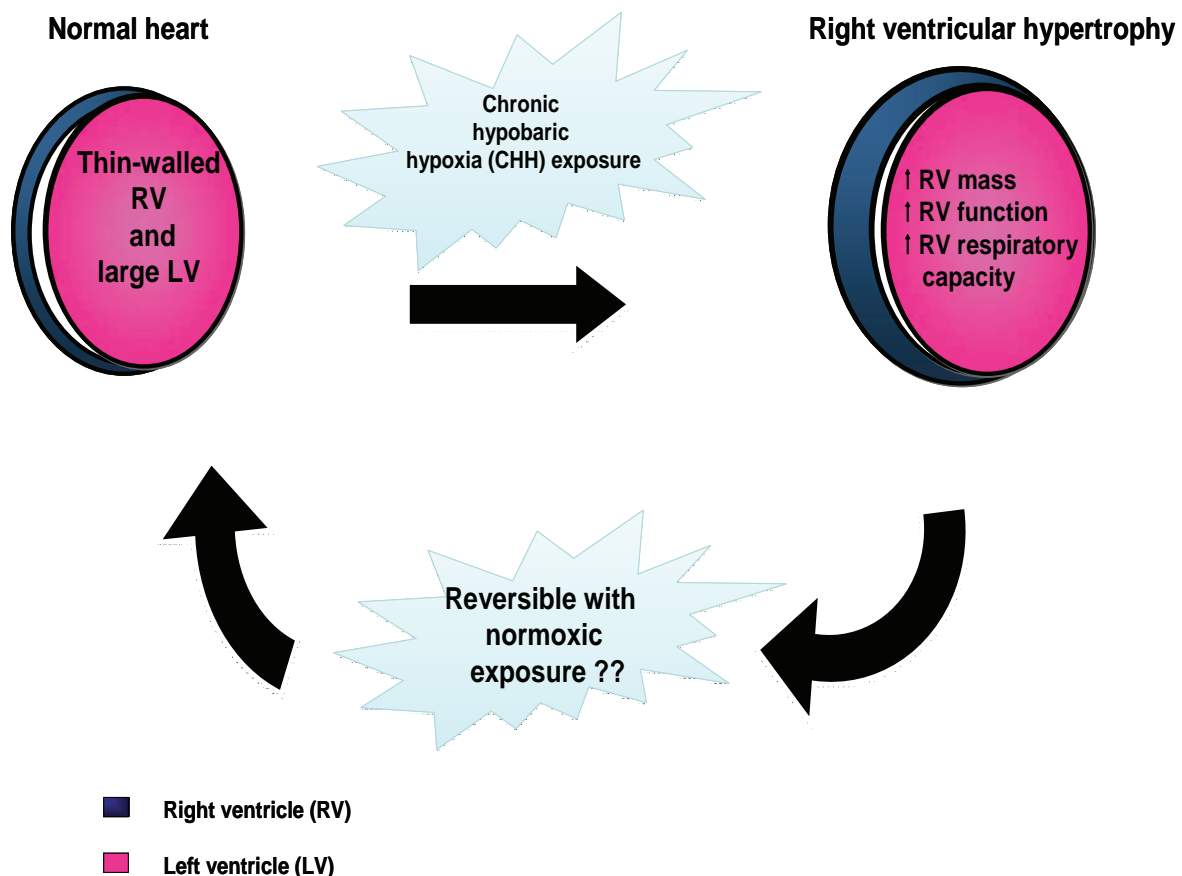


Figure 7. Description of hypothesis.

1.5 Aims

1. To investigate hypobaric hypoxia-induced right ventricular hypertrophy and assess functional parameters and mitochondrial respiratory capacity.
2. Assess whether hypoxia-induced right ventricular phenotype can be reversed upon normoxic exposure for 3- and 6-weeks, respectively.

Chapter 2

Materials and

Methods

2.1 Experimental design

In this study 3-month old Male Wistar rats (187.2 ± 3.1 g), were used. Rats were randomly assigned to either a hypoxic ($n=67$) or normoxic ($n=67$) group. The rats assigned to the hypoxic group were placed in an in-house developed hypobaric hypoxia chamber in which the air pressure was kept at 45 kPa ($\sim 11\%$ O_2).

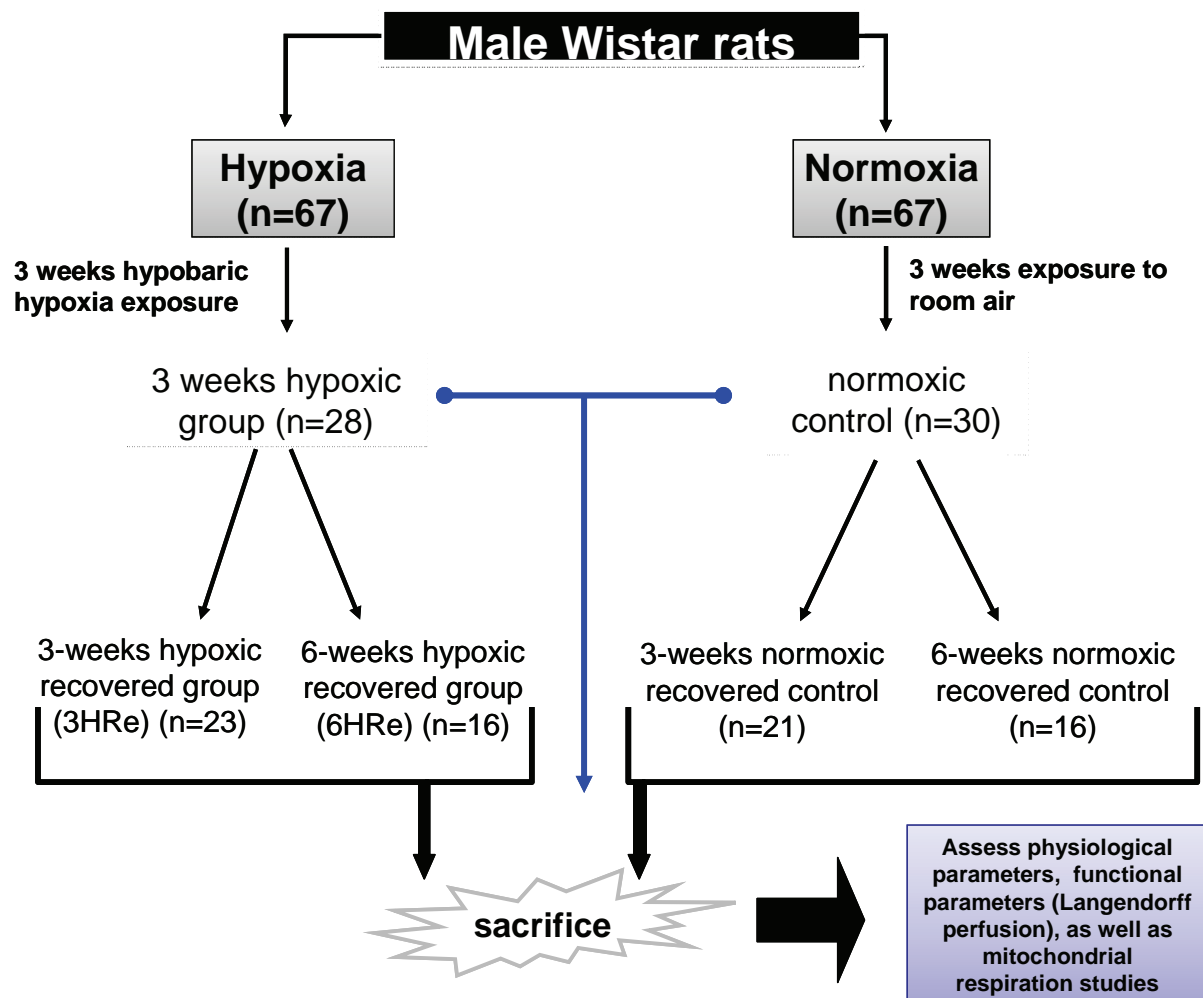


Figure 1. Experimental study design. In this study, three experimental groups were investigated a) a chronic hypobaric hypoxia (CHH) group, exposed to CHH for 3-weeks, b) a 3-week hypoxic recovered (3HRe) group, after CHH were exposed to 3 weeks of normoxia and c) a 6-week hypoxic recovered (6HRe) group, following CHH were exposed to 6 weeks of normoxia.

Animals in the hypoxic group were exposed to hypobaric conditions for a period of 3 weeks and compared to age-matched normoxic controls. For this study, we

investigated 3 experimental groups, i.e. a) chronic hypobaric hypoxia (CHH) group (n=28), were exposed to the hypobaric hypoxic environment for 3- weeks, b) 3-week hypoxic recovered (3HRe) group (n=23), were exposed to CHH for 3 weeks and allowed to recover in normoxia for an additional 3 weeks and c) 6-week hypoxic recovered (6HRe) group (n=16), were exposed to CHH for 3 weeks and allowed to recover for 6 weeks under normoxic conditions (Figure 1).

At the end of each experimental point, rats were sacrificed and heart tissue samples collected for mitochondrial respiratory studies. Blood was also collected from each group for metabolite analysis. Lastly, we dissected out intact hearts for *ex vivo* functional analysis.

The chamber was opened twice a week for no longer than 20 minutes for routine animal care, i.e. cleaning cages and providing fresh food and water. The matched control rats were kept in the same room as the hypoxic group but under normoxic conditions and were similarly handled as the hypoxic group. Experimental animals were kept on a 12-12h reverse light-dark cycle (lights off at 6AM Zeitgeber time [ZT12] and lights on at 6PM [ZT0]) and were generally sacrificed between ZT15 and ZT18, since they are more metabolically active during this time (Young, 2006). All experimental groups were allowed free access to standard rodent chow and water for the duration of the experiment.

2.2 Heart tissue collection

At the end of each experimental time point, rats were anaesthetized by pentobarbital sodium (100 mg/body weight, i.p) (see Appendix A). While sedated, animals were

weighed to determine final body weights. Rats were thereafter placed on a dissection board and the foot pinched to check for any nerve sensation. When no visible pedal reflex was observed, dissection was immediately initiated. Blood was collected directly from the *vena cava inferior*. The heart was rapidly excised, immediately placed on ice and connective tissue pieces carefully removed and hearts thereafter weighed. Atria were trimmed off and discarded. The right ventricle (RV) was dissected from the left ventricle plus interventricular septum (LV+S), and separately weighed.

2.3 Blood collection and hematocrit determination

Blood was collected via the *vena cava inferior* (as previously mentioned) for each experimental group described. Collected blood was centrifuged at 3,500 rpm for 15 minutes at 4°C in a refrigerated centrifuge (PK121R, ALC International, Milan, Italy). After centrifugation, plasma was collected and stored at -80°C and 2-8°C for further analysis (as presented in Figure 2).

Hematocrit levels were determined by collecting blood in heparinised capillary tubes (Marienfeld, Germany) followed by centrifugation at 100 xg for 3 minutes in a micro-hematocrit centrifuge (E2/12, Ecco, RSA) as previously described by Sharma et al. (2004). Following centrifugation, the total height of the sample and the height of the plasma column was determined by a micro-hematocrit reader (Hawksley, Great Britain) and expressed as a percentage thereafter.

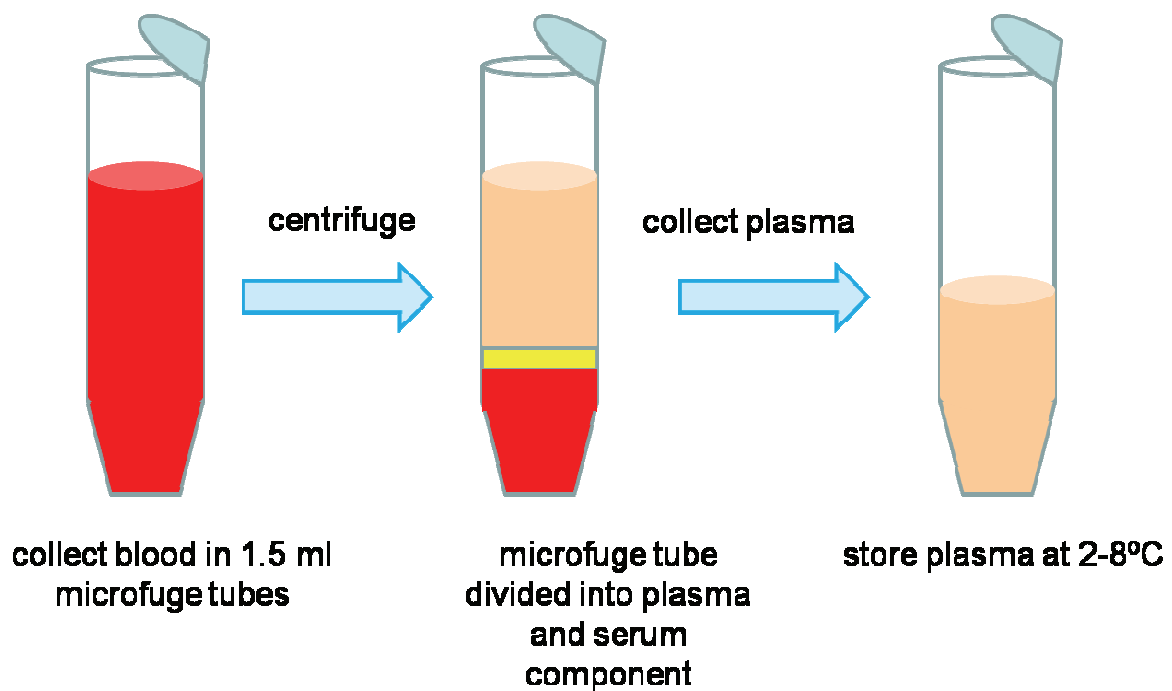


Figure 2. Diagrammatic illustration of plasma collection. *Blood was collected in 1.5 ml microfuge tubes and centrifuged at 3,500 rpm for 15 minutes at 4 °C. Plasma was collected and stored at 2-8 °C for metabolite analysis.*

2.4 Determination of plasma metabolite levels

Following blood collection, plasma glucose concentrations were rapidly measured using a hand-held glucometer (Accu-check active, Roche, Germany). A small drop of blood was placed on a disposable glucose test strip (Accu-check active, Roche, Germany) at a specific indicated region. The plasma glucose concentrations were calculated and immediately displayed as millimoles per liter (mmol/L). Triglyceride (TG) levels were also measured using a standard triglyceride reader (Accutrend GCT, Roche, Germany) and disposable TG strips (Accutrend triglycerides, Roche, Germany). Non-esterified fatty acid (NEFA) levels were determined using a commercially available colorimetric assay kit (Roche, Germany) by following instructions as detailed in the protocol booklet supplied by the manufacturer (see Appendix B).

2.5 Histological analysis

Following sacrifice, hearts were removed and rinsed with distilled water and placed in a fixative, i.e. formaldehyde. Fixation was the first step in a series of steps to prepare for subsequent microscopy as presented in Figure 3.

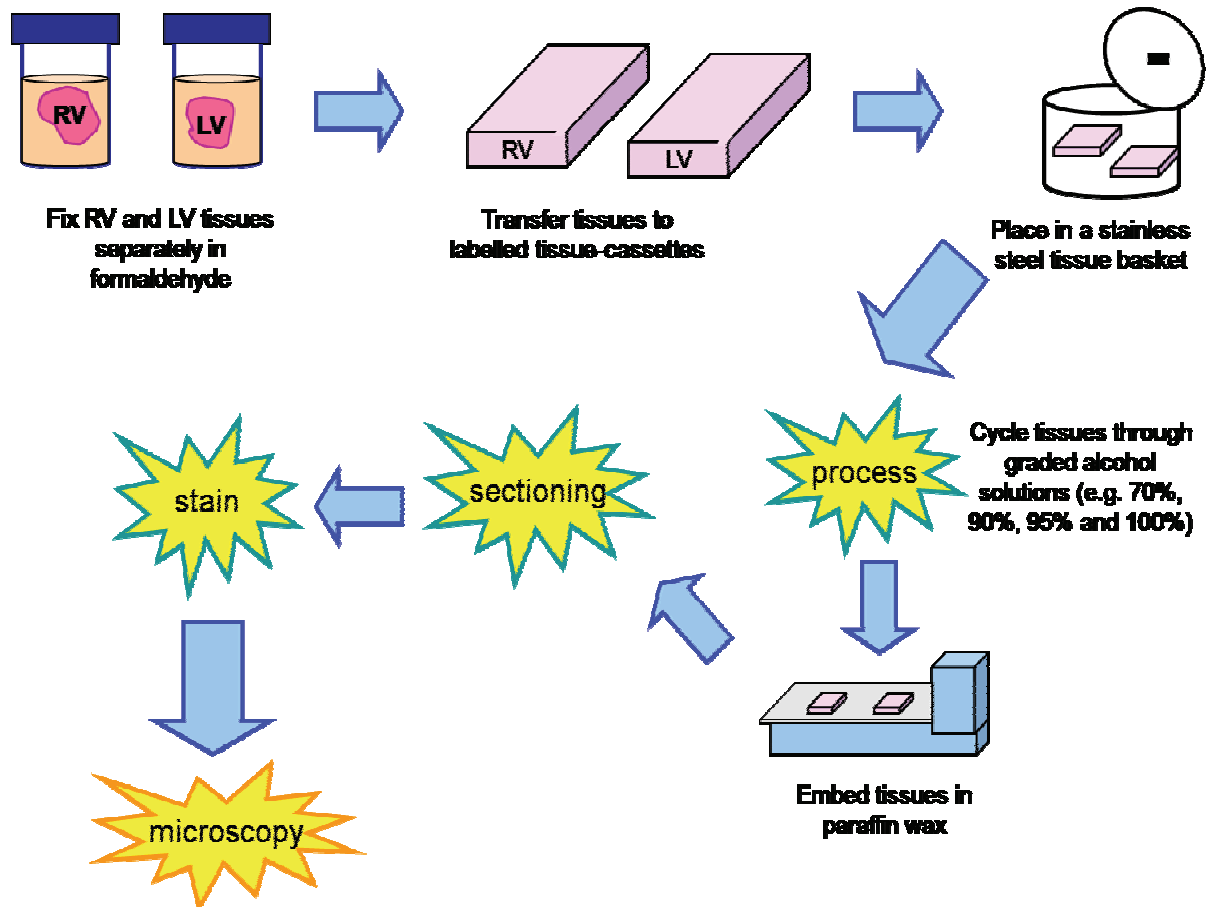


Figure 3. Schematic illustration of histo-analysis. Cardiac tissues were first fixed with formaldehyde, whereafter the tissues were put in tissue-cassettes to be process. After processing, tissues were embedded in paraffin wax to prepare for sectioning using a microtome. Slides were stained with H & E and Sirius red for microscopy.

Firstly, formaldehyde-fixed tissue samples were placed in labeled (marked with a lead pencil) plastic tissue-cassettes to prepare for subsequent tissue processing. Tissue processing is the embedding of fixed tissue in paraffin wax (WebPath, 2008). However, for this to occur all the water must first be removed from the tissue

samples, since water and paraffin are immiscible. This was accomplished using an automatic tissue processor (Tissue-Tek II, tissue processor, model 4634, Tokyo, Japan) that moves a basket filled with tissue-cassettes through different graded alcohol solutions (e.g. 70%, 90%, 95% and 100%) for 1½ to 2 hours each. This step is usually referred to as dehydration, i.e. removal of water from tissues (WebPath, 2008).

Following dehydration, tissues were cleared using xylene as a clearing agent, since it is miscible with paraffin. Note, that “clearing” of the tissue specimens is important because this allows for optimal infiltration with paraffin wax (National Diagnostics, 2005). Tissues were cleared in a 2 hour two-step process to prepare for subsequent impregnation with paraffin wax (Histosec pastilles, Embedding agent for histology, Merck Chemicals, Gauteng, S A). Both the clearing and impregnation steps were performed using the automatic tissue processor.

After processing, the tissues were placed in stainless steel cassette moulds (Tissue-Tek II, Tokyo, Japan) to form paraffin wax embedded tissue blocks. Here, a piece of tissue was placed in a cassette mould (in the correct orientation) and covered with wax. To ensure for proper structure, the bottom half of the tissue-cassette was positioned on top of the cassette mould and filled with wax. Thereafter, the cassettes were placed on a cold plate (Tissue Tek II, Tissue embedding centre, Tokyo, Japan) and allowed to set. Once set, the wax tissue blocks were ready for subsequent sectioning.

Tissue sectioning were performed by using a microtome (Heidelberg, Reichert-Jung, Austria). The microtome was first set at 20 microns to cut through the wax layer covering the tissue specimen. Thereafter, it was set at 5 microns for subsequent sectioning. Tissue sections were carefully lifted with a paintbrush and placed on a glass microscope slide. Here, the tissue was dampened with 50:50% alcohol-water solution to smooth out the creases before placing it in a preheated water bath (Optolabour, Reichert-Jung, Austria).

Additionally, warm water from the water bath was also used to flatten the section. The tissue section was floated onto the water bath before lifting it out with a poly-L-lysine (Sigma-Aldrich, St Louis, MO., USA) coated microscope slide. Poly-L-lysine was used as an adhesive to prevent section loss. Coated microscope slides were first dried in a fume cupboard or kept overnight before usage. When dry, the appropriately marked slide was used to gently remove the matched tissue section from the water bath. The slides were allowed to dry overnight on a preheated hot plate (Hospital and Laboratory supplies, London, UK) before subsequent staining.

Tissues were stained with routine haematoxylin and eosin (H & E) and Sirius Red to investigate cardiac fibrosis (see Appendix C and D for experimental procedure).

2.6 Evaluation of isolated cardiac mitochondrial function

Before commencement of respiratory experiments, the oxygraph systems were first calibrated for ± 10 minutes (see Appendix E) to ensure that the system is operating perfectly.

2.6.1 Mitochondrial isolation

Hearts were excised (as previously mentioned) and rinsed in ice-cold KH buffer. Atria and connective tissues were carefully removed. Thereafter, the RV was carefully dissected from the LV+S whereafter RV and LV+S were minced separately in petri dishes (Figure 4) containing 5ml potassium-EDTA (KE) buffer (0.18 M KCl, 10 mM EDTA, pH 7.4) on ice. RV and LV+S were separately homogenized in 10 ml hand-held glass Dounce homogenizers containing 10 ml KE buffer.

After homogenation, homogenates were transferred to 15 ml polypropylene conical tubes (BD Bioscience, USA) and centrifuged (Allegra™ X-22R centrifuge, Beckman Coulter, Germany) at 771 xg (~2,000 rpm) for 5 minutes (4°C). The resulting supernatant were filtered through 41 µm nylon mesh (Spectrum, USA) and thereafter centrifuged at 1,510 xg (~2,800 rpm) (4°C) to produce a brown-yellow pellet (mitochondria) at the bottom of the conical tube. The mitochondrial pellet was re-suspended in 50 µl KE buffer and vortexed for 10 seconds. Hereafter, mitochondrial protein concentration was rapidly calculated using a fluorometer (Qubit Invitrogen, Carlsbad, CA, USA).

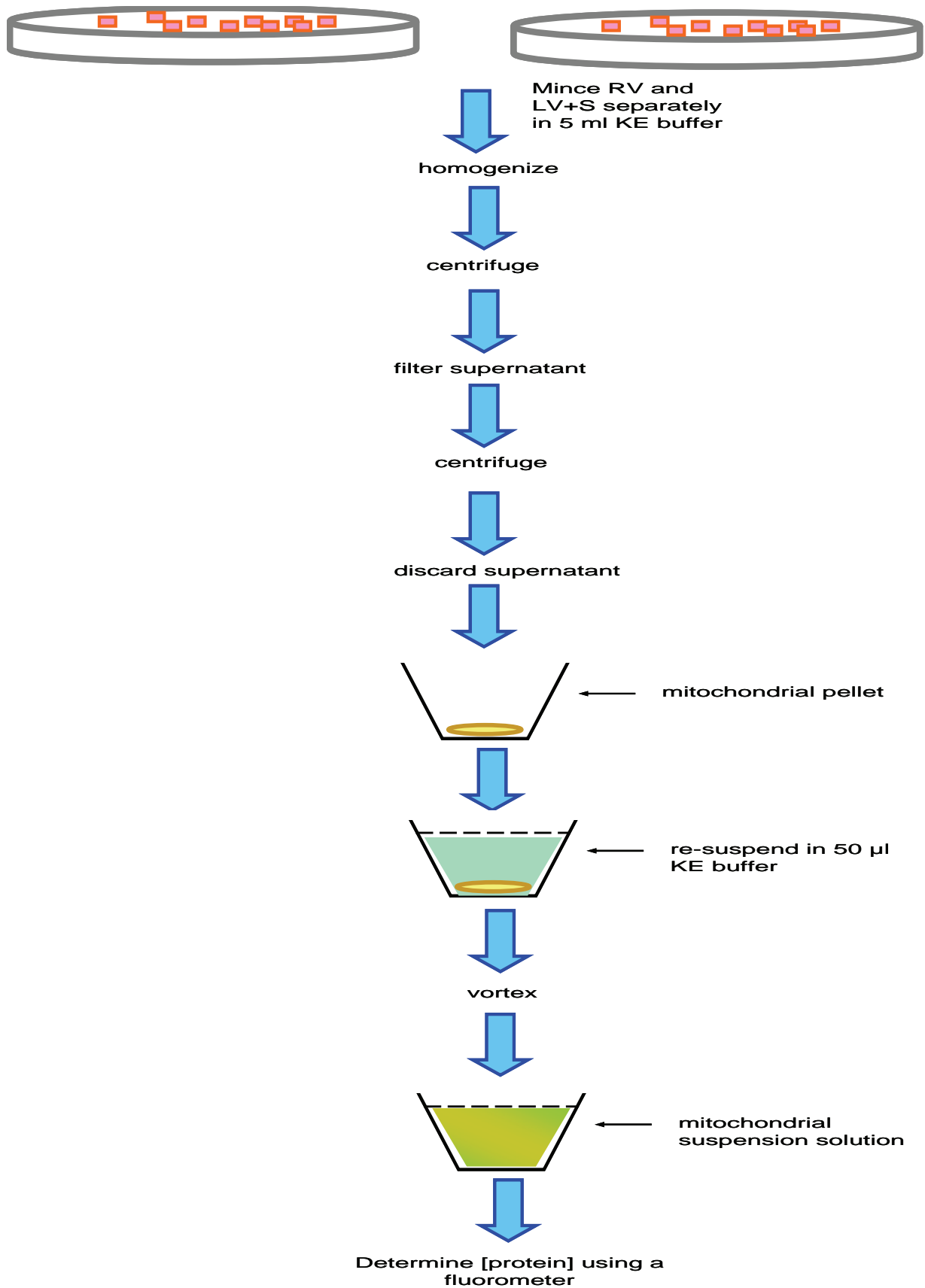


Figure 4. Mitochondrial isolation. *Ventricular mitochondria isolation were performed on ice and lasted only for 20 minutes.*

2.6.2 Mitochondrial function

Evaluation of mitochondrial function (O_2 consumption) was now immediately initiated and determined at 37°C using a Clark-type electrode (Hansatech Instruments, Norfolk, UK) with continuous stirring. The electrode prepared (Appendix E) was carefully secured (finger tight) in the oxygraph chamber thereby ensuring that a temperature of 37°C was maintained. Here, we used different combinations of oxidizable substrates to investigate glucose and fatty acid oxidation. These substrates include mixtures of a) 10 mM pyruvate plus 5 mM malate to investigate flux through pyruvate dehydrogenase, CAC and electron transport chain (Abel, 2004) and b) 40 μM palmitoyl-L-carnitine plus 5 mM malate to evaluate fatty acid β -oxidation.

Mitochondrial respiration was initiated following the addition of 25 μl of mitochondrial suspension to the electrode chamber. Respiratory measurements including state 3 was measured. State 3 (ADP-dependent) respiration was measured by adding 10 mM ADP to a final concentration of 350 μM in the electrode chamber. During this state, mitochondrial O_2 consumption was measured after the addition of ADP, since this state is also defined by phosphorylation of ADP to ATP.

All respiratory measurements were normalized to total mitochondrial protein content. Thereafter, the rates of oxygen consumption were expressed as $\text{nmol.O}_2.\text{min}^{-1}.\mu\text{g}$ protein. The experimental procedure to determine mitochondrial function is presented in Figure 5.

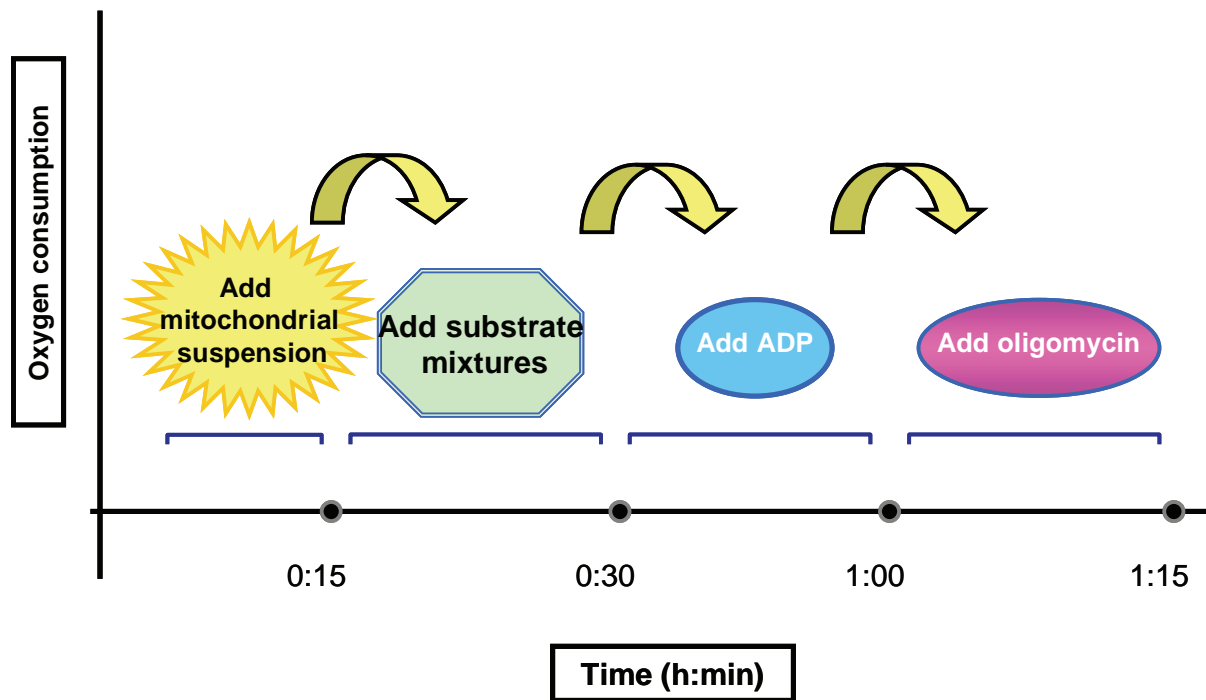


Figure 5. Evaluation of mitochondrial function. *Mitochondrial function was determined by adding various solutions to the electrode chamber at 15 min intervals.*

The respiratory control index (RCI), a ratio of State 3/State 4, was calculated and is regarded as a measure of the viability of the mitochondrial population and a value of 4 or more indicates successful mitochondrial isolation and actively respiring preparation.

2.8 Perfusion of isolated rat heart

Intact hearts were carefully removed and placed in ice-cold Krebs-Henseleit (KH) buffer (11 mM glucose, 118 mM NaCl, 25 mM NaHCO₃, 4.7 mM KCl, 1.2 mM KH₂PO₄, 1.2 mM MgSO₄·7H₂O, 1.8 mM, CaCl₂·6H₂O, pH 7.4). Once the aorta was located, the heart was transferred and cannulated onto the Langendorff perfusion apparatus (see Appendix F). The cannulated aorta was immediately tied with thread just under the aortic arch. Excess connective tissues were removed from the heart.

A retrograde perfusion of the aorta with KH buffer equilibrated with 95% O₂ and 5% CO₂ was initiated. During this mode of perfusion, the aortic valves are forced closed and the perfusion fluid moves through the coronary arteries to perfuse the entire cardiac muscle. To prevent ventricular edema, a small incision was made at the base of the aorta to relieve fluid build-up. A latex balloon connected to a pressure transducer (Powerlab/800, ADInstruments, USA) was inserted into the left atrium cavity and once in position, functional parameters were determined. This was also done for the right ventricle. Once the latex balloon was firmly in position, the heart was enclosed in a water jacket to maintain a proper working environment. The balloon was inflated with water to produce a diastolic pressure of 6-12 mmHg. Hereafter, the temperature was checked at regular intervals to ensure that the desired temperature of 37°C was maintained. The perfusion was performed at a constant hydrostatic pressure of 100 cm H₂O, thus ensuring a constant preload.

The Chart software package (ADInstruments, USA) was used to determine heart rate, systolic pressure, diastolic pressure, developed pressure, coronary pressure. Coronary flow was determined by collecting coronary effluent for 15 seconds. A 5-minute stabilization period was initially allowed, whereafter functional points were measured for a period of 30 minutes for both ventricles. Here, functional parameters were first measured in the left ventricle (for 30 minutes), followed by the right ventricle. The experimental procedure for determining cardiac function is shown in Figure 6.

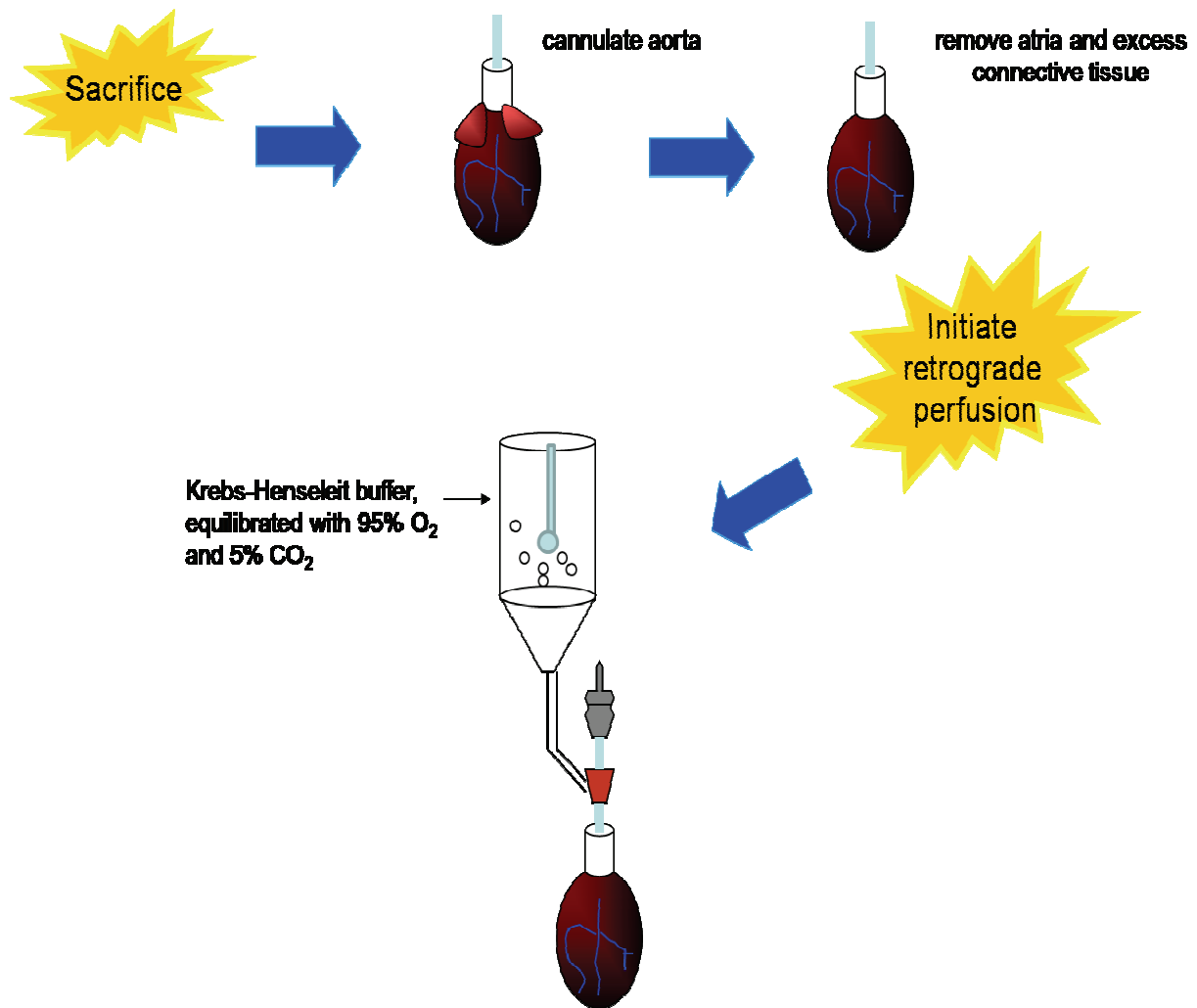


Figure 6. A simplified schematic illustration of the Langendorff heart perfusion system. The cannulated aorta was perfused in the retrograde mode with Krebs-Henseleit buffer (95% O₂, 5% CO₂) at a constant hydrostatic pressure of 100 cm H₂O and functional parameters i.e. heart rate, systolic pressure, diastolic pressure, developed pressure, coronary pressure were measured

2.9 Statistical analysis

All Statistical analyses were performed by using the Statistica version 8.00 (Statsoft Inc., Tulsa OK) and the Graphpad InStat version 3.01 (GraphPad Software Inc., San Diego CA). H&E histological stains were quantified using Simple PCI version 5.2.1 (Compix Inc., Imaging systems, USA). Sirius Red histological stains were quantified using ImageJ version 1.41o, National Institute of Health, USA). Data were analyzed

using a student's t-test to determine the difference between experimental and matched control groups. Repeated measures one-way analysis of variance (ANOVA) and one-way ANOVA followed by the Bonferroni post-hoc test were performed to analyze functional data. A p-value of <0.05 was considered statistically significant. All data are represented as mean \pm standard error of the mean (mean \pm SE).

Chapter 3

Results

3.1 Effects of chronic exposure to hypobaric hypoxia

Hypobaric hypoxia exposure, albeit intermittent or chronic, have been reported to induce an increase right ventricular size, promoting right ventricular hypertrophy (RVH) (Kolar and Ostadal, 2004; Ostadal and Kolar, 2007). This hypertrophic response is mainly due to the developing pulmonary hypertension, since left ventricular mass is unchanged (Sharma et al., 2004). Chronic hypobaric hypoxia (CHH) exposure may induce various physiological alterations or adaptations to the presenting stressor, including a) decreased body mass, b) altered ventricular weights and c) elevated hematocrit levels (Tanaka et al., 1997).

3.1.1 *Body weight (BW)*

To test our hypothesis, we exposed rats to 3 weeks of CHH followed by recovery in normoxia for a period of 3- and 6-weeks respectively. Here, we found that in response to 3 weeks of CHH exposure, BW was dramatically decreased in comparison with matched controls (311.13 ± 6.1 vs. 269.81 ± 6.3 , $p < 0.05$). To test whether these findings are reversible, rats were exposed to 3- and 6-weeks normoxia, respectively. At both normoxia-recovery time points, it was evident that BW increased. However, the increase in BW observed in the 3HRe (387.2 ± 9.0 vs. 317.3 ± 8.3 , $p < 0.001$ vs. matched controls) and 6HRe group (425.9 ± 7.8 vs. 377.92 ± 7.2 , $p < 0.01$ vs. matched controls) did not match that of their controls.

As indicated in Figure 1, increases in body weight occurred at a slower rate in the hypoxia-recovery group and did not catch up to control levels.

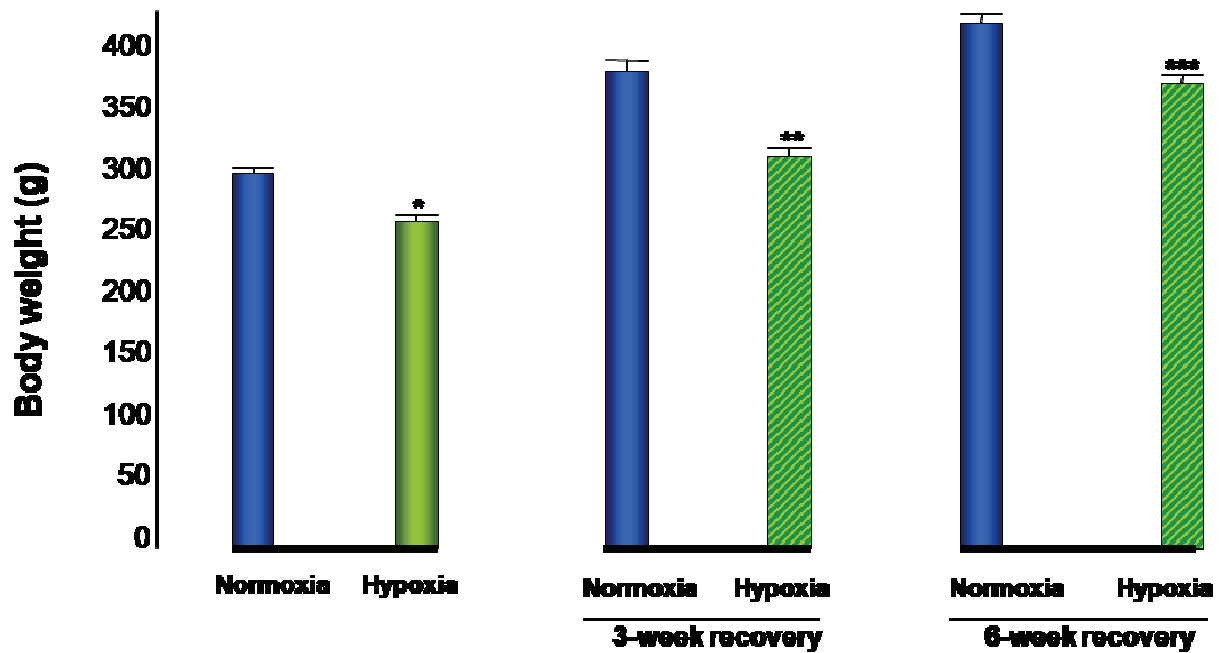


Figure 1. Effects of CHH and normoxia recovery on body weight. *CHH exposure resulted in a decrease in body weight and persisted during the recovery period. * p<0.05, ** p<0.001 ***p<0.01 vs. matched control.*

3.1.2 Morphological characteristics

We investigated the increase in RV mass in relation to the LV+S. After 3-weeks adaptation to CHH RV to LV+S ratio were increased (223.5 ± 7.03 vs. 397.4 ± 29.8 , $p<0.001$ versus normoxic controls). When allowed to recover in normoxia for 3-weeks, RV to LV+S ratio was still increased but to a lesser extent, i.e. (244.7 ± 11.2 vs. 349.64 ± 3.8 , $p<0.001$ versus normoxic controls) (Figure 2). This increase was still evident at the 6-week recovery point, 269.3 ± 14.03 vs. 333.9 ± 11.7 , $p<0.0001$ vs. matched controls.

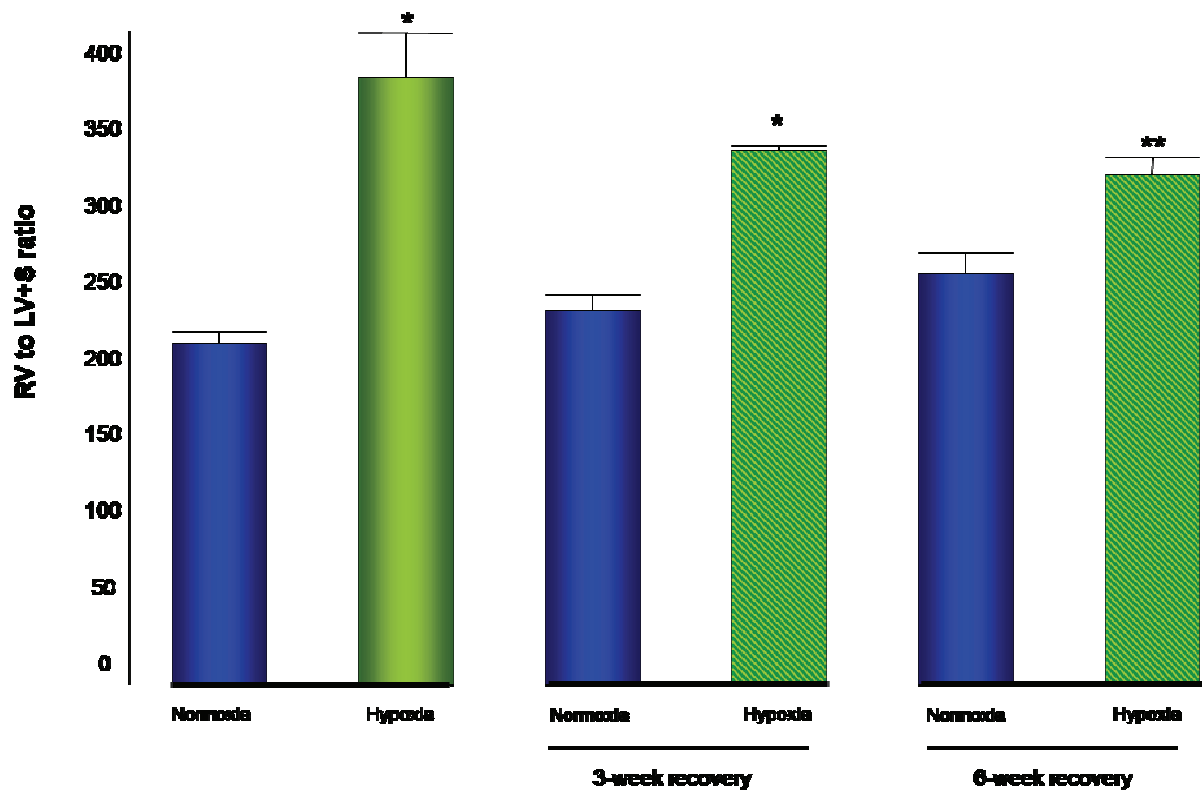


Figure 2. Regression of right ventricular hypertrophic response after normoxic exposure. All values are represented as means \pm SE. RV to LV+S ratio was significantly increased with CHH exposure. This hypertrophic response was still present following recovery for 3- and 6-weeks, respectively. * $p < 0.001$ and *** $p < 0.0001$ vs. matched controls.

In agreement with our hypothesis, CHH exposure induced a significant increase in RV to BW ratio (0.53 ± 0.01 vs. 0.93 ± 0.064 , $p < 0.001$). However, this response was lower (0.54 ± 0.03 vs. 0.77 ± 0.01 $p < 0.005$ vs. normoxic controls) after 3-weeks of normoxic recovery. Although RV to BW ratio gradually normalized, it was still increased following 6-weeks of normoxia recovery (0.58 ± 0.03 vs. 0.77 ± 0.05 , $p < 0.05$ vs. normoxic control).

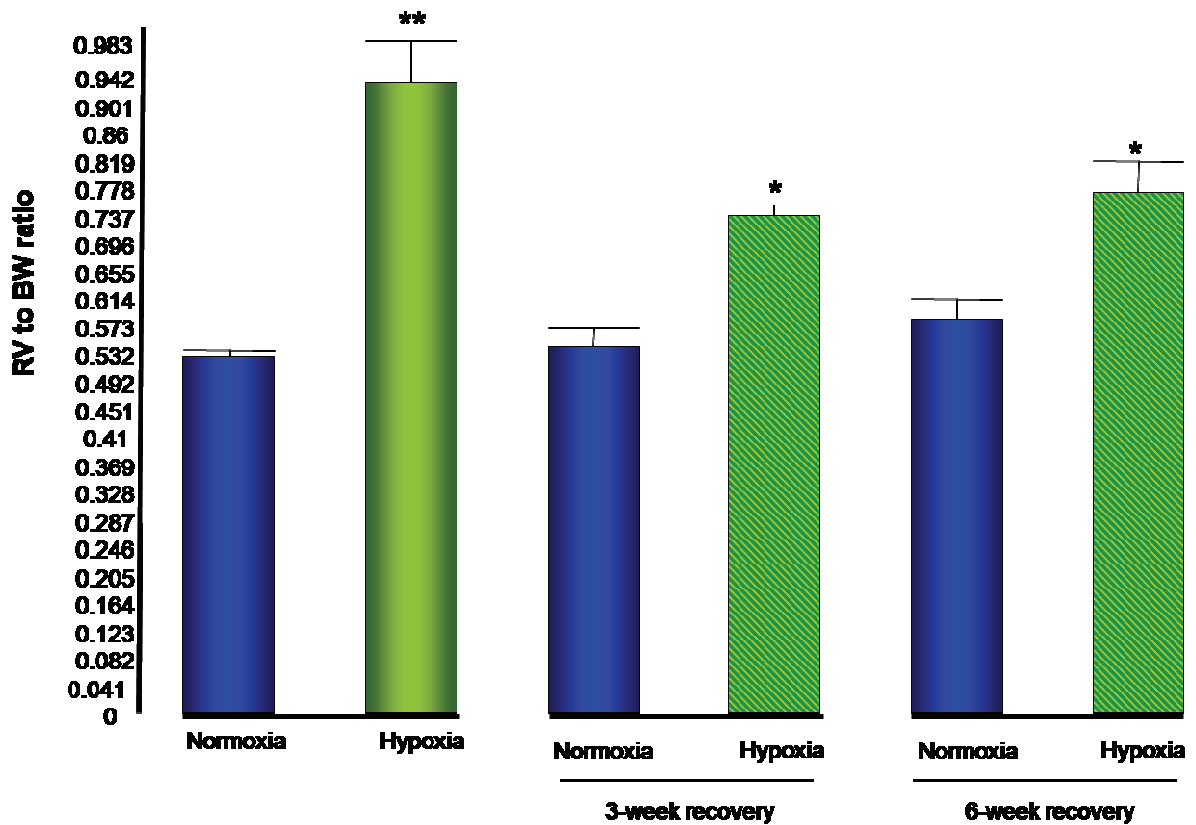


Figure 3. Regression of right ventricular hypertrophic response after normoxic exposure. *RV to BW ratio was determined to investigate the increase in right ventricular size following CHH exposure and recovery in normoxia. All values are represented as means ± SE. * $p < 0.001$ and ** $p < 0.05$ versus matched controls.*

In support of this hypertrophic response in the RV, we observed no significant difference in the LV to BW ratio between experimental animals and their matched normoxic controls, thereby indicating that the hypertrophic response is due to the developing pulmonary hypertension (Figure 4).

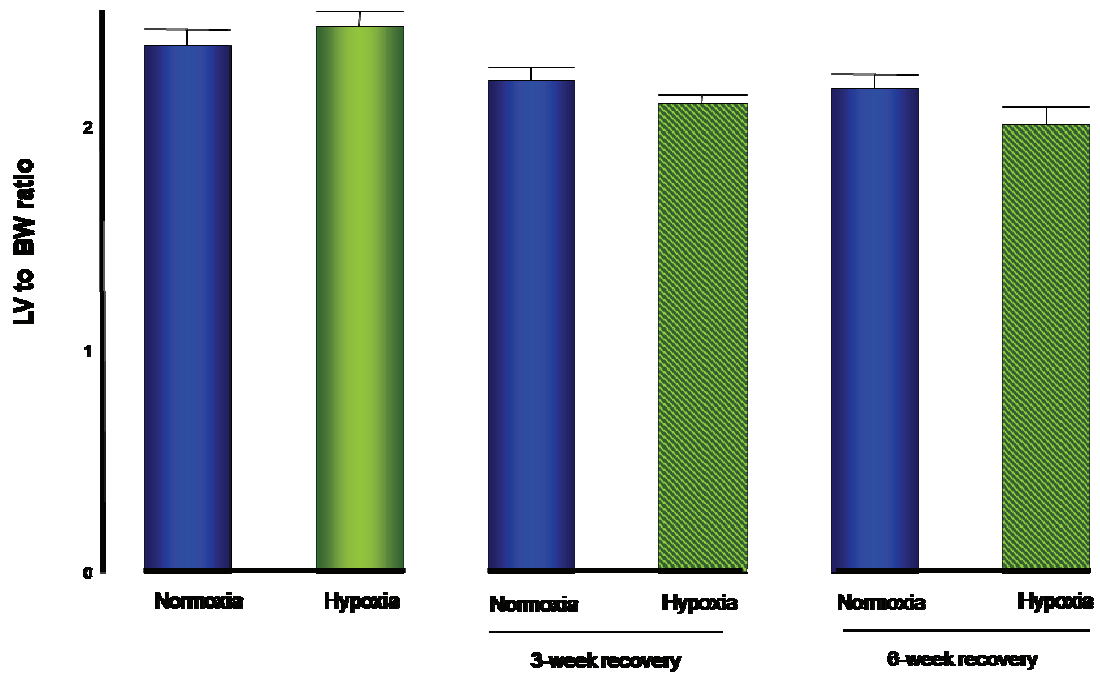


Figure 4. Unaltered LV to BW ratio in response to experimental conditions. *To investigate whether the left ventricle (LV) was altered by hypoxia-treatment, the LV to BW ratio was determined. The LV to BW ratio remained unchanged between experimental groups. All data are represented as means \pm SE.*

3.1.2 Physiological parameters

It is well known that CHH exposure leads to elevated hematocrit levels (Savourey et al., 2004; Tanaka et al., 1997). In this study, we found that in response to CHH exposure, hematocrit levels were significantly increased (42.67 ± 0.7 vs. 60.25 ± 1.6 , $p < 0.001$ vs. age-matched normoxic controls) to compensate for the reduced oxygen supply (Figure 5). However, hematocrit levels were completely normalized following recovery in normoxia for 3- and 6-weeks, respectively (Figure 5).

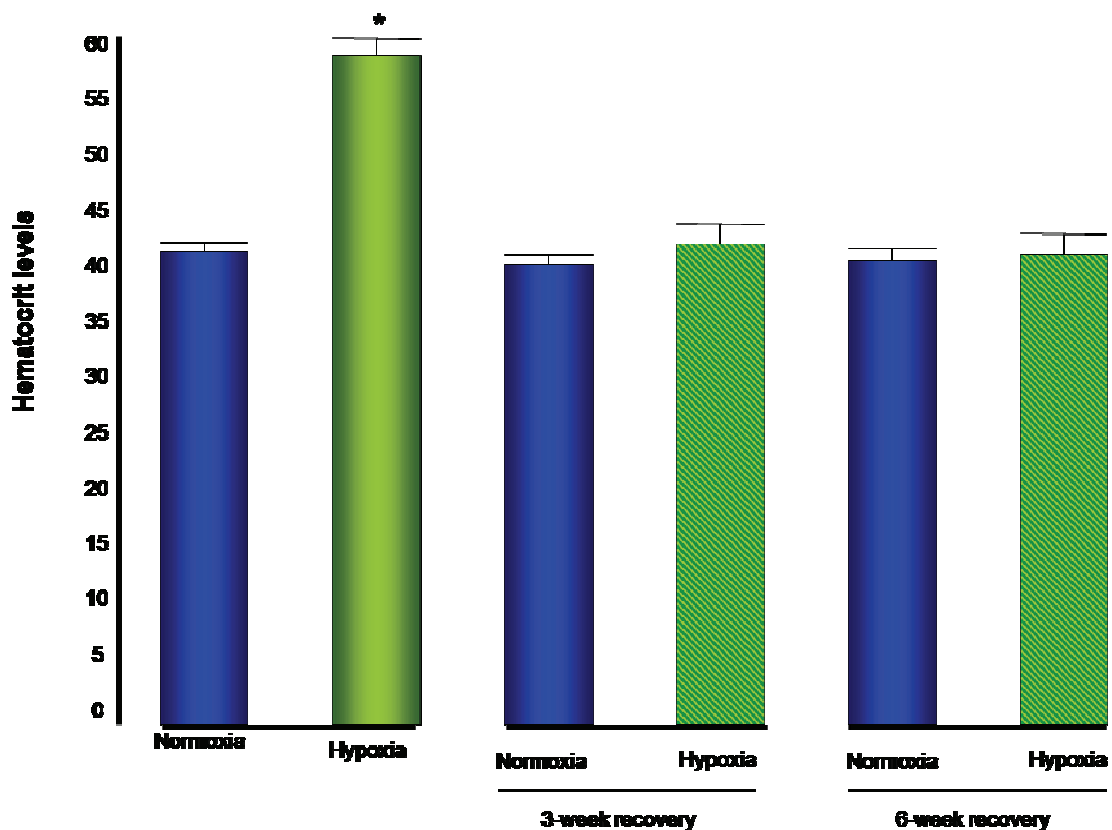


Figure 5. Complete regression of hematocrit levels after 3- and 6-weeks of normoxia. CHH exposure induced a significant difference in hematocrit levels of the hypoxia group. However, following 3- and 6-weeks recovery hematocrit levels were normalized. All values are represented as means \pm SE. * $p < 0.001$ vs. matched controls.

3.2 Histo-analysis to investigate cardiac fibrosis

In our study, we hypothesized that the changes brought about by CHH exposure is reversible, thereby proposing that this may be a model of physiological cardiac hypertrophy. Normally, physiological hypertrophy is characterized by the absence of fibrosis. Therefore, we investigated cardiac fibrosis by performing both routine H&E stains and a stain specific for collagen, i.e. Sirius Red. We assessed the increase in cardiomyocyte size by measuring the diameter across the nucleus. Although this is

not the preferred method, we employed this technique to gain some insight regarding hypertrophy. In the future, cardiomyocyte diameter will be evaluated .

Presented in Figures 6 H&E histological data show that CHH increased RV cardiomyocyte size increased in comparison with their matched controls. This increase persisted after 6-weeks normoxia-recovery (Figure 7).

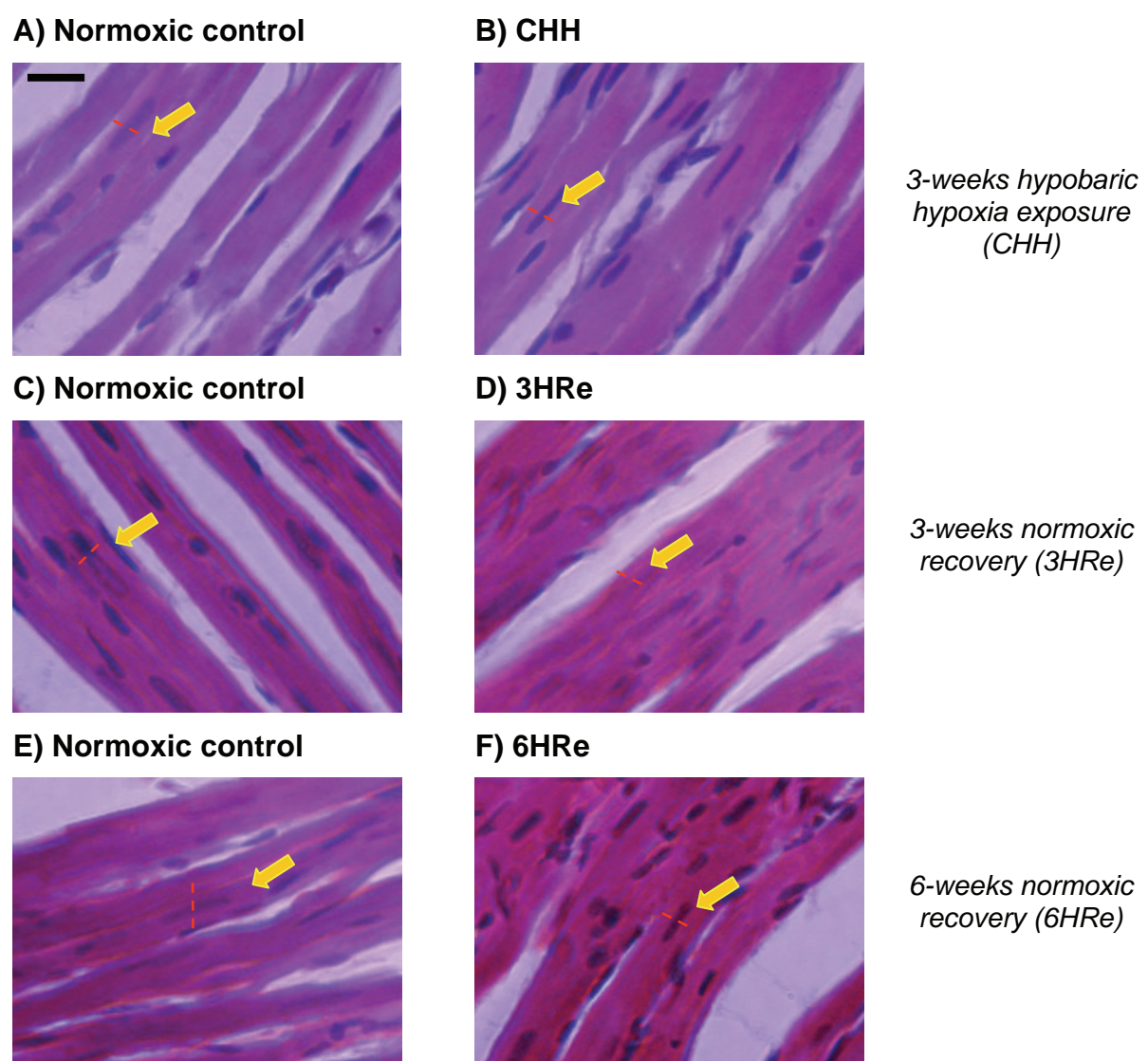


Figure 6. H&E stained histological sections at different experimental time points. In these stains, the difference in cardiomyocyte diameter of the RV induced by hypobaric hypoxia exposure versus normoxia exposure is clearly distinguishable. Magnification = 40X.

Scale bar = 5µm. Indicates how diameter was measured.

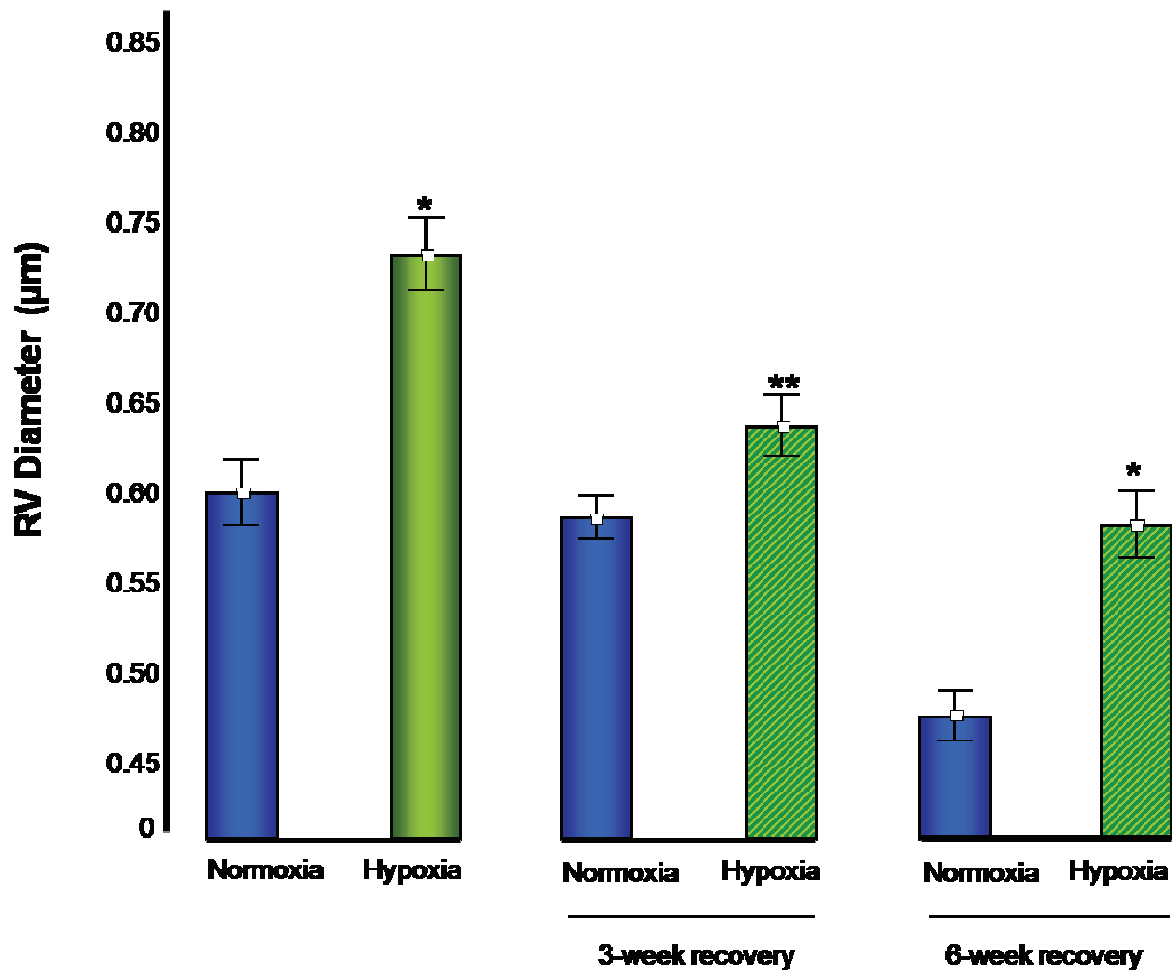
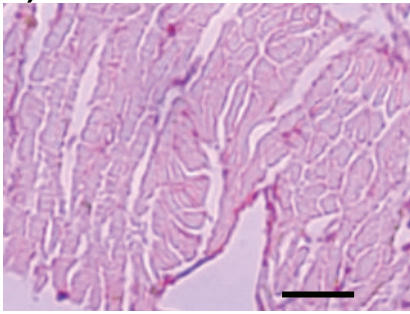


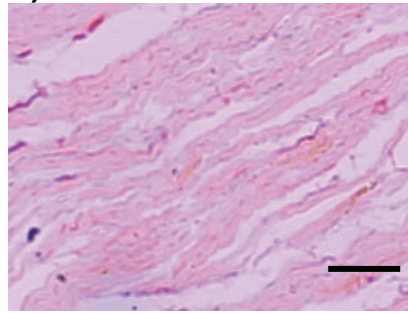
Figure 7. Evaluating regression of right ventricular cardiomyocyte size after normoxic exposure. *CHH exposure induced a 20.51 ± 2.58 % increase in right ventricular cardiomyocyte size. After recovery in normoxia for 3-and 6-weeks respectively, right ventricular cardiomyocyte size did not regress. * $p < 0.0001$ and ** $p < 0.002$ versus matched controls.*

We employed a stain specific for collagen, e.g. Sirius Red. Here we found that the amount of collagen calculated was the same in both the control and experimental groups (see Figures 8 and 9). This observation further supports our hypothesis, i.e. that this is a physiological model of RVH.

A) Normoxic control

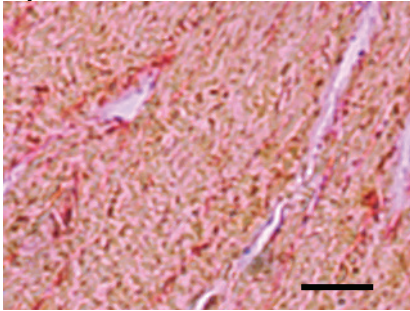


B) CHH

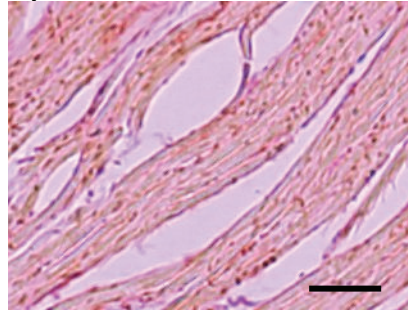


3-weeks hypobaric hypoxia exposure (CHH)

C) Normoxic control

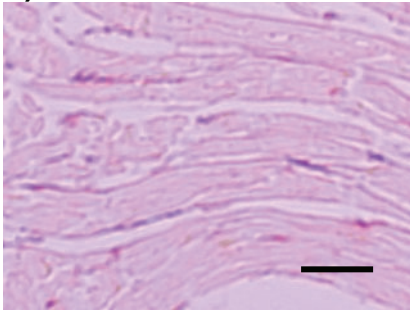


D) 3HRe

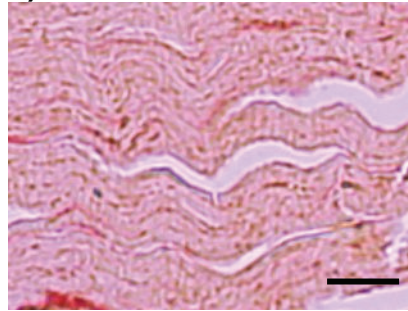


3-weeks normoxic recovery (3HRe)

E) Normoxic control



F) 6HRe



6-weeks normoxic recovery (6HRe)

Figure 8. Sirius red staining demonstrates lack of fibrosis. *The degree of fibrosis was calculated by measuring the amount of red stain surrounding cardiomyocytes. Magnification=10X. Scale bar  = 200 μ m.*

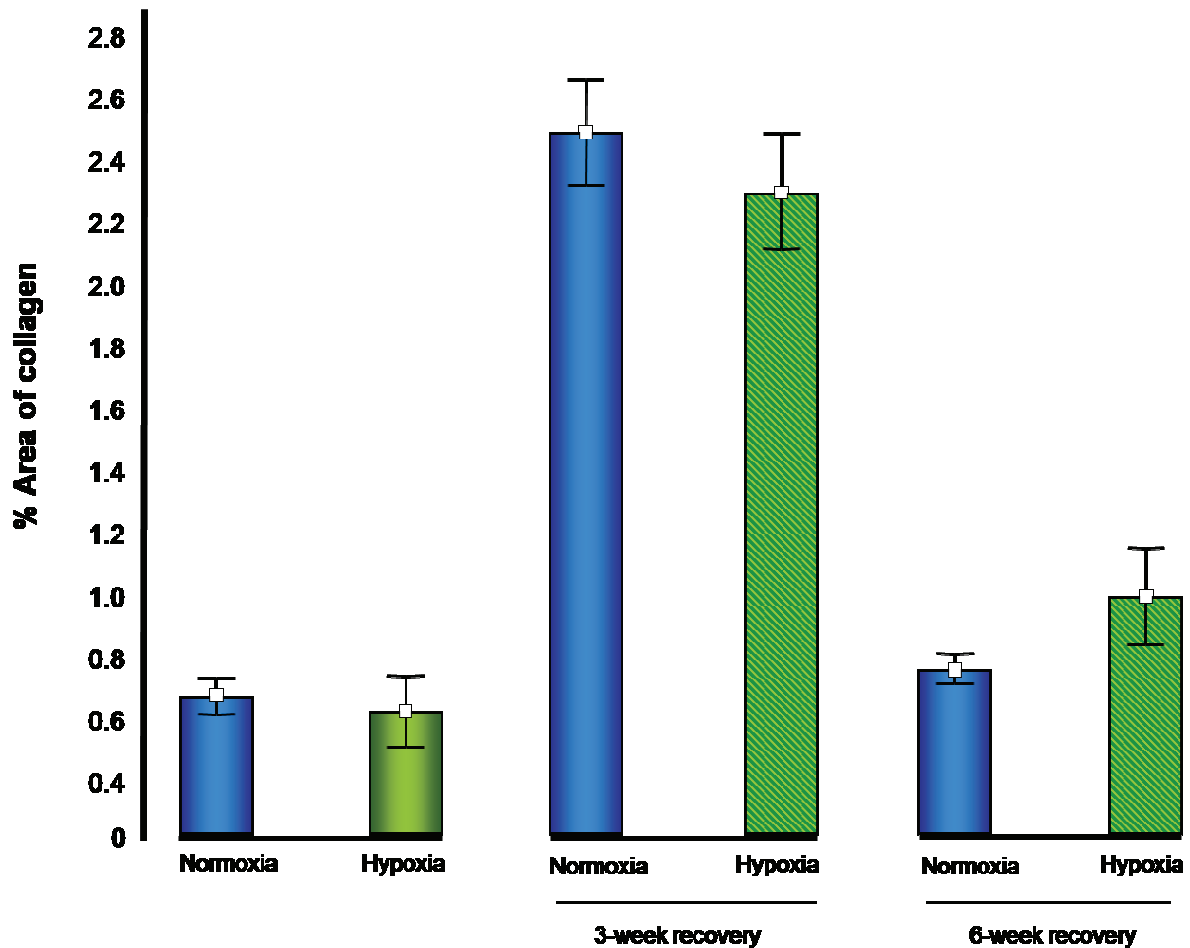


Figure 9. Fibrosis remained unchanged for both experimental and control groups. *CHH exposure induced no change in collagen composition after 3-weeks in the hypoxic environment. This remained constant until the 6-week recovery point.*

3.3 Plasma metabolite levels

To further investigate our hypothesis we determined plasma glucose, plasma TG and NEFA levels.

For the hypoxia-treated animals, plasma glucose levels remained relatively low, when compared to matched normoxic controls (11.25 ± 1.52 vs. 5.67 ± 0.3 mmol/L, $p < 0.001$). However, following 3- and 6-weeks recovery, respectively, there was no significant difference between the 3HRe and 6HRe groups versus their matched normoxic control groups (Figure 10).

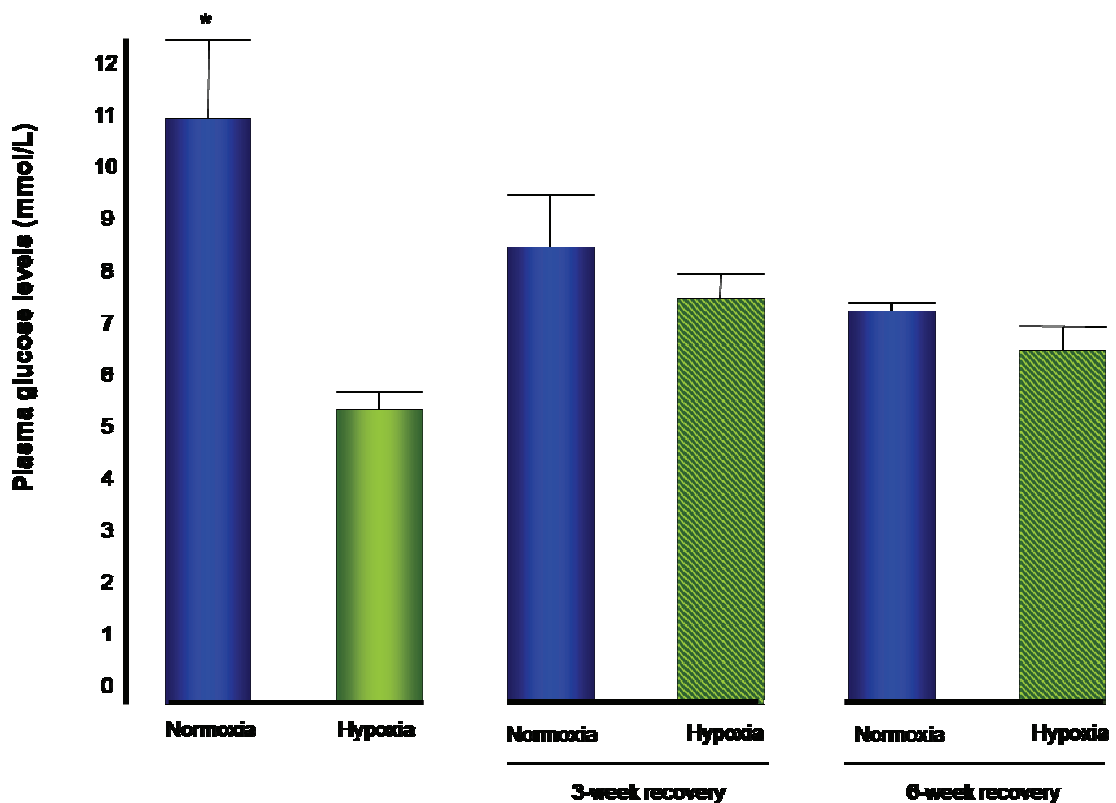


Figure 10. Plasma glucose levels normalize following normoxic exposure. *CHH* exposure resulted in a significant decrease in plasma glucose levels. However, plasma glucose levels were normalized following 3- and 6-weeks recovery, respectively. All values are represented as means \pm SE.

* $p < 0.005$ versus matched controls.

In view of this, we investigated plasma TG and NEFA levels to provide clues whether fatty acid utilization may be increased during CHH. Surprisingly, TG levels remained unchanged in the CHH and 3HRe groups versus controls (Figure 11). However, plasma TG levels in the 6HRe group were increased when compared to matched controls (1.15 ± 0.1 vs. 1.66 ± 0.2 mmol/L, $p < 0.005$). Our preliminary data show that NEFA levels were not dramatically altered in response to CHH. Moreover, the 6HRe show a large increase in NEFA levels, although more samples need to be tested to generate statistically valid data.

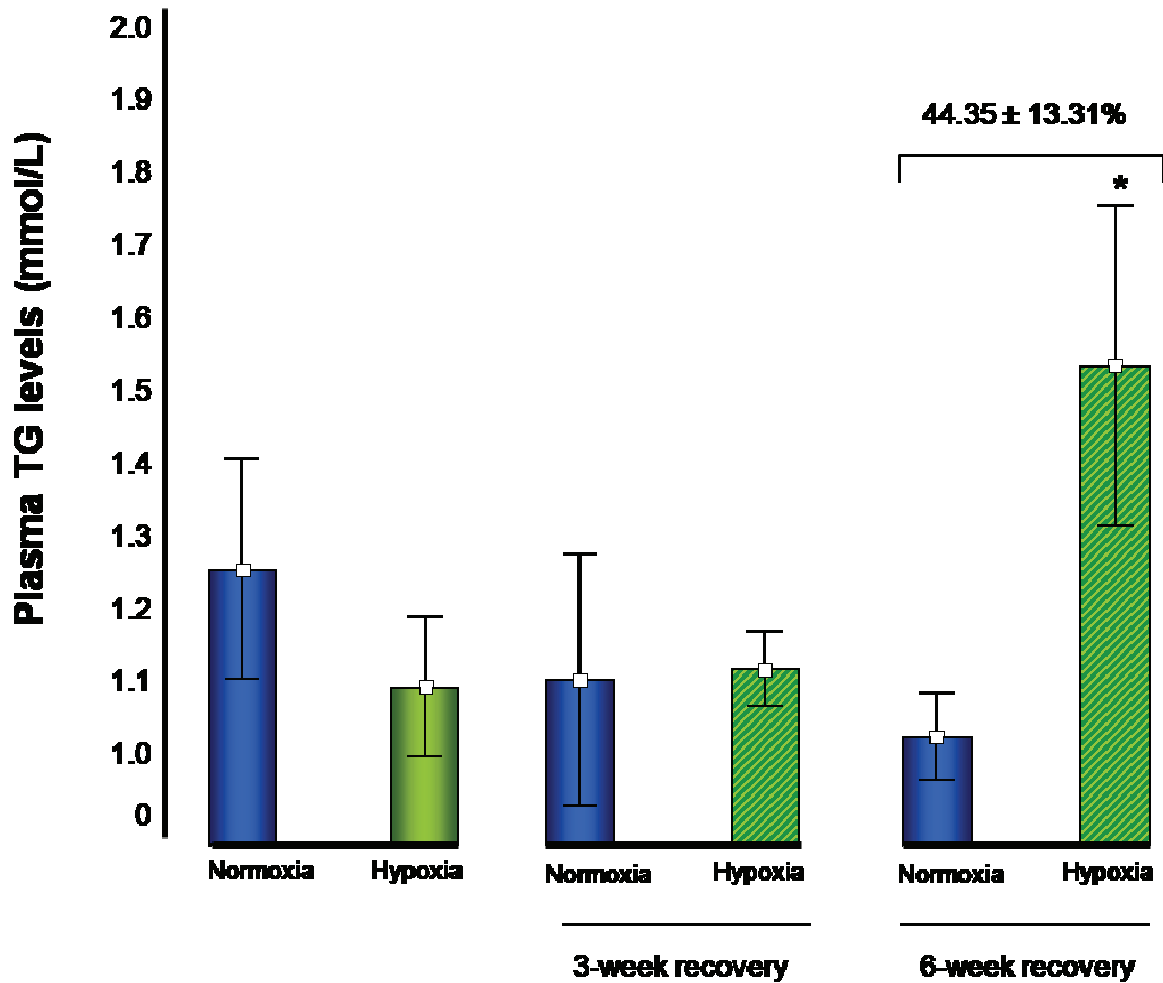


Figure 11. Increased TG levels after 6-weeks normoxic exposure. *CHH exposure did not result in significant difference in TG levels. However, the 6HRe groups displayed an increase in TG levels compared to controls. All values are represented as means \pm SE. * $p < 0.005$ versus matched controls.*

3.4 Mitochondrial respiration

To investigate mitochondrial respiratory capacity, we measured state 3 respiration using carbohydrate and fatty acid fuel substrates, respectively. This technique was rather new to me and part of setting up new techniques.

With pyruvate as substrate, we found no significant difference in RV state 3 respiration in response to CHH (Figure 12). However, the 3HRe group displayed

higher rates of pyruvate utilization when compared to normoxic controls ($p < 0.04$ vs. matched controls). When a fatty acid fuel substrate was employed, we found that RV state 3 respiration remained unchanged in the CHH and 3HRe group (Figure 13). However, at the 6-week recovery point fatty acid utilization was dramatically increased (Figure 13). These changes in mitochondrial substrate utilization were not observed for the LV (Figures 14 and 15). We only investigated state 3 respiration, since method in process of being setup. Other mitochondrial parameters were not measured since this technique was fairly new to me, but will be assessed in the future.

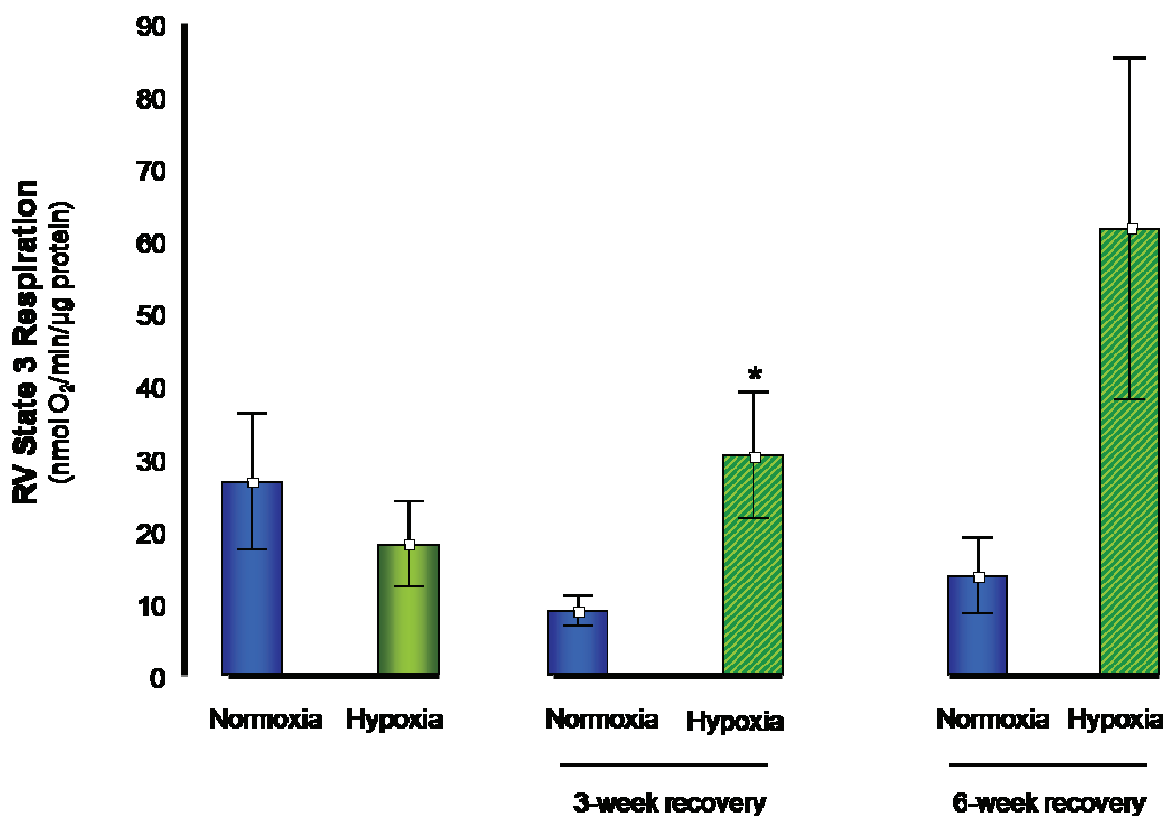


Figure 12. Effects of CHH on mitochondrial respiratory capacity-pyruvate.

*Pyruvate utilization was increased at the 3-week recovery point. * $p < 0.04$ vs. matched controls.*

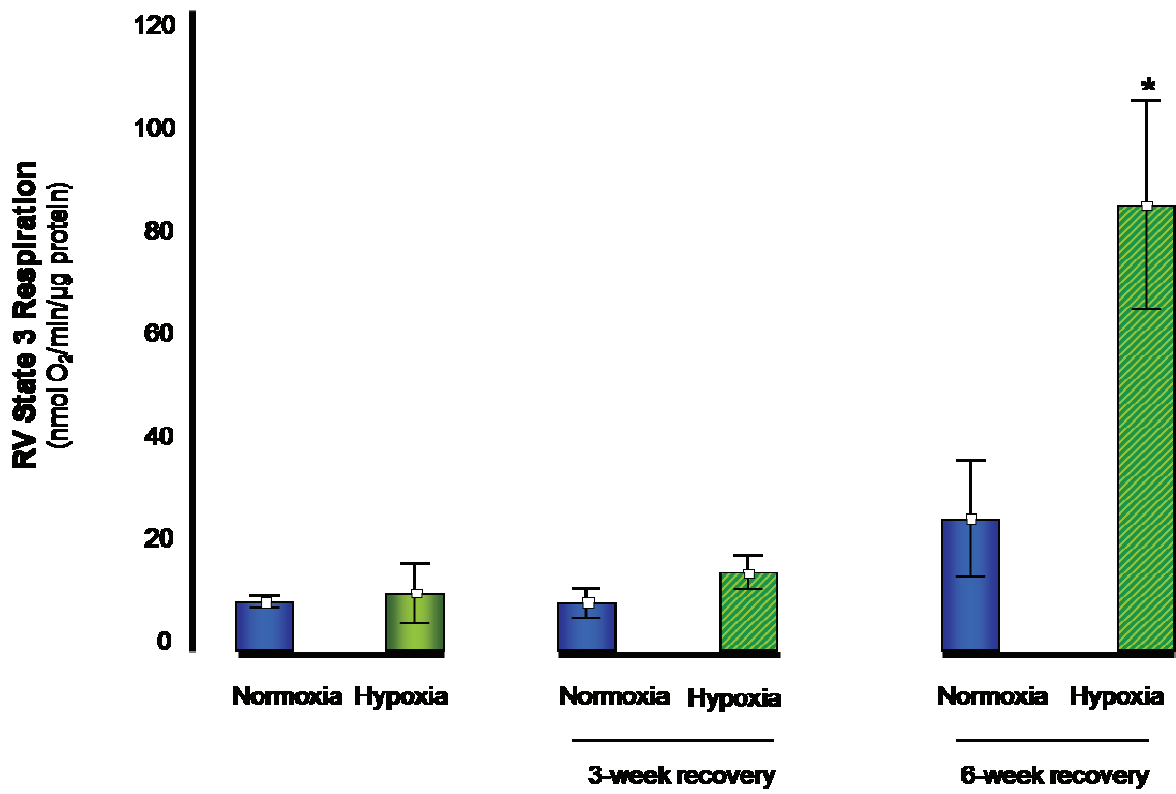


Figure 13. Effects of CHH on mitochondrial respiratory capacity-palmitoylcarnitine. Palmitoyl carnitine utilization was increased at the 6-week recovery point. * $p < 0.03$ vs. matched controls.

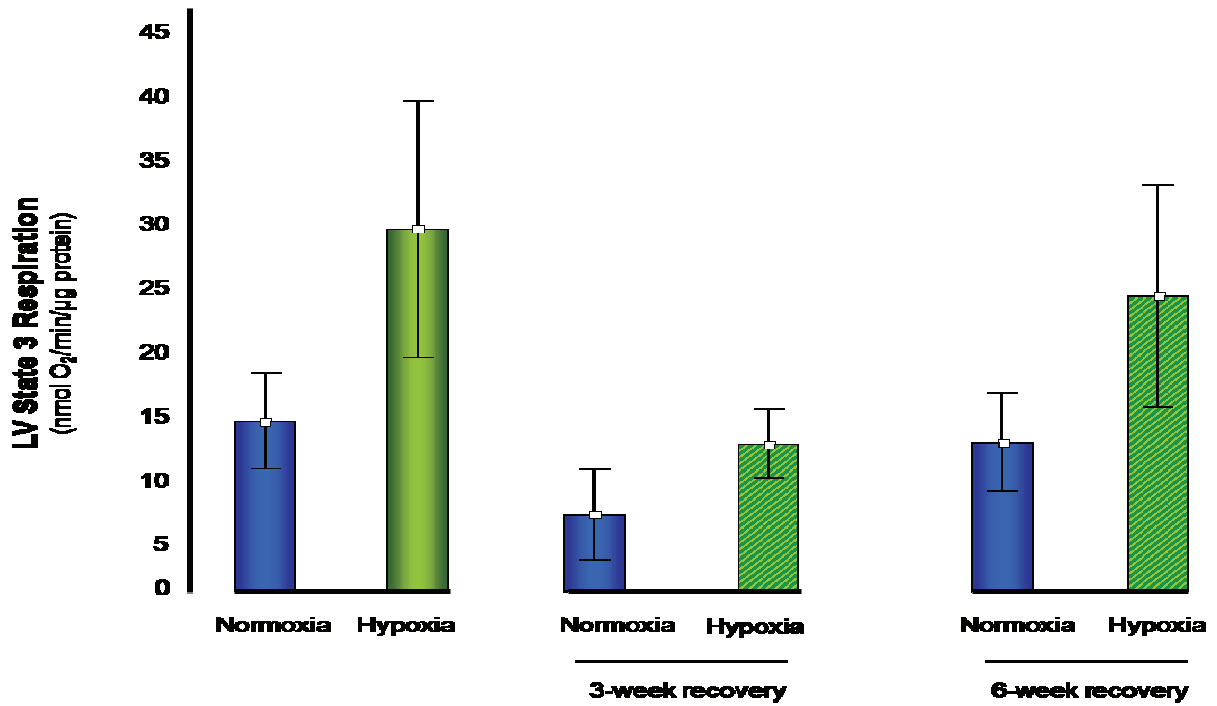


Figure 14. Mitochondrial respiratory capacity (pyruvate) remained unchanged in control and experimental groups.

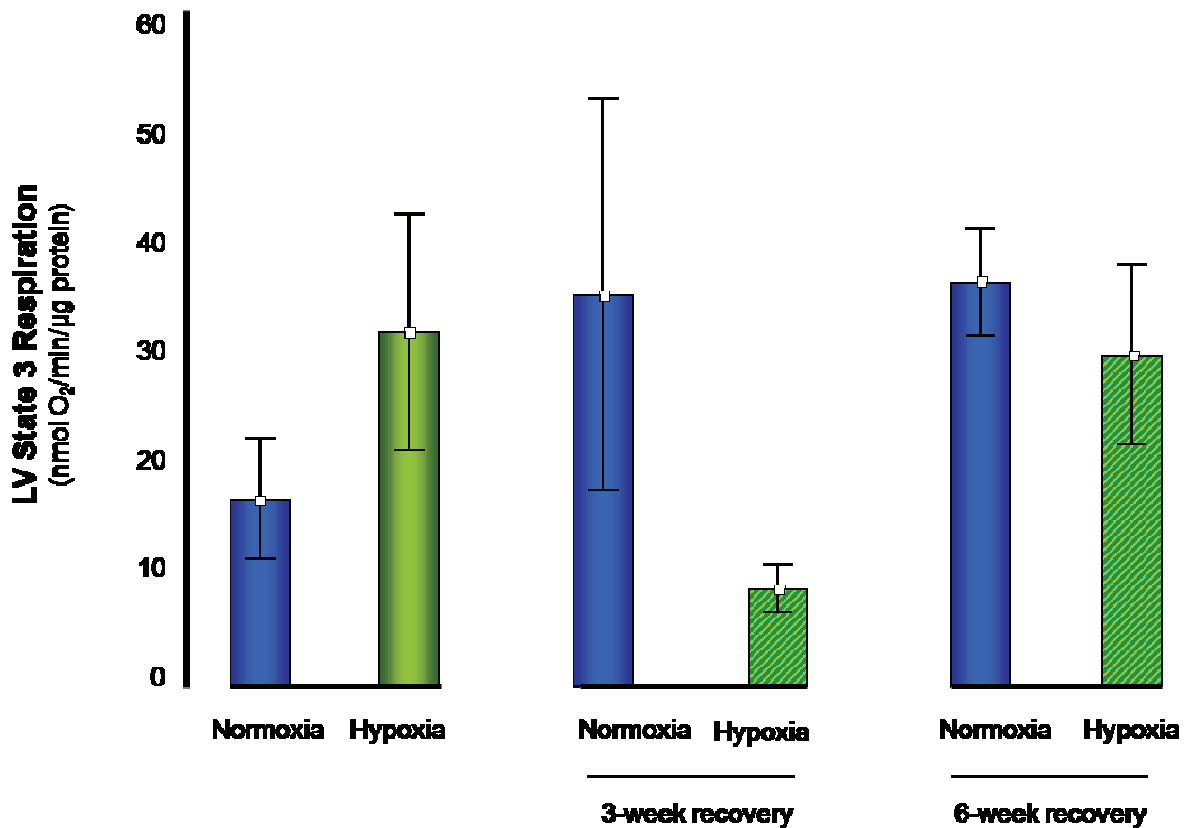


Figure 15. Mitochondrial respiratory capacity (palmitoylcarnitine) remained unchanged in control and experimental groups.

3.5 Determination of cardiac function via the Langendorff perfusion mode

Recent studies have shown that RVH induced by CHH is an adaptive response to pressure-overload to preserve cardiac function (Adrogue et al., 2005, Sharma et al., 2004; Zungu et al., 2007). Therefore, we investigated cardiac function by performing a retrograde perfusion through the aorta.

Here, functional measurements were determined for both the left- and right ventricles. In this study, we observed that functional parameters remained unchanged in the LV, i.e. for controls and all experimental groups (Table 2).

Table 1. Functional measurements investigated at each experimental time point.

	3 weeks		3 weeks Recovery		6 weeks Recovery	
	Normoxia (n=6)	Hypoxia (n=6)	Normoxia (n=5)	Hypoxia (n=6)	Normoxia (n=5)	Hypoxia (n=6)
Left ventricle:						
Heart rate (beats/min)	330.67 ± 17.6	341.67 ± 17.4	227.40 ± 31.5	278.83 ± 17.7	317.00 ± 17.9	321.67 ± 16.4
Systolic pressure (mmHg)	109.83 ± 13.0	93.50 ± 6.5	107.80 ± 4.8	95.50 ± 11.1	106.80 ± 3.0	110.50 ± 5.7
Diastolic pressure (mmHg)	9.33 ± 0.5	8.50 ± 0.3	8.00 ± 0.0	7.83 ± 0.2	7.8 ± 0.5	6.33 ± 0.8
Coronary pressure (mmHg)	69.67 ± 1.0	68.33 ± 0.6	69.12 ± 1.8	69.50 ± 0.8	68.80 ± 0.7	71.83 ± 1.1
Coronary flow (ml/min)	11.83 ± 0.8	12.17 ± 0.7	10.30 ± 1.2	11.50 ± 0.5	13.36 ± 0.7	13.00 ± 0.8
Right ventricle:						
Heart rate (beats/min)	350.16 ± 13.2	346.33 ± 17.9	205.4 ± 14.5	258 ± 24.3	314.00 ± 14.7	316.67 ± 26.4
Systolic pressure (mmHg)	50.50 ± 3.46	71.00 ± 1.4 ^a	51.60 ± 1.4	64.50 ± 3.6 ^b	50.00 ± 0.9	49.5 ± 3.4
Diastolic pressure (mmHg)	9.26 ± 0.8	9.83 ± 0.8	6.40 ± 0.4	7.00 ± 0.4	6.00 ± 0.0	6.83 ± 0.7
Coronary pressure (mmHg)	70.83 ± 1.5	69.67 ± 0.6	66.60 ± 0.2	68.67 ± 0.9	68.40 ± 0.9	70.00 ± 0.7
Coronary flow (ml/min)	12.50 ± 0.6	13.50 ± 0.9	8.36 ± 0.7	10.50 ± 1.3	12.64 ± 0.4	13.83 ± 0.7

All values are represented as means ± SE. ^a p<0.0001 and ^b p<0.04 versus matched controls.

In response to 3 weeks of CHH, RV systolic pressure was significantly increased ($p < 0.0001$ vs. matched controls). This difference in systolic pressure was sustained after 3-weeks of normoxia-recovery ($p < 0.04$ vs. matched controls). However at the 6-week point these values were completely normalized to match that of their controls.

RVDP was significantly increased in the hypoxic group following CHH exposure (47.98 ± 2.98 , $p < 0.001$ vs. matched controls) (Figure 16). Here, we observed that this functional adaptation was still present in the 3HRe group ($p < 0.05$ vs. matched controls), but at the 6-week recovery point had normalized. LVDP remained the same for all three experimental groups and their respective controls (Figure 17).

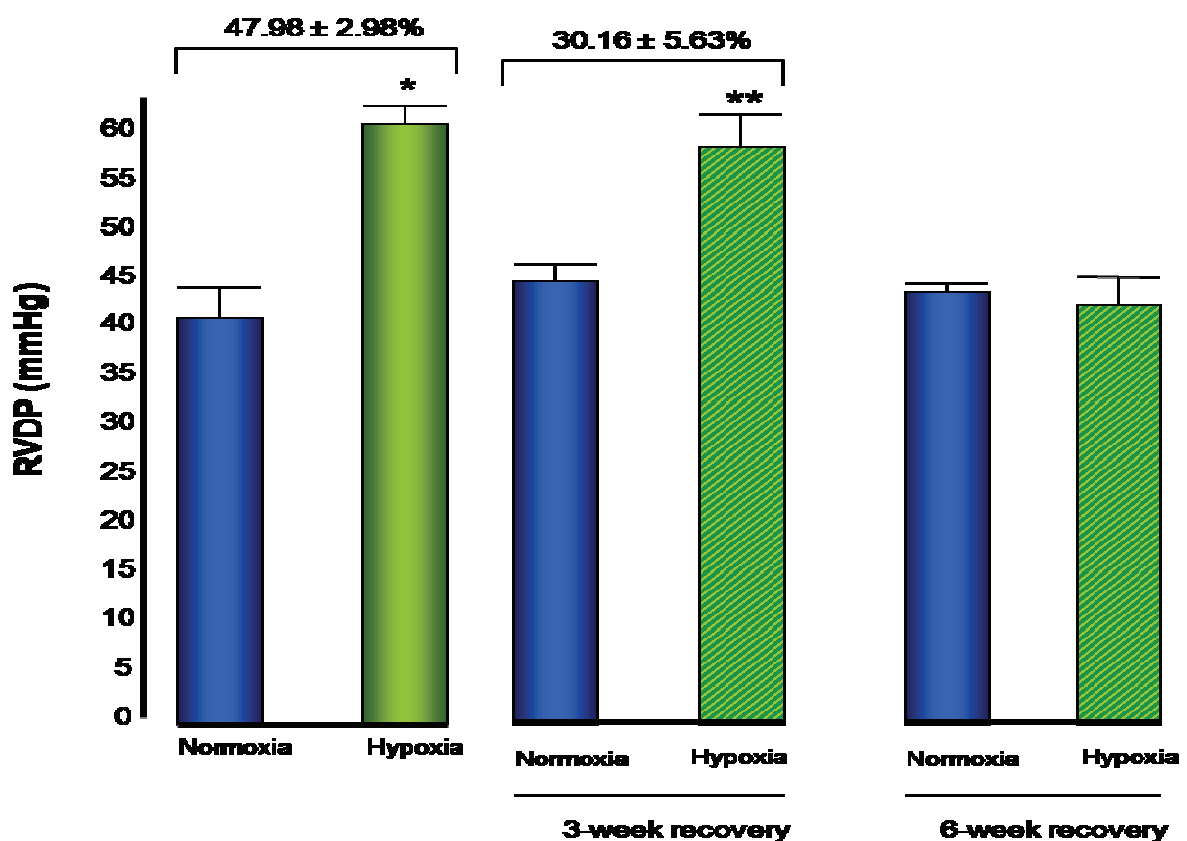


Figure 16. Normalization of right ventricular developed pressure (RVDP) in response to normoxic exposure.

*RVDP was significantly increased following CHH exposure and 3-weeks recovery in normoxia. However, RVDP normalized after 6-weeks of normoxic exposure. * $p < 0.001$ and ** $p < 0.05$ versus matched controls.*

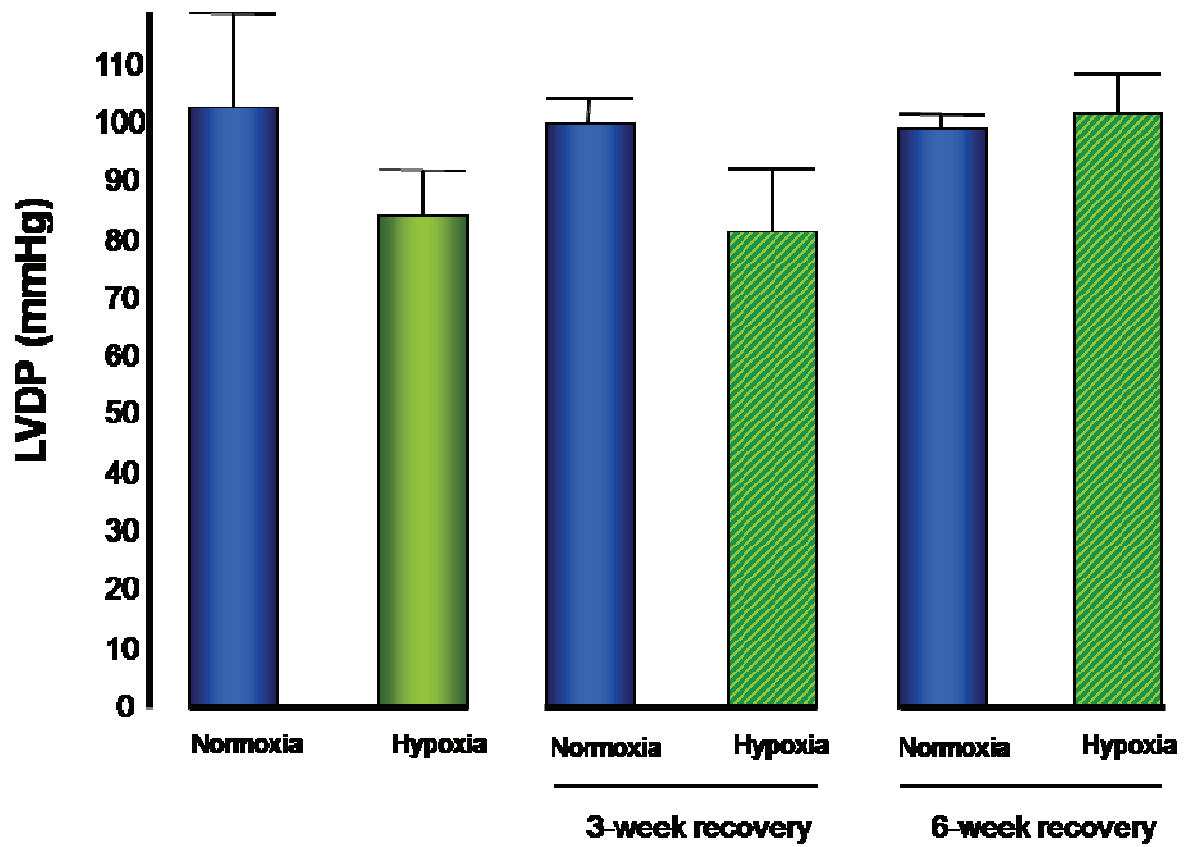


Figure 17. Left ventricular developed pressure (LVDP) remained unaltered during experimental period. *LVDP remained the same in both the experimental and control groups.*

Chapter 4

Discussion

Physiological and pathological cardiac hypertrophic responses are triggered by regulatory mechanisms in the heart to maintain energy homeostasis (Czubryt and Olson, 2004). However, these responses are triggered by different intracellular signaling cascades (Heineken and Molkentin, 2006). Unlike pathological cardiac hypertrophy, physiological hypertrophy is reversible with the absence of heart failure development (McMullen and Jennings, 2007).

For this study, we have investigated a model of physiological hypobaric hypoxia-mediated RV hypertrophy (RVH). Here our hypothesis was that previous changes observed in the RV in response to chronic hypobaric hypoxia (increased RV mass, function and respiratory capacity) (Zungu et al., 2007) are reversible. To test our hypothesis we exposed male Wistar rats to 3 weeks of CHH and thereafter removed the hypoxic stimulus for 3 and 6 weeks, respectively. The main findings of this study are 1) complete reversal of cardiac contractile function at the 6-week normoxia recovery time point, 2) a return to adult cardiac phenotype (i.e. return to fatty acid utilization at the plasma and mitochondrial level following 6-weeks of normoxic recovery) and 3) normalization of chronic hypobaric hypoxia-induced adaptive changes in the hypertrophied RV in response to normoxic exposure.

We found a robust increase in RV mass after 3-weeks of hypobaric hypoxia exposure. In support, the RV/LV+S and RV/BW ratios were increased, while H & E histological staining clearly showed that the diameter of right ventricular cardiomyocytes were increased in response to hypobaric hypoxia. These data therefore show a robust hypertrophic response in the RV and adds to our currently established model of hypoxia-induced RVH, i.e. characterization of the 3-week time point. The right ventricular hypertrophic response at 3-weeks shows that the trophic

response previously found at 2 weeks still persists (Sharma et al., 2004). Together these data show that the hypertrophic response in the RV is initiated fairly early on in response to chronic hypobaric hypoxia , i.e. after 1 week (Sharma et al., 2004), peaks at 2 – 4 weeks (Sharma et al., 2004; Zungu et al., 2007), thereafter remaining relatively high after 10 - 12 weeks exposure (Adroque et al., 2005). The robust increase in RV mass at the 3-week time point was associated with the absence of fibrosis development, agreeing with previous findings from our laboratory (Sharma et al., 2004).

Hematocrit levels were increased after 3 weeks of CHH exposure, in agreement with previous findings in our laboratory (Adroque et al., 2005; Sharma et al., 2004). A well-recognized consequence of CHH exposure is decreased body weight. In this study, we observed that body weight was decreased at the 3-week point, in line with investigations at the 2- and 4-week points (Sharma et al., 2004; Zungu et al., 2007; Zungu et al., 2008). Also, we found that plasma glucose levels were reduced in the hypoxic animals. In support, a study performed by Chen et al. (2007) demonstrated reduced plasma glucose levels after 15 days of hypobaric hypoxia exposure. They further reported that plasma insulin levels were significantly decreased, while corticosterone and glucagon levels were increased in hypoxic animals.

Glucagon secretion is increased during hypobaric hypoxia to enhance hepatic glycogenolysis to promote glucose release for anaerobic energy production and fuel substrate supply to the brain, thus ensuring survival (Chen et al., 2007). It is well-documented that glucocorticoids (i.e. corticosterone in rodents) and insulin play an important role in regulating the hypothalamic-pituitary-adrenal (HPA) axis and food intake (Dallman et al., 2007; Warne et al., 2007). Thus, increased HPA activity found by Chen et al. (2007) may contribute to decreased plasma glucose and insulin levels

observed. We propose that this scenario may hold for our experimental system, i.e. increased HPA activity mediated by hypobaric hypoxia may result in lowered blood glucose levels. Plasma NEFA and TG levels were not significantly increased in response to 3 weeks of CHH. Interestingly

Together these data show that there is a robust increase in RV mass, enhanced hematocrit levels and decreased body weight in response to 3 weeks of CHH exposure.

I next evaluate my hypothesis, i.e. whether changes in the RV in response to 3 weeks of CHH are reversible and therefore strengthen the concept that this is indeed a model of physiological RV hypertrophy. Here we re-exposed hypoxic animals to normoxic conditions for 3 and 6 weeks, respectively, to allow for “recovery” after CHH exposure. After 3 weeks of normoxia-recovery, RV function and respiratory capacity were completely reversed, whereas morphological changes, i.e. increased RV mass, and cardiomyocyte diameter still persisted. Though this increase in RV mass was not associated with fibrosis formation, we did observe an increase in collagen content at the 3-week normoxia-recovery time but the precise mechanism involved in promoting this increase in collagen content requires further investigation. In agreement, a study performed by Pelouch et al., 1997 demonstrated that following sixty days after the last hypoxic exposure, collagen concentration was increased in both ventricles.

Our data suggest that the 3-week recovery time point appears to be a mid-stage of reversion. Here, body weights began to increase while hematocrit levels were fully

normalized. Although body weights further increased after 6 weeks of recovery, the increase occurred at a slower rate compared to controls. After 6 weeks of normoxia-recovery, the adaptive changes in RV function were largely reversed. However, mitochondrial respiratory capacity demonstrated a different pattern, i.e. pyruvate utilization was increased after 3-weeks of normoxia-recovery but remained unchanged at the 6-weeks of normoxia recovery time point. Interestingly, palmitoyl carnitine utilization were increased at the 6-week recovery point, agreeing with the increase in plasma TG levels observed at the 6-week recovery time point. We are uncertain regarding the significance of these findings. However, we propose that it may reflect longer-term severe programming that is triggered by this hypertrophic stimulus since the physiological hypertrophic response is linked with both increased cardiomyocyte size and mitochondrial density (with upregulation of PGC-1 α and NRF-1) (Goffart et al., 2004; Zungu et al., 2007) we propose this may explain increased respiratory capacity at the 3- and 6-week points, respectively. This proposal, however requires further investigation.

RV changes were still present at the structural level following 6 weeks of recovery. For example, the hypertrophic response still persists at this time point. These findings are in line with a study reported by Chouabe et al. (2002) who also investigated a physiological model of hypobaric hypoxia-induced RVH. Here, they exposed rats to 20 days of CHH and then allowed them to recover for 20 and 40 days, respectively, under normoxic conditions. They reported that RV function was completely normalized after 20 days following CHH exposure. However, the changes in right ventricular weight persisted for much longer, i.e. after 40 days of recovery.

Why does the RV hypertrophic response persist after normalization? This finding is still unclear. However, we speculate that a robust gene program may induce the observed hypertrophic response, thus taking much longer to reverse. Possible candidate factors for such long-term gene programming include GATA-4, -5, -6, MEF-2, HDAC class I and class II transcription factors (Carreño et al., 2006). Whether these transcriptional modulators are induced in our experimental system requires further investigation. Another question that arises is how to explain the apparent disconnection between increased ventricular mass and size and normalization of RV function. Again, it is not clear what may explain this intriguing phenomenon. We speculate that mitochondrial biogenesis (observed at the 2-week time point by Zungu et al. [2007]) may still persist at the 3-week time point, thereby enhancing mitochondrial ATP production. Greater ATP supply will therefore underpin normal RV function despite increased RV mass. We are currently pursuing this proposal in our laboratory.

What are the implications of these findings for physiological cardiac hypertrophy in general? Although this is a model of hypobaric hypoxia-induced RV hypertrophy I am of the opinion that these findings will have general application, i.e. may also apply to the LV. However, this postulate requires further investigations in rodent models of LVH. Moreover, I have successfully established a reversible model of hypertrophy at the 3-week point and the value of this experimental system is that it may be a useful tool to exploit. For example, it provides an opportunity to test novel hypotheses which we believe may disrupt the physiological hypertrophy response. We are currently planning to investigate PI3K/Akt and GSK-3 β signaling pathways (Heineken and Molkenin, 2006; Sugden et al., 2008), key intracellular signaling cascades in promoting physiological cardiac hypertrophy, in our experimental system. We predict

that disruption of these pathways (e.g. siRNA) would result in the transition of physiological to pathological cardiac hypertrophy. In this case, the reversibility of the RV hypertrophic response would be lost. We would also like to test the significance of mitochondrial biogenesis in physiological hypertrophy (Zungu et al., 2007). Here our laboratory previously proposed that increased mitochondrial biogenesis plays an important role to underpin physiological cardiac hypertrophy. In light of this, an experiment designed to administer *in vivo* siRNA (against PGC-1 α) to the RV should result in attenuated mitochondrial biogenesis in the hypertrophied RV. We predict that this intervention will contribute to the transition from physiological to pathological RVH. Again, we will be able to test this proposal by assessment of RV hypertrophic reversibility under normoxic conditions.

In summary, we found that exposure to CHH resulted in various adaptive physiological changes, i.e. enhanced hematocrit levels and increased RV mass linked to greater RV contractility and respiratory function. It is important to note that all these changes only occurred in the RV and not in the LV. In our experimental model there are two major stimuli, i.e. a) hypobaric hypoxia and b) hypertrophy. Thus, changes in the LV are due to hypoxia *per se* while changes that are observed in the RV only (not LV) are due to hypertrophy. Furthermore, when a normoxic recovery period (3 and 6 weeks) were initiated, these physiological parameters were completely normalized. From these findings we can conclude that cardiac contractile function especially on the right side were enhanced under the hypobaric hypoxic environment and that only 6-weeks recovery in normoxia is necessary to completely reverse these changes. Interestingly, RV function and respiratory capacity normalized when re-exposed to normoxic conditions despite structural hypertrophic

changes. These data suggest that RVH structural adaptations possibly occur as a result of more longer-term gene programming.

Chapter 5

References

Abel D. Evaluation of mitochondrial function. *Animal Models of Diabetic Complications Consortium AMDCC protocols(1):* 1-3, 2004.

Adroque JV, Sharma S, Ngumbela K, Essop MF and Taegtmeyer H. Acclimatization to chronic hypobaric hypoxia is associated with a differential transcriptional profile between the right and left ventricle. *Molecular and Cellular Biochemistry* 27: 71-75, 2005.

Allard M F. Adaptive and maladaptive cardiac hypertrophy. *Heart Metabolism* 26: 5-9, 2005.

An D and Rodrigues B. Role of changes in cardiac metabolism in development of diabetic cardiomyopathy. *American Journal of Physiology and Heart Circulatory Physiology* 291:H1489-H1506, 2006.

Arad M, Seidman C E and Seidman J G. AMP-activated protein kinase in the heart: role during health and disease. *Circulation Research* 100:474-488, 2007.

Berenji K, Drazner M H, Rothermel B A and Hill J A. Does load-induced ventricular hypertrophy progress to systolic heart failure? *American Journal of Physiology and Heart Circulatory Physiology* 289: H8-H16, 2005.

Bers D M. Cardiac excitation-contraction coupling. *Nature* 415: 198-205, 2002.

Bertrand L, Harman S, Beauloye C and Vanoverschelde J-L. Insulin signalling in the heart. *Cardiovascular Research* p1-11, 2008.

Bökel C and Brown N H. Integrins in development: Moving on, responding to, and sticking to the extracellular matrix. *Developmental Cell* 3:311-321, 2002.

Brownsey R W, Boone A N and Allard M F. Actions of insulin on the mammalian heart: Metabolism, pathology and biochemical mechanisms. *Cardiovascular Research* 34: 3-24, 1997.

Brower G L, Gardner J D, Forman M F, Murray D B, Voloshenyuk T, Levick S P, Janicki J S. The relationship between myocardial extracellular matrix remodeling and ventricular function. *European Journal of Cardio-thoracic Surgery* 30:604-610, 2006.

Calvani M, Reda E and Arrigoni-Martelli E. Regulation by carnitine of myocardial fatty acid and carbohydrate metabolism under normal and pathological conditions. *Basic Research in Cardiology* 95:75-83, 2000.

Carreño J E, Apablaza F, Ocarranza M P and Jalil J E. Cardiac hypertrophy: Molecular and cellular events. *Rev Esp Cardiol* 59(5):473-486, 2006.

Chandrasekar B, Mummidi S, Claycomb W C, Mestril R and Nemer M. Interleukin-18 is a pro-hypertrophic cytokine that acts through a phosphatidylinositol

3-kinase-phosphoinositide-dependent kinase-1-Akt-GATA4 signaling pathway in cardiomyocytes. *Journal of Biological Chemistry* 6(11): 4553-4567, 2005.

Chakraborti S, Das S, Kar P, Ghosh B, Samanta K, Kolley S, Ghosh S Roy S and Chakraborti T. Calcium signalling phenomena in heart disease: A perspective. *Molecular and Cellular Biochemistry* 298: 1-40, 2007.

Chen X-Q, Du J-Z and Wang Y S. Regulation of hypoxia-induced release of corticotrophin-releasing factor in the rat hypothalamus by norepinephrine. *Regulatory Peptides* 119: 221-228, 2004.

Chen X-Q, Dong J, Niu C-Y, Fan J-M and Du J-Z. Effects of hypoxia on glucose, insulin, glucagon and modulation by corticotrophin-releasing factor receptor Type I in the rat. *Endocrinology* 148: 3271-3278, 2007.

Chouabe C, Amsellem J, Espinosa L, Ribaux P, Blaineau S, Mégas P and Bonvallet R. Reversibility of electrophysiological changes induced by chronic high-altitude hypoxia in adult rat heart. *American Journal of Physiology and Heart Circulatory Physiology* 282: H145-H1460, 2002.

Coort S L M, Bonen A, van der Vusse G J, Glantz J F C and Luiken J J F P. Cardiac substrate uptake and metabolism in obesity and type-2 diabetes: role of sarcolemmal substrate transporters. *Molecular and Cellular Biochemistry* 299: 5-18, 2007.

Corno A F, Milano G, Samaja M, Tozzi P, von Segesser L K. Chronic hypoxia: a model for cyanotic congenital heart defects. *Journal of Thoracic and Cardiovascular Surgery* 124(1): 105-112, 2002.

Czubryt M P and Olson E N. Balancing contractility and energy production: the role of myocyte enhancer factor 2 (MEF2) in cardiac hypertrophy. *Endojournals* 150-124, 2004.

Dallman M F, Warne J P, foster M T and Pecoraro N C. Glucocorticoids and insulin both modulate caloric intake through actions on the brain. *Journal of Physiology* 583(2): 431-436, 2007.

Damasceno A, Gotter G, Dzudie A, Sliwa K and Mayosi B M. Heart failure in Sub-Saharan Africa: Time for Action. *Journal of American College of Cardiology* 50(17): 1688-1693, 2007.

DeBosch B, Treskov I, Lupu T S, Weinheimer C, Kovacs A, Courtois M and Muslin A J. Akt 1 is required for physiological cardiac growth. *Circulation* 113: 2097-2104, 2006.

Diwan A and Dorn G W 2nd. Decompensation of cardiac hypertrophy: cellular mechanisms and novel therapeutic targets. *Physiology* 22: 56-64, 2007.

Diwan A, Wansapura J, Syed F M, Matkovich S J, Lorenz J N and Dorn G W 2nd. Nix-mediated apoptosis links myocardial fibrosis, cardiac remodelling, and hypertrophy decompensation. *Circulation* 117: 396-404, 2008.

Dolinsky V W and Dyck J R B. Role of AMP-activated protein kinase in healthy and diseased hearts. *American Journal of Physiology and Heart Circulatory Physiology* 291: H2557-2569, 2006.

Dorn G W 2nd and Force T. Protein kinase cascades in the regulation of cardiac hypertrophy. *Journal of Clinical Investigation* 115(3): 527-537, 2005.

Dorn G W 2nd. The fuzzy logic of physiological cardiac hypertrophy. *Hypertension* 49: 962-970, 2007.

Duffy H S. Cardiac connections- The antiarrhythmic solution? *New England Journal of Medicine* 358: 1397-1398, 2008.

Duncan J G and Finck B N. The PPAR α -PGC-1 α axis controls cardiac energy metabolism in healthy and diseased myocardium. *PPAR Research* 2008.

Engelman J A, Luo L and Cantley L C. The evolution of phosphatidylinositol 3-kinases as regulators of growth and metabolism. *Nature Reviews* 7: 606-619, 2006.

Essop M F. Cardiac metabolic adaptations in response to chronic hypoxia. *Journal of Physiology* 584(3): 715-726, 2007.

Finck B N. The PPAR regulatory system in cardiac physiology and disease. *Cardiovascular Research* 73: 269-277, 2007.

Finck B N and Kelly D P. Peroxisome proliferator-activated receptor γ coactivator – 1 (PGC-1) regulatory cascade in cardiac physiology and disease. *Circulation* 115: 2540-2548, 2007.

Folmes C D L and Lopaschuk G D. Role of malonyl-CoA in heart disease and the hypothalamic control of obesity. *Cardiovascular Research* 73: 278-287, 2007.

Frey N and Olson E N. Cardiac hypertrophy: The good, the bad, and the ugly. *Annual Reviews in Physiology* 65: 45-79, 2003.

Frey N, Katus H A, Olson E N and Hill J A. Hypertrophy of the heart. *Circulation* 109:1580-1589, 2004.

Fuster V, Alexander R W, O'Rourke R A, Roberts R, King III S B, Nash I R S, Prystowsky E N. Hurst's the heart 11th ed volume 1. New York: McGraw-Hill, p15-45, 2004.

Goffart S, von Kleist-Retzow J-C and Wiesner R J. Regulation of mitochondrial proliferation in the heart: Power-plant failure contributes to cardiac failure in hypertrophy. *Cardiovascular Research* 64; 198-207, 2004.

Grimaldi P A. Regulatory functions of PPAR α in metabolism: implications for the treatment of metabolic syndrome. *Biochimica et Biophysica Acta* 1771: 983-990, 2007.

Han M K, McLaughlin V V, Criner G J and Martinez F J. Pulmonary diseases and the heart. *Circulation* 116: 2992-3005, 2007.

Hainsworth R and Drinkhill M J. Cardiovascular adjustments for life at high altitude. *Respiratory Physiology and Neurobiology* 158: 204-211, 2007.

Hardie D G. Minireview: The AMP-activated protein kinase cascade: the key sensor of cellular energy status. *Endocrinology* 144(12): 5179-5183, 2003.

Heineke J and Molkentin J D. Regulation of cardiac hypertrophy by intracellular signalling pathways. *Nature Reviews* 7: 589-600, 2006.

Heart disease and stroke statistics-2008 update. American heart association, Dallas, Texas.

Hilfiker-Kleiner, Landmesser U and Drexler H. Molecular mechanisms in heart failure: Focus on cardiac hypertrophy, inflammation, angiogenesis and apoptosis. *Journal of American College of Cardiology* 48: A56-A60, 2006.

Hill J A and Olson E N. Cardiac plasticity. *New England Journal of Medicine* 358: 130-1380, 2008.

Hislop A and Reid L. Normal structure and dimensions of the pulmonary arteries in the rat. *J Anat* 125(1): 71-83, 1978.

Howell K, Ooi H, Preston R and McLoughlin P. Structural basis of hypoxic pulmonary hypertension: the modifying effect of hypercapnia. *Experimental Physiology* 89(1): 66-72, 2004.

Hunter J J and Chien K R. Signaling pathways for cardiac hypertrophy and failure. *The New England Journal of Medicine* 341(17): 1276-1283, 1999.

Huss J M and Kelly D P. Mitochondrial energy metabolism in heart failure: A question of balance. *The Journal of Clinical Investigation* 115(3): 547-555, 2005.

Huss J M, Imahasi K-I, Dufour C R, Weinheimer C J, Courtois M, Kovacs A, Giguère V, Murphy E and Kelly D P. The nuclear receptor ERR γ is required for the bioenergetic and functional adaptation to cardiac pressure-overload. *Cell Metabolism* 6: 25-37, 2007.

Kemi O J, Ceci M, Wisloff U, Grimaldi S, Gallo P, Smith G L, Condorelli G and Ellingsen O. Activation or inactivation of cardiac Akt/mTOR signalling diverges physiological from pathological hypertrophy. *Journal of Cellular Physiology* 214: 316-321, 2008.

Kiernan J A. Sirius red staining protocol for collagen. [Web:] http://www.ihcworld.com/potocols/special_stains/sirius_red.htm.2007

Klinger J R and Hill N S. Right ventricular dysfunction in chronic obstructive pulmonary disease. Evaluation and management. *Chest* 99:715-723, 1991.

Kodde I F, van der Stok J, Smolenski R T and de Jong J W. Metabolic and genetic regulation of cardiac energy substrate preference. *Comparative Biochemistry and Physiology Part A* 146: 26-39, 2007.

Kolar F and Ostadal B. Molecular mechanisms of cardiac protection by adaptation to chronic hypoxia. *Physiological Research* 53(Supplement 1): S3-S13, 2004.

Lehman J J, Barger P M, Kovas A, Saffitz J E, Medeiros D M and Kelly D P. Peroxisome proliferator-activated receptor γ coactivator -1 promotes cardiac mitochondrial biogenesis. *The Journal of Clinical Investigation* 106:847-856, 2000.

Leibowitz M D, Fiévet c, Hennuyer N, Peinado-Onsurbe J, Duez H, Berger J, Cullinan C A, Sparrow C P, Baffic J, Berger G D, Santini C, Marquis R W, Tolman R L, Smith R G, Moller D E and Auwerx J. Activation of PPAR δ alters lipid metabolism in db/db mice. *FEBS letters* 473: 333-336, 2000.

Leong H S, Grist M, Parsons H, Wambolt R B, Lopaschuk G D, Brownsey R and Allard M F. Accelerated rates of glycolysis in the hypertrophied heart: Are they a methodological artifact? *American Journal of Physiology, Endocrinology and Metabolism* 282: E1039-E1045, 2002.

Leong H S, Brownsey R W, Kulpa J E and Allard M F. Glycolysis and pyruvate oxidation in cardiac hypertrophy-why so unbalanced? *Comparative Biochemistry and Physiology Part A* 135:499-513, 2003.

Liang H and Ward W F. PGC-1 α : A key regulator of energy metabolism. *Advances in Physiology Education* 30: 145-151, 2006.

Luo J, McMullen J R, Sobwiq C L, Zhang L, Dorfman A L, Sherwood M C, Logsdon M N, Horner J W, DePinho R A, Izumo S and Cantley L C. Class I_a phosphoinositide 3- kinase regulates heart size and physiological cardiac hypertrophy. *Molecular and Cellular Biology* 25 (21): 9491-9502, 2005.

Lydell C P, Chan A, Wambolt R B, Sambandam N, Parsons H, Bondy G P, Rodrigues B, Popov K M, Harris R A, Brownsey R W and Allard M F. Pyruvate dehydrogenase and the regulation of glucose oxidation in hypertrophied rat hearts. *Cardiovascular Research* 53(4): 841-851, 2002.

McMullen J R and Jennings G L. Differences between pathological and physiological cardiac hypertrophy: Novel therapeutic strategies to treat heart failure. *Clinical and Experimental Pharmacology and Physiology* 54: 255-262, 2007.

McMullen J R, Amirahmadi F, Woodcock EA, Schinke-Braun M, Bouwman R D, Hewitt K A, Mollica J P, Zhang L, Zhang Y, Shioi T, Buerger A, Izumo X, Jay P Y and Jennings G L. Protective effects of exercise and phosphoinositide 3-kinase (p110 α) signalling in dilated and hypertrophic cardiomyopathy. *PNAS* 104: 612-617, 2007.

Miner E C and Miller W L. A look between the cardiomyocytes: The extracellular matrix in heart failure. *Mayo Clin Proc* 81 (1): 71-76, 2006.

Moudgil R, Michelakis E D and Archer S L. Hypoxic pulmonary vasoconstriction. *Journal of Applied Physiology* 98: 390-403, 2005.

Nakanishi K, Tajima F, Nakamura A, Yagura S, Ookawara T, Yamashita H, Suzuki K, Tangiguchi N, and Ohno H. Effects of hypobaric hypoxia on antioxidant enzymes in rats. *Journal of Physiology* 489(3): 869-876, 1995.

National diagnostics. National diagnostics – articles - histology
Fundamentals_clearing tissue section. [Web:]
http://nationaldiagnostics.com/article_info.php/articles_id/id.html.2005

Neubauer S. The failing heart- An engine out of fuel. *The New England Journal of Medicine* 356:1140-11451, 2007.

Opie L H, Commerford P J, Gersh B J and Pfeffer M A. Controversies in ventricular remodelling. *The Lancet* 367: 356-367, 2006.

Ostadal B and Kolar F. Cardiac adaptation to chronic high-altitude hypoxia: Beneficial and adverse effects. *Respiratory Physiology and Neurobiology* 158:224-236, 2007.

Pearson T A. Cardiovascular disease in developing countries: Myths, realities and opportunities. *Cardiovascular Drugs and Therapy* 13: 95-104, 1999.

Pelouch V, Kolar F, Ostadal B, Milerova M, Cihak R and Widimsky J. Regression of chronic hypoxia-induced pulmonary hypertension, right ventricular hypertrophy and fibrosis: Effect of Enalapril. *Cardiovascular Drugs and Therapy* 11:177-185, 1997.

Petersen K F and Shulman G I. Etiology of insulin resistance. *The American Journal of Medicine* 119(5A): 10S-16S, 2006.

Pokreisz P, Marsboom G and Janssens S. Pressure overload-induced right ventricular dysfunction and remodeling in experimental pulmonary hypertension: The right heart revisited. *European Heart Journal Supplements* 9 (Supplement H):H75-H84, 2007.

Puigserver P and Spiegelman B M. Peroxisome proliferators-activated receptor γ coactivator 1 α (PGC-1 α): Transcriptional coactivator and metabolic regulator. *Endocrine Reviews* 24(1): 78-90, 2003.

Rajabi M, Kassiotis C, Razeghi P and Taegtmeyer H. Return to the fetal gene program protects the stressed heart: a strong hypothesis. *Heart failure reviews* 2007.

Razeghi P, Young M E, Alcorn J L, Moravec C S, Frazier O H and Taegtmeyer H. Metabolic gene expression in fetal and failing human heart. *Circulation* 104: 2923-2931, 2001.

Rasmussen B B and Wolfe R R. Regulation of fatty acid oxidation in skeletal muscle. *Annual Reviews in Nutrition* 19: 463-484, 1999.

Reddy K S. Cardiovascular disease in non-western countries. *New England Journal of Medicine* 350 (24): 2438-2440, 2004.

Ritchie R H and Delbridge L. Cardiac hypertrophy, substrate utilization and metabolic remodeling: cause or effect? *Proceedings of the Australian Physiological Society* 36: 35-43, 2005.

Rossetti L. Perspective: hexosamines and nutrient sensing. *Endocrinology* 144(6): 1922-1925, 2000.

Rumsey W L, Abbot B, Bertelsen D, Michael M, Hagan K, Nelson D and Erecinska M. Adaptation to hypoxia alters energy metabolism in rat heart. *American Journal of Physiology and Heart Circulatory Physiology* 276(45): H71-H80, 1999.

Saad M J, Folli F, Araki E, Hashimoto N, Csermely P and Kahn C R. Regulation of insulin receptor, insulin receptor substrate-1 and phosphatidylinositol-3-kinase in 3T3-F442A adipocytes. Effects of differentiation, insulin and dexamethasone. *Molecular Endocrinology* 8(5): 545-557, 1994.

Saeedi R, Grist M, Wambolt R B, Bescond-Jacquent A, Lucien A and Allard M F. Trimetazidine normalizes postischemic function of hypertrophied rat hearts. *Journal of Pharmacology and Experimental Therapeutics* 314:446-454, 2005.

Sambandam N, Lopaschuk G D, Brownsey R W and Allard M F. Energy metabolism in the hypertrophied heart. *Heart Failure Reviews* 7:161-173, 2002.

Sano M and Schneider M D. Energizer: PGC-1 α keeps the heart going. *Cell Metabolism* 216-218, 2005.

Savourey G, Launay J-C, Besnard Y, Guinet A, Bourrilhou C, Cabane D, Martin S, Caravel J-P, Péquignot J-M and Cottet-Emard J-M. control of erythropoiesis after high altitude acclimatization. *European Journal of Applied Physiology* 93:47-56, 2004.

Scarpulla R C. Nuclear activators and coactivators in mammalian mitochondrial biogenesis. *Biochimica et Biophysica Acta* 1576: 1-14, 2002.

Sharma S, Taegtmeyer H, Adroque J, Razeghi P, Sen S, Ngumbela K and Essop M F. Dynamic changes of gene expression in hypoxia-induced right ventricular hypertrophy. *American Journal of Physiology and Heart Circulatory Physiology* 286: H1185-H1192, 2004.

Sidhu S, Gangasani A, Korotchkina L G, Suzuki G, Fallavollita J A, Canty J M and Patel M S. Tissue-specific pyruvate dehydrogenase complex deficiency causes cardiac hypertrophy and sudden death of weaned male mice. *American Journal of Physiology, Heart and Circulatory Physiology* 295:H946-H952, 2008.

Spinale F G. Myocardial matrix remodelling and the matrix metalloproteinases: Influence on cardiac form and function. *Physiological Reviews* 87: 1285-1342, 2007.

Srivastava D and Yu S. Stretching to meet needs: integrin-linked kinase and the cardiac pump. *Genes and Development* 20: 2327-2331, 2006.

Stanley W C and Sabbah H N. Metabolic therapy for ischemic heart disease: The rationale for inhibition of fatty acid oxidation. *Heart Failure Reviews* 10: 275-279, 2005.

Stanley W C, Recchia F A and Lopaschuk G D. Myocardial substrate metabolism in the normal and failing heart. *Physiological Reviews* 85: 1093-1129, 2005.

Sugden M C. PDC deletion: the way to a man's heart disease. *American Journal of Physiology Heart and Circulatory Physiology* 295: H917-H919, 2008.

Sugden P H, Fuller S J, Weiss S C and Clerk A. Glycogen synthase kinase 3 (GSK3) in the heart: a point of integration in hypertrophic signaling and a therapeutic target? A critical analysis. *British Journal of Pharmacology* 1-17, 2008.

Swynghedauw B. Molecular mechanisms of myocardial remodeling. *Physiological Reviews* 79: 215-262, 1999.

Taegtmeyer H, Wilson C R, Razeghi P and Sharma S. Metabolic energetics and genetics in the heart. *Annals New York Academy of Sciences* 1047: 208-218, 2005.

Tanaka M, Mizuta K, Koba F, Ohira Y, Kobayashi T and Honda Y. Effects of exposure to hypobaric-hypoxia on body weight, muscular and hematological characteristics and work performance in rats. *Japanese Journal of Physiology* 47: 51-57, 1997.

Towler M C and Hardie D G. AMP-activated protein kinase in metabolic control and insulin signaling. *Circulation Research* 100: 328-341, 2007.

Tibazarwa K, Ntyintyane L, Silwa K, Gertholtz T, Carrington M, Wilkinson d and Stewart S. A time bomb of cardiovascular risk factors in South Africa: Results from the heart of Sowetho study "Heart Awareness Days". *International Journal of Cardiology* p1-7, 2008.

Ussher F R and Lopaschuk G D. Clinical implication of energetic problems in cardiovascular disease. *Heart Metabolism* 32: 9-17, 2006.

Vander A, Sherman J and Luciano D. Human physiology: The mechanisms of body function. 7thed. New York: McGraw Hill p 591-610, 1998.

Van Gaal L F, Mertens I L and De Block C E. Mechanisms linking obesity with cardiovascular disease. *Nature* 444:875-880, 2006.

Voet D and Voet J G. Biochemistry: Biomolecules, mechanisms of enzyme action, and metabolism 3rd ed vol 1. New York: Wiley pp 613-618, 768,780-781,917, 2004.

Wang X, Ren G, Liu S, Sentex E, Tappia P S and Dhalla N S. Characterization of cardiac hypertrophy and heart failure due to volume overload in the rat. *Journal of Applied Physiology* 94: 752-763, 2003(a).

Wang Y-Z, Lee C-H, Tjep S, Y R T, Ham J, Kang H and Evans R M. Peroxisome-proliferator-activated receptor δ activates fat metabolism to prevent obesity. *Cell* 113: 159-170, 2003(b).

Warne J P, Foster M T, Horneman H F, Pecoraro N C, Ginsberg A B, Akana S F and Dallman M F. Afferent signaling through the common hepatic branch of the vagus inhibits voluntary lard intake and modifies plasma metabolite levels in rats. *Journal of Physiology* 582(2): 455-467, 2007.

WebPath: The internet pathology laboratory. Histotechniques. [Web:] <http://www.library.med.utah.edu/WebPath/HISTHTML/HISTOTCH.html>.2008.

Wilkins B J, Dai Y, Bueno O F, Parsons S A, Xu J, Plank D M, Jones F, Kimball T R and Kolekentin J D. Calcineurin/NFAT coupling participates in pathological, but not physiological cardiac hypertrophy. *Circulation Research* 94: 110-118, 2004.

Wilson C R, Tran M K, Salazar K L, Young M E and Taegtmeyer H. Western diet, but not high fat diet, causes derangements of fatty acid metabolism and contractile dysfunction in the heart of Wistar rats. *Biochemical Journal* 406: 457-467, 2007.

World health organisation (WHO). Cardiovascular disease. [Web:]
<http://www.who.int/mediacentre/factsheets/fs317/en/index.html>. 2008.

Young M E, McNulty P and Taegtmeyer H. Adaptation and maladaptation of the heart in diabetes: Part II. *Circulation* 105: 1861-1870, 2002.

Young M E. The circadian clock within the heart: potential influence on myocardial gene expression, metabolism and function. *American Journal of Physiology and Heart Circulatory Physiology* 290: H1-H16, 2006.

Yusuf S, Reddy S, Ôunpuu S and Anad S. Global burden of cardiovascular diseases Part II: Variations in cardiovascular disease by specific ethnic groups and geographic regions and prevent strategies. *Circulation* 104: 2855-2864, 2001.

Yusuf S, Vaz M and Pais P. Tackling the challenge of cardiovascular disease burden in developing countries. *American Heart Journal* 148: 1-4, 2004.

Zhu H, Tannous P, Johnstone J L, Kong Y, Shelton J M, Richards J A, Le V, Levine B, Rothermel B A and Hill J A. Cardiac autophagy is a maladaptive response to hemodynamic stress. *Journal of Clinical Investigation* 117:1782-1793, 2007.

Zungu M, Alcolea M P, Garia-Palmer F J, Young M E and Essop M F. Genomic modulation of mitochondrial respiratory genes in the hypertrophied heart reflects adaptive changes in mitochondrial and contractile function. *American Journal of Physiology and Heart Circulatory Physiology* 293: H2819-H 2825, 2007.

Zungu M, Young M E, Stanley W C and Essop M F. Expression of mitochondrial regulatory genes parallels respiratory capacity and contractile function in a rat model of hypoxia-induced right ventricular hypertrophy. *Molecular and Cellular Biochemistry* 318: 175-181, 2008.

Chapter 6

Appendices

Appendix A: Experimental procedures to sacrifice and excise rat hearts

- Remove rats from cages by holding them at the highest part of the tail
- Place the animal on the floor or on a level surface
- Wrap your fingers just under its forearms and turn the rat on its back to expose the abdomen
- Inject the rat intraperitoneally with an anaesthetic e.g. pentobarbital sodium
- The amount of anaesthetic is calculated according to body weight of the rat
- Check for any nerve sensation by pinching the foot
- While sedated, weigh the rat to determine the final body weight
- Place the rat on a dissection board and open the abdominal cavity
- Neatly move the intestines to the side to expose the *vena cava inferior*
- Collect blood directly from the *vena cava inferior* via exsanguination
- Carefully remove the diaphragm
- Open the chest cavity to expose the heart
- Gently lift the heart and cut in the direction of the throat to get a great piece of the aorta
- Remove the heart and immediately place it in Krebs-Henseleit buffer [11 mM glucose, 118 mM NaCl, 25 mM NaHCO₃, 4.7 mM KCl, 1,2 mM KH₂PO₄, 1.2 mM MgSO₄.7H₂O, 1.8 mM, CaCl₂.6H₂O, pH 7.4] on ice

Appendix B: Determination of plasma NEFA levels

Bottle	Contents
1	5x 11 ml potassium phosphate buffer, pH 7.8
2	5 tablets containing ATP, coenzyme A, acyl-CoA synthetase, peroxidase, ascorbate oxidase, 4-aminoantipyrine and stabilizers
3	3 ml aqueous N-ethyl-maleinimide solution with stabilizers
4	5x acyl-CoA oxidase 0.6 ml diluted solutions and stabilizers
5	5 tablets containing acyl-CoA oxidase and stabilizers

Prepare working solutions:

Solution A

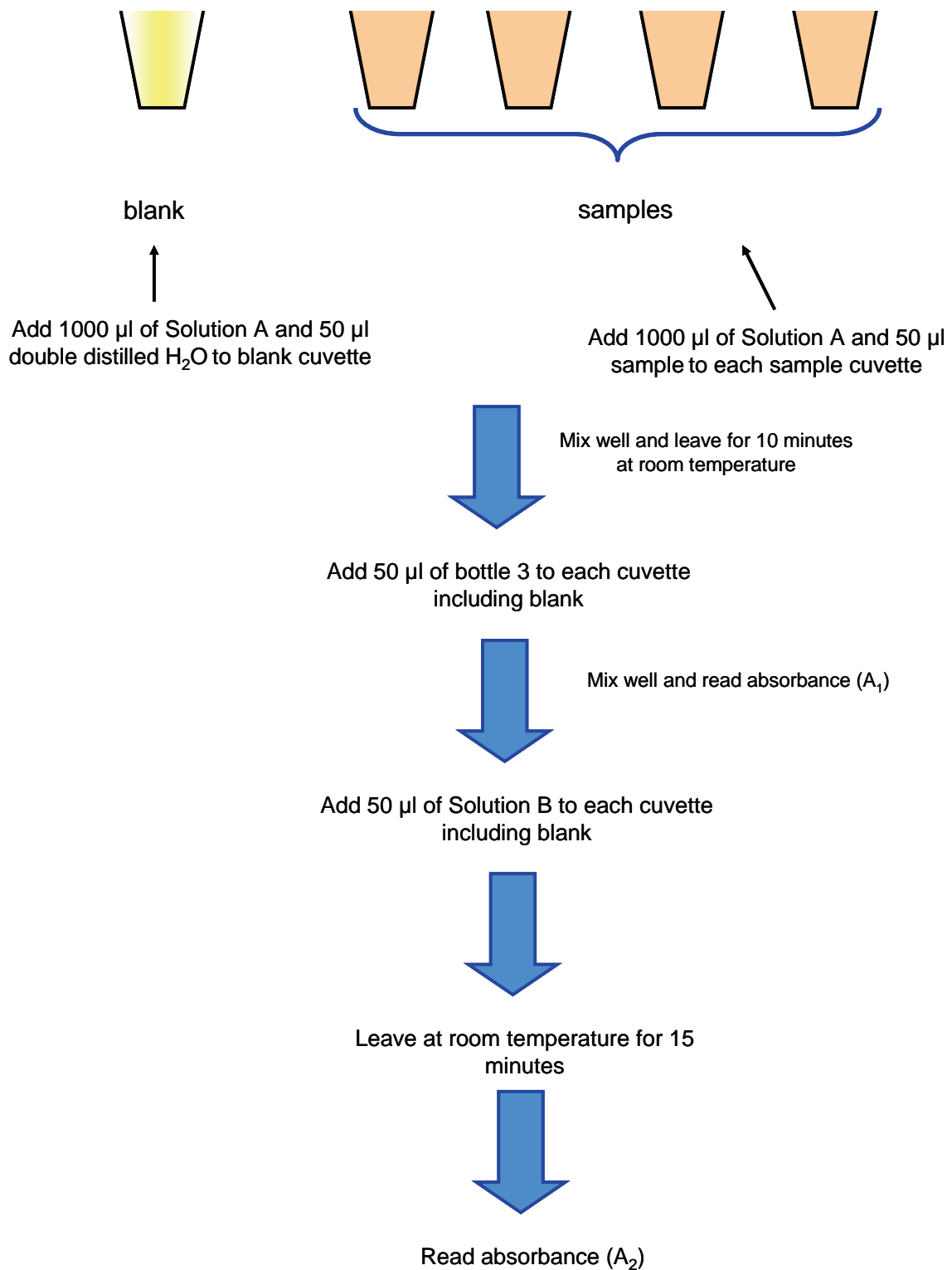
- Add 1 tablet of bottle 2 to bottle 1
- Wait until tablet is fully dissolved before usage

Solution B

- Add 1 tablet from bottle 5 to bottle 4
- Wait until tablet is completely dissolved before usage

Note: handle tablets with forceps. Working solutions are only stable for 5 days when stored at 2 to 8 °C.

Experimental procedure:



Calculations:

- Calculate absorbance differences for both blank and sample (A₂-A₁).

- Subtract the absorbance difference of the blank (ΔA_b) from the absorbance difference of the sample (ΔA_s) to give ΔA .

Thus, $c = (V/\epsilon \times d \times v) \times \Delta A$

Where V = final volume (ml)

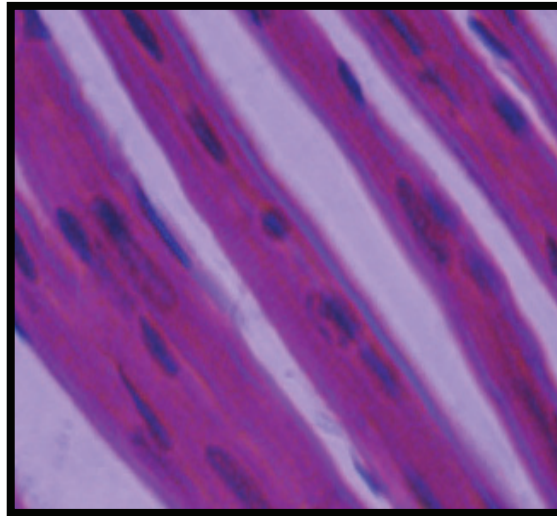
v = sample volume (ml)

d = light path (cm)

ϵ = absorption coefficient of the dye at 546 nm

= 19.3 [$1 \times \text{mmol}^{-1} \times \text{cm}^{-1}$]

Appendix C: Haematoxylin and Eosin staining protocol



Materials:

1. Xylo
2. 100% or absolute alcohol
3. 95% alcohol
4. 70% alcohol
5. Distilled water
6. Haematoxylin

For staining:

- Filter 100 ml haematoxylin stock solution through two filter papers
- Add 4 ml glacial acetic acid per 100ml haematoxylin

7. Acid alcohol (75%)
8. Tap water
9. Eosin

Stock solution:

- 10 g Eosin dissolved in 1 L distilled water

Working solution:

- Add 10 ml eosin stock solution to 90 ml distilled water (note: must be freshly prepared daily)

For staining:

- Add 2-3 drops of glacial acetic acid per 100 ml working

10. Mounting media

Staining procedure:

Note: Haematoxylin and Eosin are water soluble dyes, therefore paraffin still present in the tissue sections must be removed (“deparaffinise”)

1. Deparaffinise

- Place in xylol for 10 minutes
- Put in absolute alcohol for 20 seconds
- Place in 95% alcohol for 20 seconds
- Place in 70% alcohol for 10 seconds
- Rinse in distilled water

2. Haematoxylin stain:

- Leave in Harris haematoxylin solution for 3 to 5 minutes
- Rinse of excess stain in distilled water
- Place in acid alcohol to remove excess stain
- Rinse in distilled water
- Rinse in tap water

- Rinse in distilled water

3. Eosin stain:

- Leave haematoxylin-stained slides in eosin for 2 minutes
- Rinse in distilled water

4. Dehydrate and clear:

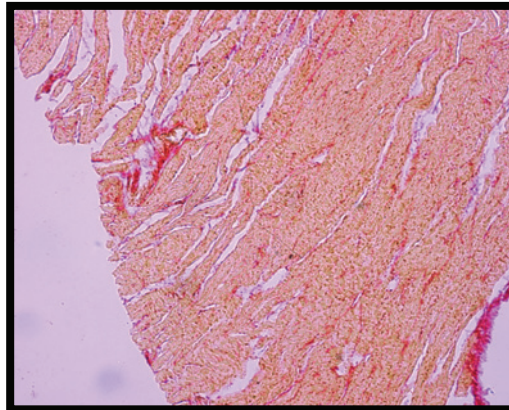
- Place in 70% alcohol for 10 seconds
- Place in 95% alcohol for 20 seconds
- Place in 100% alcohol for 20 seconds
- Leave in xylol for 60 seconds

5. Coverslip mounting

- Add enough mounting medium (Etellan, Merck, Germany) on the coverslip to cover the entire stained tissue section
- Carefully place the coverslip (at an angle) down over the tissue section to avoid air bubbles
- Once firmly in place, wipe with a dry paper towel to evenly spread the mounting medium over tissue section
- Leave to dry overnight

Note: It's important that the mounting medium covers the whole of the tissue section, since it protects the staining dyes and keeps the section moist, thus ensuring long-term preservation.

Appendix D: Pico-Sirius red stain for collagen (Kiernan, 2007)



Materials:

Pico-Sirius red solution

- 0.5 g Sirius red F3B (C.I. 35782)
- 500 ml Saturated aqueous solution of picric acid (Note: add a little solid picric acid to ensure saturation)

Acidified water

- Add 5 ml glacial acetic acid to 1L tap water

Weigert's haematoxylin

Experimental procedure

1. de-wax and hydrate paraffin sections
2. stain nuclei with Weigert's haematoxylin for 8 minutes, and wash the slides for 10 minutes in running tap water.
3. stain in pico-sirius red for 1h

4. wash in two changes of acidified water
5. physically remove most of the water from the slides by vigorous shaking
6. dehydrate in three changes of 100% ethanol
7. clear in xylene

Appendix E: Preparation and calibration of electrode

- Polish the center silver and platinum section of the electrode with the supplied polish paste using a cotton bud
- Rinse with distilled water and dry with a cotton bud.
- Cut a small square piece of Rizzla cigarette paper and nick in the middle
- Place onto of electrode and wet with saturated KCl solution
- Carefully cut an equally big piece of membrane and place it on top of the Rizzla
- paper. (Remember to handle membrane with forceps and to wear gloves).
- Gently apply the small O-rings to secure membrane
- Secure electrode in chamber and assemble system
- Switch on water bath
- Set calibration settings and allow to calibrate for 10 minutes

Appendix F: Langendorff perfusion protocol

- Remove heart as described in Appendix A and Option B
- Place in ice-cold Krebs-Henseleit buffer
- Locate aorta, transfer to the perfusion apparatus and cannulate
- Bind the aorta with thread or a piece of string just under the aortic arch
- Remove excess connective tissue
- Make a small incision just at the base of the aorta to prevent fluid build-up
- Make small openings in the right and left atrium to insert a latex balloon connected to a pressure transducer
- Check the temperature and pressure of the perfusion buffer at regular intervals
- If all is fine, allow for a 5 minute stabilization period
- Measure functional measurements every 15 minutes for right and left ventricle, respectively
- Functional measurements were first taken for the left ventricle (30 minutes), followed by functional measurements of the right ventricle (30 minutes)

**Establishing the Nature of
Reversible Cardiac Remodeling
in a
Rat Model of Hypobaric Hypoxia-
induced Right Ventricular
Hypertrophy**

Aretha van der Merwe



Thesis presented in partial fulfillment of the requirements
for the degree of Masters of Physiological Sciences at
Stellenbosch University

Supervisor: Prof M. Faadiel Essop

March 2009